Involvement of autophagy in the metabolism of Amyloid Precursor Protein and effects of familial Alzheimer's disease-associated mutations of Presenilin-1

Dissertation

zur

Erlangung des Doktorgrades (Dr. rer. nat.)

der

Mathematisch-Naturwissenschaftlichen Fakultät

der

Rheinischen Friedrich-Wilhelms-Universität Bonn

Vorgelegt von

Nguyễn, Thành Tiền

aus Hai Duong, Viet Nam

Bonn, 2014

Angefertigt mit Genehmigung der Mathematisch-Naturwissenschaftlichen Fakultät der
Rheinischen Friedrich-Wilhelms-Universität Bonn

Contents

1. Introduction

1.1. Alzheimer's disease

Alzheimer's disease (AD) is characterized by a progressive neurodegeneration that leads to memory and language impairment, disordered cognitive function as well as other neuropsychiatric symptoms and behavioral disturbances (Alonso et al., 1997; Selkoe, 2001). The World Health Organization cites AD as the leading cause of dementia and the sixth most common cause of death worldwide. It was estimated that approximately 18 million people worldwide were affected by AD in 2010 and it is expected that this number will be doubled by the year 2050 (O'Brien and Wong, 2011), but no cure or preventive therapy is available yet (Tanzi and Bertram, 2005). The etiology of the disease is not completely understood and it can only be diagnosed with certainty by brain autopsy (Tannenberg et al., 2004).

AD causes a loss of brain weight and volume, and affects neurons in several brain regions including the entorhinal cortex, hippocampus, parahippocampal gyrus, amygdale, frontal, temporal, parietal and occipital association cortices, and certain subcortical nuclei projecting to these regions; with the hippocampus and entorhinal cortex being the first affected regions (Gomez-Isla et al., 1996; Selkoe, 2001). Loss of brain weight is mainly caused by the shrinkage and loss of neuronal processes (Gomez-Isla et al., 1996; Selkoe, 2001). Neuronal synapses and dendrites are particularly vulnerable to AD. Loss of synapses and dendritic spines correlates with cognitive decline in AD (Palop and Mucke, 2010).
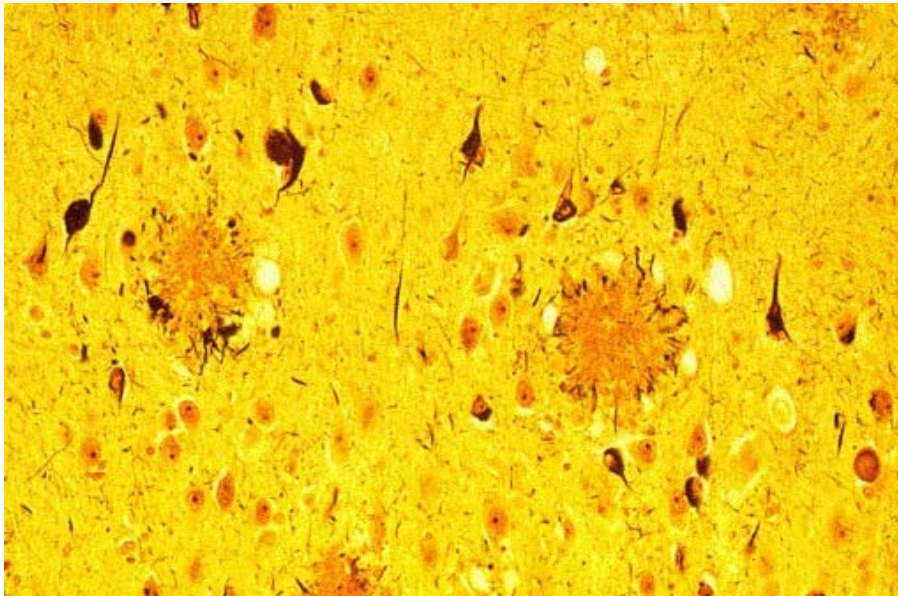
Figure 1.1: Photomicrograph of an AD brain section demonstrates the neuropathological lesion of the disease. Amyloid plaques are visible as large compacted and spherical structures. Neurofibrillary tangles are darkly stained masses occupying much of the perinuclear cytoplasm. The image is taken from Selkoe (Selkoe, 1998).

Neuropathologically, AD is characterized by the combined accumulation of extracellular amyloid plaques consisting of amyloid-beta (Aβ) peptides and intraneuronal neurofibrillary tangles composed of hyperphosphorylated tau (p-tau) protein (Alonso et al., 1996; Selkoe, 2001).

Abnormal folding of tau leads to the generation of paired helical filaments (PHFs) and NFTs (Alonso et al., 1996). In addition to PHFs, hyperphosphorylated tau also exists as a soluble pool in AD brain (Kopke et al., 1993). The tau levels, especially p-tau, are strongly increased in AD brains as compared to age-matched control brains (Khatoon et al., 1992).

Amyloid plaques and neurofibrillary tangles can occur independently of each other (O'Brien and Wong, 2011; Selkoe, 2001). Tau aggregate-composed tangles have also been described in more than a dozen less common neurodegenerative diseases that lack Aβ deposits and neuritic plaques. These indicate tau itself as a disease-causing agent (Mandelkow and Mandelkow, 2012). NFTs pathology correlates better with AD symptoms than amyloid plaques (Buerger et al., 2006; Buerger et al., 2002). Importantly, tau reduction prevents Aβ-mediated neuronal deficits in cell culture and hAPP transgenic mice (Morris et al., 2011). However, Aβ deposits also occur in brains of cognitively normal-aged humans in the virtual absence of tangles (Selkoe, 2001). In addition, there are also infrequently AD cases with only few NFTs the neocortex, despite abundant Aβ plaques (Terry et al., 1987).

AD is categorized into early-onset AD (EO-AD; <65 years) and late-onset AD (LO-AD; >65 years). They both exhibit progressive cognitive decline, amyloid plaques and neurofibrilary tangles (NTFs) (Lee et al., 2011b). They also share other neuropathological features including defects in axonal transport, loss of synapses and selective neuronal death (Goldstein, 2012; Holtzman et al., 2011).

1.1.1. Early-onset familial AD

1–6% of AD cases are early onset (< 65 years old), of which about 60% are familial AD. It usually occurs at the age of 40s or in the early 50s, although many cases of onset at the 30s and early 60s have been reported (Campion et al., 1999; Rocca et al., 1991).

Three genes have been identified that are associated with early-onset familial AD (EO-FAD) which encode the Amyloid precursor protein (APP), Presenilin 1 (PS1) and Presenilin 2 (PS2) (Campion et al., 1999). More than 190 mutations in PS1, 26 mutations in PS2 and 25 mutations in APP have been indentified to be associated with FAD so far (http://www.alzforum.org/mutations, http://www.molgen.vib-ua.be/ADMutations). Most FAD cases containing APP mutations have the age of onset in the mid-40s and 50s (Hardy, 2001).

1.1.2. Late-onset and sporadic AD

LO-AD refers to the age of onset above 65 years and accounts for about 95% of all AD cases. Unlike early-onset cases, LO-AD is caused by multiple factors including genetic and epigenetic changes, and additional age-related factors (Campion et al., 1999). Aging is the most important risk factor for AD.

Moreover, hypertension, diabetes, obesity and environmental factors such as head injury, low education, also increase the risk of developing AD (Rosendorff et al., 2007; Van Den Heuvel et al., 2007). However, the relative contribution of these factors to the risk for AD remains controversial (Daviglus et al., 2010). The major genetic factor for LO-AD is Apolipoprotein E4 (ApoE4) allele (Caselli et al., 2011; Haan et al., 1999).

In the brain, ApoE is expressed predominantly by astrocytes and microglia (Grehan et al., 2001; Pitas et al., 1987). The ApoE gene comes in three well known isoforms encoding proteins (designated ApoE2, ApoE3, and ApoE4) that differ at two amino acids (Mahley et al., 2006). It has a gene-dosage-dependent effect on increasing the risk and lowering the age of onset and potentially also of the progression of the AD (Corder et al., 1993; Farrer et al., 1997). The most compelling role in AD is its ability to bind Aβ and affect Aβ deposition. While ApoE3 stimulates Aβ clearance, ApoE4 is strongly related to increased Aβ accumulation and increased amyloid plaque formation (Huang and Mucke, 2012; Mahley et al., 2006). Indeed, the crossing between APP-transgenic (Tg) mice (PDAPP and Tg2576 models) that develop Aβ deposition in the brain with ApoE$^{-/-}$ mice led to less Aβ deposition and a strong decrease in amyloid plaque load (Bales et al., 1999; Holtzman et al., 2000). Many studies have suggested that ApoE may influence Aβ seeding and fibrillogenesis (Castano et al., 1995), as well as the clearance of soluble Aβ (Castellano et al., 2011). Most studies show that the efficiency of complex formation between lipidated ApoE and Aβ follows the order of ApoE2 > ApoE3 >> ApoE4 (Ma et al., 1994). Thus, the ApoE4 allele is strongly associated with increased brain Aβ deposition (Tiraboschi et al., 2004), whereas ApoE2 and -E3 diminish Aβ deposition (Holtzman et al., 1999). The ApoE4 allele increases the risk for AD threefold in individuals carrying one copy and 15-fold for homozygous individuals (Singh et al., 2006).

Besides its critical role in AD, ApoE has also a potential role in other neurological diseases and traumatic brain injury (Mahley et al., 2006). In the brain, ApoE is a major lipid transporter. ApoE-containing lipoproteins have been proposed to play a role in reverse cholesterol transport, deliver cholesterol and other lipids to neurons to support synapses, thereby affecting CNS lipid and cholesterol homeostasis. Their receptors belong to the low-density lipoprotein receptor (LDLR) family (Mauch et al., 2001). ApoE maintains a constant supply of neuronal lipids for membrane synthesis thus ensuring efficient neurotransmitter release and the propagation of action potentials (Bales, 2010). This raises the possibility that a dysfunction of the lipid transport system associated with compensatory sprouting and synaptic remodelling could be central to the AD process (Mauch et al., 2001). Additionally, the role of ApoE in the CNS is particularly important in relation to the function of the cholinergic system which relies to a certain extent on the integrity of phospholipid homeostasis in neurons (Poirier, 1996).

Lipid metabolism has been shown to play important role not only in AD, but also in other neurodegenerative diseases (Kolter et al., 2005; Walter and van Echten-Deckert, 2013b).

Particularly, impairment of degradation and transport of cholesterol and sphingolipids in endo-lysosomal compartments are the cause of many neurodegenerative diseases (Settembre et al., 2008). Furthermore, neurodegeneration diseases share pathological similarities with AD such as extensive neurodegeneration, intracellular tau protein aggregates and neuroinflammation (Jeyakumar et al., 2003; Rojo et al., 2008). In addition, the generation Aβ takes place in endocytic compartments (Greenfield et al., 1999; Haass et al., 1993a), suggesting the involvement of membrane lipids in subcellular transport, activity, and metabolism of AD-related proteins (Walter and van Echten-Deckert, 2013).

1.1.3. APP processing and Aβ generation

APP is a member of a small protein family, also including the amyloid precursor-like proteins 1 and 2 (APLP1 and APLP2) in mammals, and orthologs also found in other species, like Drosophila. They are single-pass transmembrane proteins with large extracellular domains and short intracellular domains that are posttranslationally modified and processed in a similar manner (Bayer et al., 1999; Selkoe, 2001). The APP gene is located on human chromosome 21 and contains 19 exons. Alternative splicing of the APP mRNA generates three main isoforms, APP695, APP751 and APP770 (according to the number of amino acids), in which APP695 is predominantly expressed in neurons (Bayer et al., 1999; Selkoe, 2001). In addition, APP isoforms can undergo posttranslational modification while moving through secretory pathway, including proteolytic processing, addition of N-and O-linked sugars, glycosylation, sulfation and phosphorylation (Weidemann et al., 1989).

Understanding the real physiological function of APP is still challenging. So far, most of the studies have shown that APP overexpression exerts neurotrophic effects. Transient transfection of APP in cells or transgenic mice overexpressing wild-type APP showed a positive effect on cell growth, motility, neurite outgrowth, and cell survival. These functions can also be reproduced by the soluble ectodomain of APP as well (O'Brien and Wong, 2011; Oh et al., 2009). Additionally, intracerebral injections of the APP ectodomain improved cognitive function and synaptic density (Meziane et al., 1998; Roch et al., 1994). By extension, injection of APP RNAi into embryonic rodents resulted in abnormalities in neuronal migration (Young-Pearse et al., 2007). However, deletion of APP in mice is not deleterious to the adult animal (O'Brien and Wong, 2011). Duplication of APP gene or trisomy of chromosome 21 (Down syndrome) causes early-onset AD (Huang and Mucke, 2012), whereas partial trisomy 21 excluding the APP gene is not linked to AD (Prasher et al., 1998).

Amyloid deposits in the AD brains are classified in three morphological variants: diffuse deposits, in which Aβ peptides are not aggregated into clusters; primitive deposits, in which the Aβ peptides are aggregated into clusters and associated with dystrophic neurites and helical filaments; and classic deposits, in which Aβ peptides are highly aggregated to form a central cluster "core" surrounded by a "ring" of dystrophic neuritis (Armstrong, 2011).

4
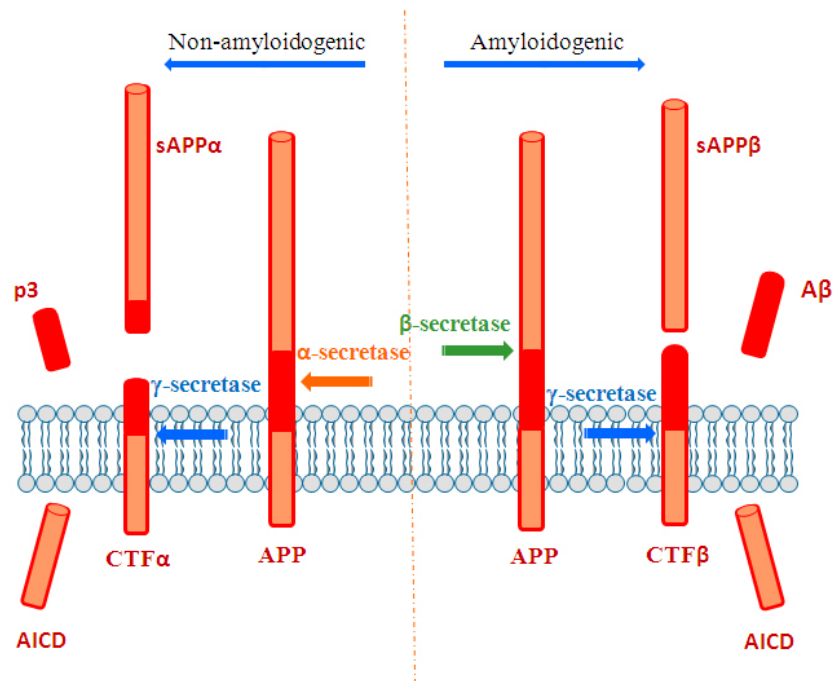
Figure 1.2: Proteolytic prcessing of APP. APP can be processed in either a non-amyloidogenic or an amyloidogenic pathway. The non-amyloidogenic pathway involves α- and γ-secretase processing to release soluble APPα (sAPPα), APP–C-terminal fragment α (CTFα), APP intracellular domain (AICD) and p3. The amyloidogenic pathway involves β- and γ-secretase processing to generate sAPPβ, CTFβ, AICD and Aβ peptides.

APP is synthesized in the endoplasmic reticulum (ER) and then transported through the Golgi apparatus to the trans-Golgi-network (TGN) (Greenfield et al., 1999; Xu et al., 1997). From the TGN, APP can be transported in TGN-derived secretory vesicles to the cell surface (Sisodia, 1992). From the plasma membrane, APP can be re-internalized via endocytosis and sorted to endosomal/lysosomal degradation pathways (Caporaso et al., 1994). Following endocytosis, APP is delivered to endosomes and a fraction of endocytosed APP is recycled to the cell surface (Haass et al., 2012). On the cell surface, APP is mainly proteolyzed in non-amyloidogenic pathway involving α- and γ-secretases. In endocytic compartments, APP is cleaved in amyloidogenic pathway by β- and γ-secretases (O'Brien and Wong, 2011). However, there is some α- and β- secretase activity in the TGN as well (Mills and Reiner, 1999).

In the non-amyloidogenic pathway, APP is first cleaved by α-secretase at a position 83 amino acids from the carboxy (C) terminus, generating a soluble APP (N)-terminal ectodomain (sAPPα) which is secreted to the extracellular milieu (Kojro and Fahrenholz, 2005). The remaining C-terminal fragment α (CTFα) with 83-amino-acid (C83) is subsequently cleaved within its transmembrane domain by γ-secretase to generate the p3 fragment (Haass et al., 1993b). Importantly, cleavage by α-secretase occurs within the Aβ region, thereby preventing Aβ formation. In the amyloidogenic pathway, APP is cleaved to generate Aβ peptides. The initial proteolysis is mediated by β-secretase

to release a soluble APP (N)-terminal ectodomain (sAPPβ) which is secreted to the extracellular milieu and the CTFβ with 99-amino-acid (C99) retained within the membrane. Subsequent cleavage of the CTFβ between residues 38 and 43 by γ-secretase generates Aβ peptides of different length (Jarrett et al., 1993).

β-Secretase predominantly localizes to the late Golgi/TGN and endosomes (Koo and Squazzo, 1994); whereas γ-secretase complex is present in multiple compartments including the ER, ER-Golgi intermediate compartment, Golgi, TGN, endosomes, and plasma membrane. Many lines of evidence have shown that Aβ is generated mainly in the TGN and endosomal/lysosomal compartments (Greenfield et al., 1999; Haass et al., 1993a). Aβ peptides are then degraded in the lysosomes or released into extracellular fluids through vesicle recycling (O'Brien and Wong, 2011).

The role of Aβ peptides on behaviour and cognition have not been clearly identified yet (Luo et al., 2001). Most of the Aβ peptide produced has 40 amino acids (Aβ40), whereas the 42 amino acid peptide (Aβ42) only accounts for approximately 10%. Importantly, the Aβ42 variant is more hydrophobic and more prone to aggregate than Aβ40 (Jarrett et al., 1993), and is the major constituent of senile plaques in AD brains (Glenner and Wong, 1984; Masters et al., 1985). Many studies indicate that insoluble Aβ fibrils found in amyloid plaques and monomeric Aβ are less pathogenic than soluble, nonfibrillar assemblies of Aβ such as Aβ dimers, trimers, and oligomers (Huang and Mucke, 2012). Aggregated Aβ peptides can trigger neuroinflammation, neuronal cell death and gradual cognitive decline (Selkoe, 1999).

Besides the major amount of extracellular secretion, Aβ peptides are also found intracellularly. Importantly, intracellular Aβ42 is most abundant in neurons compared to Aβ40 (Gouras et al., 2000). Intracellular Aβ accumulation has been implicated as an early event in the pathogenesis of AD and Down syndrome. In the hippocampus and entorhinal cortex of patients with mild cognitive impairment (MCI), intraneuronal Aβ immunoreactivity has been reported to be a predictor of the development of early AD pathology (Gouras et al., 2000). Similarly, it has been shown that intracellular Aβ accumulation precedes extracellular plaque formation in Down syndrome patients (Gyure et al., 2001).

All FAD-associated APP mutations are localized within and around the Aβ domain (Selkoe, 2001). These mutations accelerate Aβ production by diverse mechanisms. For examples, the Swedish mutation at the amino terminus of the Aβ region represents a better substrate for β-secretase activity, thereby increasing total Aβ production (such as Aβ40 and Aβ42) (Cai et al., 1993; Citron et al., 1992). Mutations in the middle region of Aβ such as the Arctic (Nilsberth et al., 2001) and the Dutch mutations (Levy et al., 1990), affect the Aβ structure and enhance its aggregation propensity. Mutations located just beyond the carboxyl terminus of Aβ (such as the Austrian, Iranian, French, German, London, and Florida mutations) cause increased production of Aβ42. The Flemish mutation

is located in an apparent substrate inhibitory domain that negatively regulates γ-secretase activity by binding to an unknown allosteric site within the complex. Therefore, the Flemish mutation reduces the activity of this inhibitory domain and consequently increase Aβ generation (Tian et al., 2010). In addition, mutations at residue 717 in APP can accelerate Aβ42 generation (Cai et al., 1993; Sherrington et al., 1995). Besides the pathogenic mutations, the substitution of alanine by threonine at position 673 in APP gene (A673T) results in a protection against Alzheimer's disease (Jonsson et al., 2012), likely by decreasing the processing by β-secretase.

1.1.4. α-and β-secretases

α-Secretase activity could be exerted by members of the ADAM (a disintegrin and metalloprotease) family such as ADAM9, ADAM10, ADAM17/TACE (tumour necrosis factor- α- converting enzyme) and ADAM19. ADAMs are membrane-anchored proteins with several domains, containing a metalloprotease domain which requires a zinc co-factor for activity (Allinson et al., 2003).

Stimulation of phosphorylation of protein kinase C (PKC) by phorbol esters stimulates α-secretase processing and secretion of the APP ectodomain (Buxbaum et al., 1990). The PKC-dependent α-secretase has also been shown to compete with β-secretase for cleavage of APP (Fahrenholz et al., 2000).

Besides APP, α-secretases also mediate the ectodomain shedding of Notch, p75, TNFα receptor, cadherins and IL-6 receptor, EGF receptor ligands, and several other type I transmembrane proteins (Sisodia, 1992). Therefore, they play roles in many biological aspects including cell proliferation, differentiation, remodeling of extracellular matrix and signaling (Primakoff and Myles, 2000).

The β-secretase or β-site APP-cleaving enzyme 1 (BACE1), is a type I integral membrane protein belonging to the pepsin family of aspartyl proteases (Sinha et al., 1999; Vassar et al., 1999). BACE1 is highly expressed in neuronal cells, but also at lower levels in non-neuronal cells and tissues (Cole and Vassar, 2008). Besides the cleavage of APP at the N-terminus of the Aβ peptide sequence, BACE1 can also cleave at the Glu11 site of the Aβ peptide which leads to decreased Aβ production (Cai et al., 2001; Fluhrer et al., 2002).

The BACE gene is located on chromosome 11 and consists of nine exons. It codes for a protein of 501 amino acids (Stockley and O'Neill, 2008). Pre-mRNA of BACE1 can undergo alternative splicing in exon 3 and 4, leading to the production of four variants with 501, 476, 457 and 432 amino acids. Among them, the longer variants have stronger cleavage activity for APP compared to the shorter variants (Mowrer and Wolfe, 2008).

Besides BACE1, BACE2 - a homologous protease was also identified (Vassar 2004). While BACE1 is involved in neuronal Aβ generation, BACE2 is predominantly expressed in glia and peripheral tissue. BACE2 was shown to cleave APP in the middle of the Aβ domain between phenylalanines 19 and 20.

Thus, it is not involved in amyloidogenesis and appears to process APP somewhat similar to α-secretase (Basi et al., 2003; Fluhrer et al., 2002).

BACE1 is an attractive potential target in AD therapy as its expression levels increase with age (Fukumoto et al., 2004), and are particularly elevated in the brain cortex of AD patients (Fukumoto et al., 2004). Moreover, inhibition of BACE1 not only reduces Aβ levels but also prevents the accumulation of APP-CTFβ, the precursor protein for Aβ production. This is very important, because APP-CTFβ accumulation may cause additional toxic effects to neurons (Citron et al., 1992). However, although BACE1 knockout mice are not lethal, they have myelination deficit (Walter, 2006).

1.1.5. γ-Secretase and Presenilins
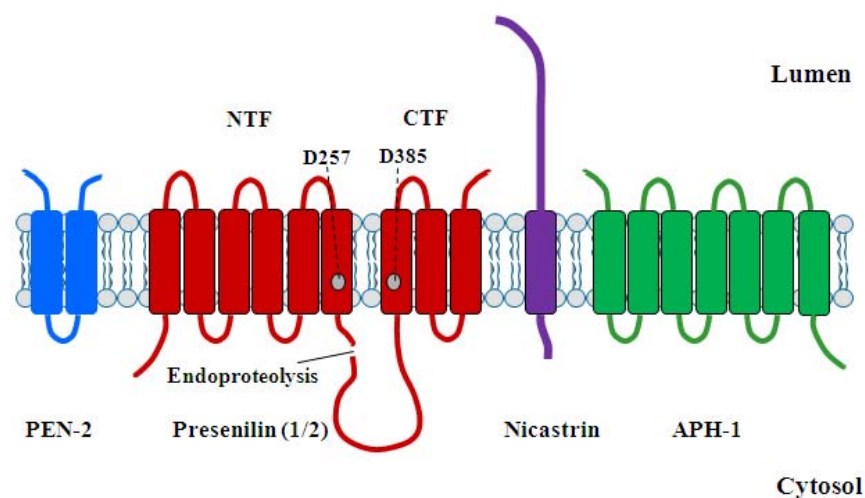
Figure 1.3: Model of the core components of the γ-secretase complex and their membrane topologies. Presenilin (1 or 2) forms the catalytic component of the complex. It is proteolytically processed into the N-terminal fragment (NTF) and C-terminal fragment (CTF) during maturation of the complex. Presenilin has two catalytic aspartic acid residues D257 and D385 in transmembrane domain 6 and 7, respectively. Other components of the complex are nicastrin, anterior pharynx defective (APH-1), and presenilin enhancer 2 (PEN-2).

γ-Secretase is a multiprotein complex composed of presenilin 1 or 2 (PS1/2), nicastrin, anterior pharynx defective 1a or 1b (APH-1a/1b) and presenilin enhancer 2 (PEN-2); in which, PSs are the catalytic subunits of the complex (Francis et al., 2002; Levitan et al., 2001; Steiner et al., 2002; Wolfe et al., 1999; Yu et al., 2000). Knockout of both PS1 and PS2 completely abolished γ-secretase activity (Zhang et al., 2000).

PSs are polytopic transmembrane (TM) proteins which are cleaved endoproteolytically in their cytoplasmic loop between transmembrane domains 6 and 7 to release N- and C- terminal fragments (Steiner and Haass, 2000). PS1 and PS2 have two aspartyl residues (D257 in TM6 and D385 in TM7)

that are important for γ-secretase intramembranous cleavage. Mutagenesis of these residues reduces cleavage of APP and Notch1 (De Strooper et al., 1999; Wolfe et al., 1999).

The biological functions of nicastrin, APH-1, and PEN-2 have been demonstrated. Nicastrin is a type I transmembrane glycoprotein with a large extracellular domain, which is heavily glycosylated and tightly folded after maturation (Shirotani et al., 2003). It probably acts as a size-selective substrate receptor, which might forward the substrates to the active site in PS (Dries et al., 2009; Shah et al., 2005). PEN-2 has two transmembrane domains. It facilitates PS endoproteolysis and stabilizes PS within the γ-secretase complex (Hasegawa et al., 2004). APH-1 has 7 TM domains and it is suggested to act as a scaffold for the initial binding of nicastrin and assembly of the complex (LaVoie et al., 2003). It influences PS conformation and therefore contributes to the proteolytic activity of the γ-secretase in situ (Serneels et al., 2009). The γ-secretase complex containing APH-1a is crucial for Notch signaling during embryogenesis (Serneels et al., 2005).

The γ-secretase complex has a predicted 1:1:1:1 stoichiometric complex, based on molecular mass estimated in blue native electrophoresis, immunobloting analysis, and electron microscopy studies of the purified complex (De Strooper et al., 2012). Nicastrin initially binds APH-1 to forms a subcomplex in the endoplasmic reticulum. The subcomplex then interacts with the PS and PEN-2 subcomplex. The carboxy-terminal domain of PS interacts with APH-1 and the TM domain of nicastrin (De Strooper et al., 2012)

The γ-secretase complex cleaves type 1 transmembrane proteins. Over the years, at least 90 proteins have been found to undergo proteolysis by this enzyme (Beel and Sanders, 2008; De Strooper et al., 1999). The most well known substrates include APP, Notch receptors and ligands, Erb4 receptor and Cadherin (Wakabayashi and De Strooper, 2008). It is clear that Notch is an important substrate of γ-secretase as its signaling is involved in cell growth, differentiation, and proliferation (De Strooper et al., 1999). Notch phenotypes are reported to be predominant in presenilin-deficient animals. Importantly, the greatest concern when developing γ-secretase inhibitors for AD therapy is their interference with the Notch signaling pathway (McCarthy et al., 2009). Other well studied substrates of γ-secretase are N- and E-cadherins, which form complexes with PS1 and α-/ β-catenins at the cell surface. The N-methyl-D-aspartate (NMDA) agonists-regualted γ-secretase-mediated proteolysis of E-cadherin leads to the release of the associated α-/ β-catenins (De Strooper et al., 2012).

The cleavage of APP as well as other substrates by γ-secretase does not take place at a single site. It rather appears that they are cleaved several times within their transmembrane domains at the so-called ε-, ζ-, and γ-sites which are separated by approximately three amino acids (Takami et al., 2009; Weidemann et al., 2002). It is even more complicated when the final γ-cleavage occurs under physiological conditions at least between amino acids 37 and 43 of the Aβ (Haass and Selkoe, 2007).

PS1 and PS2 are highly homologous proteins and their mutations are the main cause of FAD (Selkoe, 2001; Steiner and Haass, 2000). PSs are primarily localized in the ER and Golgi apparatus, and small fraction at the cell surface (Walter et al., 1996). They are predominantly present as N- and C-terminal fragments, while the PS full-length (PS-FL) is only faintly detectable. This is explained by the short half-life time (~1.5 h) and rapid turnover of PS-FL compared to the endoproteolytic fragments with a half-life of ~24 h (Walter et al., 1997). Endoproteolytic cleavage of PS-FL takes place primarily in the ER. Consequently, γ-Secretase complex is formed at the ER and subsequently transported to the Golgi and the plasma membrane where it functions as γ-secretase (De Strooper et al., 2012).

PSs have a highly conserved GXGD motif at the catalytic site, and the two conserved aspartate residues, within the GXGD motifs of TMD6 and TMD7, are essential for the γ-secretase activity (Haass and Steiner, 2002).

Given the central role in AD, the function of PSs in the CNS is of crucial interest. Lack of PSs is lethal in mouse embryos (Golde and Kukar, 2009). The conditional knockout of PSs in the forebrain (using an αCaMKII promoter to drive Cre expression) led to an impairment in hippocampal memory and synaptic plasticity followed by age-dependent neurodegeneration (Saura et al., 2004). These deficits support the hypothesis that loss of PS function might contribute to the pathogenesis of sporadic AD independently of Aβ generation (Shen and Kelleher, 2007). However, the absence of Aβ deposition might not constitute a model of AD (De Strooper et al., 2012).

As the major cause of early-onset, autosomal dominant AD, PS mutations cause the most aggressive form of inherited AD, in some cases with the disease onset below the age of 30 (Selkoe, 2001). Importantly, FAD-linked mutations of PS alter γ-secretase activity, leading to increased Aβ42/Aβ40 ratio either by increasing Aβ42 peptide or/and decreasing Aβ40 peptide production and triggering Aβ accumulation in the brain (Repetto et al., 2007; Selkoe, 2011). It was initially suggested that PS mutations act via a toxic gain-of-function mechanism because they increase the relative amount of Aβ42 versus Aβ40 in vivo and in vitro paradigms (Borchelt et al., 1996; Duff et al., 1996). On the other hand, reduced AICD production in PS mutants suggested a loss-of-function mechanism (Moehlmann et al., 2002). However, further analyses clarified that the increase in Aβ42/Aβ40 ratio does not necessarily indicate an increase in Aβ42 levels, but it can also be the consequence of a decrease in Aβ40 levels. Actually, many mutations have been observed to reduce one or both Aβ42 and Aβ40 levels (Koch et al., 2012; Kulic et al., 2000). These observations rather support a loss-of-function mechanism of γ-secretase activity in FAD-linked mutations of PS1, resulting in decreased proteolytic processing of different substrates and compromising intracellular signaling pathways (Kelleher and Shen, 2010; Shen and Kelleher, 2007).

Besides the role as catalytic subunits of the γ-secretase complex to cleave type I transmembrane proteins, PSs also involves in γ-secretase-independent processes such as protein trafficking and

turnover, calcium homeostasis, regulation of β-catenin signaling, cell adhesion, apoptosis, neurite outgrowth, and synaptic plasticity (De Strooper et al., 2012; Shen and Kelleher, 2007). Moreover, PS1/γ-secretase is involved in ephrinB phosphorylation and Src activation by regulating ephrinB2-CTF production, which further activates Src. This indicates the possibility that FAD-linked mutations of PS1 interfere with Src and ephrinB2 functions in the CNS (Georgakopoulos et al., 2006). Besides these roles, with at least 40 interacting partners, possible presenilin functions are immense (Wakabayashi et al., 2009).

Furthermore, presenilins are also reported to play a role in Ca^{2+} homeostasis. There is a consensus that PS mutants disturb the Ca^{2+} pool in the ER (Bezprozvanny and Mattson, 2008). However, the proposed mechanisms appear unclear, and might involve regulation of the Ryanodine receptor (Hayrapetyan et al., 2008), stimulation of inositol-3-phosphate-induced ER Ca^{2+} release (Cheung et al., 2008) and stimulation of sarco(endo)plasmic reticulum Ca^{2+}-ATPase (SERCA) pumps (Green et al., 2008). In addition, PSs might act as Ca^{2+} leak channels themselves (Tu et al., 2006).

Recently, presenilins have also been implicated in cellular trafficking and turnover of proteins. The mechanisms, however, are still debated between studies. The initial study reported that FAD-linked mutations of PS led to increased lysosomal pathology in both mouse model and humans (Cataldo et al., 2004). In addition, PS1 deficiency and FAD mutations have been shown to prevent autophagic turnover of long-lived proteins. The effect was caused by an impaired lysosomal acidification (Lee et al., 2010). However, Coen and colleagues recently demonstrated that lysosomal Ca^{2+} homeostasis, rather than lysosomal acidification, is affected by PS1 deficiency. This provides an alternative hypothesis that accounts for impaired lysosomal fusion capacity observed in PS deficiency, leading to endo-lysosomal defects in PS1 deficient cells (Coen et al., 2012). Despite this growing consensus on a role of PS proteins and γ-secretase in endolysosomal function, the above-mentioned studies provided conflicting mechanisms by which PS1 deficiency and FAD mutations could affect autophagic activity.

1.2. Lysosomal function and autophagy

1.2.1. The lysosomal system

The lysosome is a single-membrane cytoplasmic organelle in eukaryotic cells that contains more than 50 different hydrolases (phosphatases, nucleases, glycosidases, proteases, peptidases, sulphatases and lipases), which can digest all of the major macromolecules of the cell in an acidic environment for metabolic reuse (Maiuri et al., 2007b). Among the lysosomal hydrolases, proteases (especially cathepsins) play a major role in degrading proteins (Mullins and Bonifacino, 2001). Lysosomal pH is maintained at an average of ~4.7 through the action of a proton pump and multiple ion channels in the lysosomal membrane (Demarchi et al., 2006).

Most newly synthesized acidic hydrolases are processed post-translationally by modification of carbohydrates to mannose-6-phosphate moieties and subsequently form a complex with the mannose-6-phosphate receptor (MPR) in the trans-Golgi network, which targets them to endosomes (Kroemer and Jaattela, 2005). The acidic environment in endosomes during maturation to lysosomes triggers the dissociation of the complexes and the proteolytic processing of some enzymes from proforms to active forms (Demarchi et al., 2006). For example, Cathepsin D (Cat D) is a glycoprotein synthesized as pro-Cat D that is proteolytically processed to an intermediate during its transport to the lysosome. In the lysosome, the intermediate Cat D is further processed to generate the active fragment (Richo and Conner, 1994). The lysosomal substrates for degradation are delivered to lysosomes by two general pathways including heterophagy (receptor-mediated endocytosis, pinocytosis, phagocytosis) for extracellular constituents and autophagy for intracellular constituents (Nixon, 2007). The lysosomal breakdown products (amino acids, mono- and oligo-saccharides, and nucleotides) can be transported back to the cytosol by specific transporter proteins in the lysosomal membrane or to the extracellular space through calcium-induced exocytosis (Kroemer and Jaattela, 2005).

Principally, the acidic luminal pH is generated by v-ATPase, a multi-subunit complex that mediates the ATP-driven transport of protons across biological membranes. Given its important role in maintaining the lysosomal acidic lumen, v-ATPase function is especially critical in autophagy, where fusion of autophagosomes with lysosomes requires rapid proton import to re-acidify newly formed autolysosomes (Wolfe et al., 2013). Besides the function in maintaining lysosomal pH, v-ATPase can influence diverse functions of lysosome such as receptor-ligand trafficking, modulation of lysosomal Ca^{2+} levels (Mindell, 2012), transport of degradative axonal compartments (Lee et al., 2011a), and membrane fusion events (Williamson and Hiesinger, 2010).

1.2.2. Autophagy

Autophagy refers to any cellular degradative pathway that delivers cytoplasmic constituents to the lysosome for degradation (Levine and Kroemer, 2008). At least three major forms of autophagy have been indentified so far - including chaperone-mediated autophagy (CMA), microautophagy and macroautophagy – that differ in molecular mechanisms of cargo delivery to the lysosome for degradation (Levine and Kroemer, 2008).

Chaperone-mediate autophagy (CMA) is involved in the translocation of cytosolic proteins across the lysosomal membrane. The proteins that contain a KFERQ motif are recognized by Hsc70 for CMA, which facilitates unfolding and delivery of proteins to lysosome-associated membrane protein 2a (LAMP2a). Subsequently, LAMP2a serves as a pore for translocation of the selected proteins across the lysosomal membrane. It should be noted that APP also contains a KFERQ domain (Massey et al., 2004).

Microautophagy describes the process by which the lysosomal membrane invaginates non-selectively and engulfs small quantities of cytoplasm which are then pinched off for digestion within the lumen (Levine and Kroemer, 2008).

Macroautophagy (herein called autophagy unless otherwise indicated) is the major regulated catabolic mechanism that eukaryotic cells use to degrade cytoplasmic constituents and recycle nutrients via double membrane vesicles (Klionsky, 2007; Kundu and Thompson, 2008).
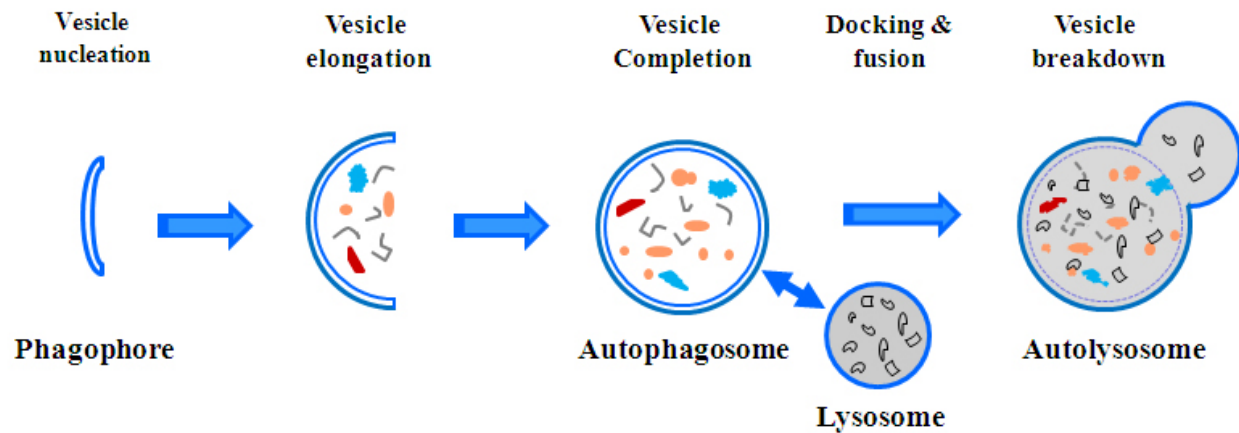
Figure 1.4: The process of autophagy (macroautophagy). The process of autophagy follow stages: Vesicle nucleation (formation of the isolation membrane or phagophore), vesicle elongation and completion (formation of autophagosome), the docking and fusion of autophagosome with lysosome to form autolysosome, lysis of autophagosome inner membrane and contents by lysosomal hydrolases.

Autophagy initiates with the formation of a phagophore. Subsequently, cytoplasmic materials are engulfed by the phagophore and the phagophore membrane is then elongated and finally closes to form an autophagosome, a double-membrane vesicle. This is followed by the fusion between the outer membrane of the autophagosome with the lysosome to form the autolysosome or autophagolysosome, where the engulfed materials and autophagosome inner membrane are degraded (Levine and Kroemer, 2008).

Autophagy is particularly relevant in cellular quality control in neurons, where the amount of cytosolic constituents, altered proteins and damaged organelles cannot be reduced by cell division. (Nixon et al., 2008; Winslow and Rubinsztein, 2008). Autophagic vacuoles are quite scarce in the healthy brain. This raised the suggestion that neuronal autophagy is relatively inactive: However, many studies have proven that basal levels of autophagy in neurons are quite active, leading to fast degradation of autophagosomes (Nixon, 2007). Furthermore, autophagic activity is also essential for normal development of the nervous system. Autophagic degradation of synaptically localized proteins regulates synapse formation (Rowland et al., 2006). In the developed animal, autophagy plays a critical role in neuronal protein homeostasis. This is supported by the finding that a deficiency of basal autophagy in the mouse brain neurons causes neurodegeneration associated with the accumulation of ubiquitinated protein aggregates (Hara et al., 2006; Komatsu et al., 2006).

A critical physiological role of autophagy is to maintain intracellular energy resources to meet cellular and organismal demands. It is rapidly upregulated in cells during nutrient starvation, growth factor withdrawal, or in response to high bioenergetic demands to provide building blocks for important biosynthetic pathways, nutrients and energy (Levine and Kroemer, 2008). Furthermore, autophagy also functions in the elimination of aggregated proteins, defective proteins and organelles, and intracellular pathogens. Thus, it is critical for a protective mechanism against aging, cancer, neurodegenerative diseases, and infection (Levine and Kroemer, 2008).

Autophagy can be a non-selective or selective process. Non-selective, bulk degradation of cytoplasm and organelles by autophagy provides essential materials for metabolism during starvation. Selective autophagy rather involves degradation of protein aggregates and of organelles such as mitochondria (mitophagy), ribosomes (ribophagy), endoplasmic reticulum (reticulophagy), peroxisomes (pexophagy), and lipids (lipophagy). Mechanisms regulating selective autophagy are more elaborate and occur in specific situations. As protein aggregates and organelle-associated proteins are decorated with ubiquitin. One possibility of selective autophagy could be that ubiquitin-conjugated substrates are recognized and bound by p62/sequestosome-1 (SQSTM1) or neighbor of BRCA1 gene 1 (NBR1) receptors, which have LC3-interacting domain and bound to LC3, leading to deliver cargo to autophagosomes (Rabinowitz and White, 2010). Furthermore, proper turnover of p62 by autophagy also prevent spontaneous aggregate formation (Komatsu et al., 2007a).

1.2.2.1. Autophagosome formation

The phagophore membrane has been suggested to derive from the ER (Axe et al., 2008; Hayashi-Nishino et al., 2009; Yla-Anttila et al., 2009). Recently, many studies indicated that initiation of phagophore formation is dependent on ER-mitochondria connections (Hailey et al., 2010; Hamasaki et al., 2013) and the ER is the most plausible candidate to activate autophagosome formation upon nutrient starvation (Lamb et al., 2013). However, contributions from the Golgi, mitochondria or PM are also very important, especially when autophagy is induced by other stimuli (Lamb et al., 2013).

Several important molecular components are involved in the initiation of autophagy, including the autophagy-related protein 1 (Atg1)/unc-51-like kinase (ULK) complex, Beclin 1 (BECN1)/class III phosphatidyl-inositol-3-kinase (PI3K) complex, the two transmembrane proteins (Atg9 and vacuole membrane protein 1 (VMP1)), two ubiquitin-like protein (Atg12 and Atg8/LC3) conjugation systems, and proteins that mediate fusion between autophagosomes and lysosomes (Yang and Klionsky, 2010).

ULK1 and ULK2 are the mammalian orthologs of yeast Atg1. They play a key role in autophagic induction by acting downstream of the mammalian target of rapamycin complex 1 (mTORC1) (Efeyan and Sabatini, 2010) and other regulatory signaling pathways, such as adenosine monophosphate-activated protein kinase (AMPK). When nutrients are abundant, binding of the ULK

with the mTOR inhibits autophagy. In contrast, nutrient starvation dissociates mTORC1 from the complex and trigger autophagosome nucleation and elongation. Activated ULK1 has been shown to phosphorylate vacuolar protein sorting 34 (Vps34), thereby promoting phosphatidylinositol-3-kinase (PI3K) complex activation (Lamb et al., 2013). Once activated and targeted for autophagic initiation, the ULK complex and PI3K complex regulate the formation of phosphatidylinositol-3-phosphate (PI3P), which has been implicated in promoting autophagy and retrograde trafficking from the endosomes to the Golgi (Backer, 2008).

Autophagosome nucleation also requires a complex containing Atg6 (mammalian homolog, BECN1) (Rabinowitz and White, 2010). The so-called BECN1 core complex or the class III PI3K complex includes BECN1, Vps15, Vps34, and likely Ambra1 (Fig. 1.5) (He and Levine, 2010). The complex initiates the allosteric activation of the class III PI3K Vps34 to generate PI3P, which recruits effectors such as the double FYVE domain-containing protein 1 (DFCP1) (Axe et al., 2008) and WD-repeat protein interacting with phosphoinositides (WIPI) family proteins (Polson et al., 2010) to mediate the autophagosome formation. Numerous proteins have been indentified to interact with BECN1 that induce or inhibit autophagy such as: Atg14 (also called Atg14L or Barkor), an autophagic inducer that is essential for PI3K activity; UVRAG (UV radiation resistance-associated gene), which may promote PI3K activity by competing with Atg14 for binding to BECN1, and also promotes autophagosome fusion with the lysosome; Bif-1/endophilin B1, which interacts with BECN1 via UVRAG to positively regulate the PI3K complex; and Rubicon (BECN1 interacting and cysteine-rich protein), which negatively regulates autophagy (Kroemer et al., 2010).
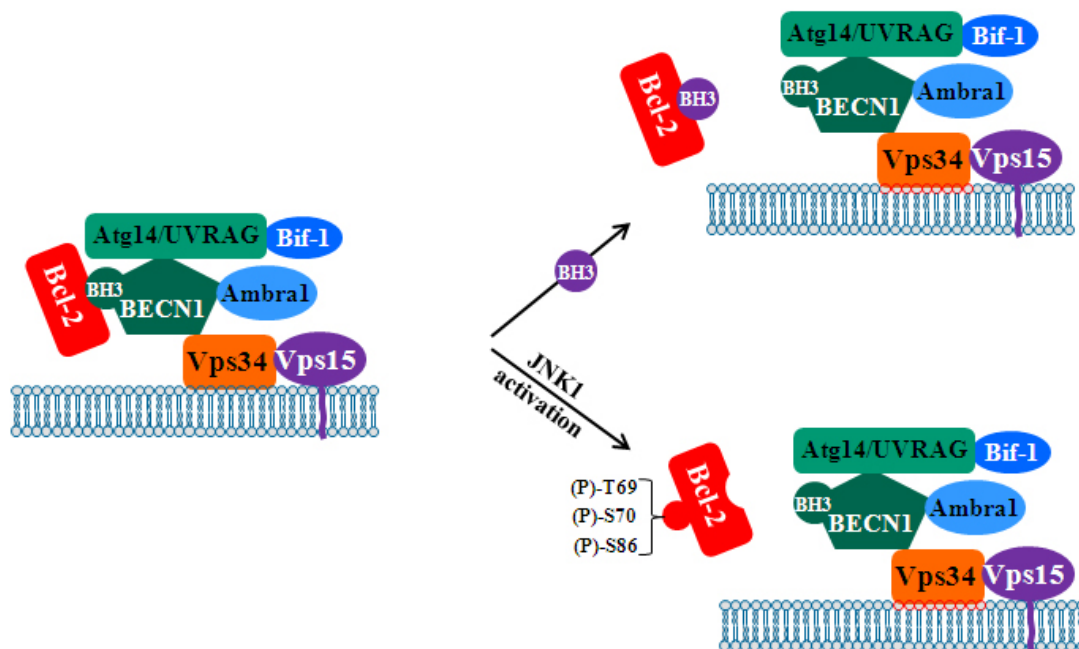
Figure 1.5: The BECN1 core complex and its inhibitory interaction with Bcl-2 homologs in the regulation of autophagy. The so-called BECN1 core complex and its interaction proteins consist of Beclin 1, Vps15, Vps34, either Atg 14 or UVRAG, Ambra1 and Bif-1. The interaction of Bcl-2 homologs with the BH3 domain of BECN1 inhibits the assembly of an autophagy-competent complex (left). Disruption of this inhibitory interaction either by other BH3 domain-containing proteins (upper right) or by JNK1-mediated phosphorylation of Bcl-2 at T69, S70 and S86 (lower right) results in the assembly of an autophagy-competent complex. The lipid kinase activity of the complex then catalyses the conversion of phosphatidylinositol (PI) to PI3P (shown with red circles) mediating the formation of autophagosome. The image was adapted and modified from Sinha et al (Sinha and Levine, 2008).

Furthermore, antiapoptotic family members (such as Bcl-2, Bcl-XL, and Mcl-1) are known to negatively regulate autophagy through an inhibitory interaction with the BH3 domain of BECN1 (Maiuri et al., 2007a; Pattingre et al., 2005). Several mechanisms have been proposed to induce autophagy by disrupting this inhibitory interaction including competitive binding of the BH3 domain of BECN1 by proapoptotic BH3-only proteins (such as BNIP3, Bad, Bik, Noxa, Puma, and BimEL) (Maiuri et al., 2007a), phosphorylation of the BH3 domain by death-associated protein kinase (DAPK) (Zalckvar et al., 2009), or phosphorylation of Bcl-2 by c-Jun N-teminal kinase-1 (JNK1) (Pattingre et al., 2009; Wei et al., 2008).

Atg9 may function in providing lipids to the isolation membrane. This requires Atg1/ULK1, Vps34 and probably Bif-1. Vacuole membrane protein 1 (VMP1), a BECN1 integrator, may function as a transmembrane protein that recruits components of the BECN1 complex to the phagophore (Yang and Klionsky, 2010).

1.2.2.2. Vesicle elongation, completion and membrane retrieval

Expansion and completion of the phagophore membrane to form the autophagosome involves two ubiquitin-like conjugation systems. The first pathway is the covalent conjugation of Atg12 to Atg5, in which the E1-like enzyme Atg7 and the E2-like enzyme Atg10 are involved. This conjugate is associated with Atg16 in a noncovalent linkage to form the Atg12-Atg5-Atg16 complex (Yang and Klionsky, 2010). The second pathway is the lipid conjugation of yeast Atg8/ mammalian LC3 with phosphatidylethanolamine (PE) at a glycine (Gly) residue by the sequential action of Atg4, the E1-like enzyme Atg7, and the E2-like enzyme Atg3. This lipidation leads to the conversion of the soluble cytsolic form of LC3 (named LC3-I) to the membrane associated form LC3-II. LC3-II is stably associated with the autophagosome membrane, and widely used as the major maker to assess autophagy (Yang and Klionsky, 2010). During nucleation, the ATG12–ATG5–ATG16 complex is recruited to the membrane, where it functions as the E3 ligase to mediate the lipidation of LC3. This enables them to associate with the phagophore membrane. Before the closure of the phagophore to form the autophagosome, the membrane-bound ATG proteins are dissociated, except LC3-II. After closure, lipidated LC3 is only bound to the inner layer of the autophagosome (Lamb et al., 2013).
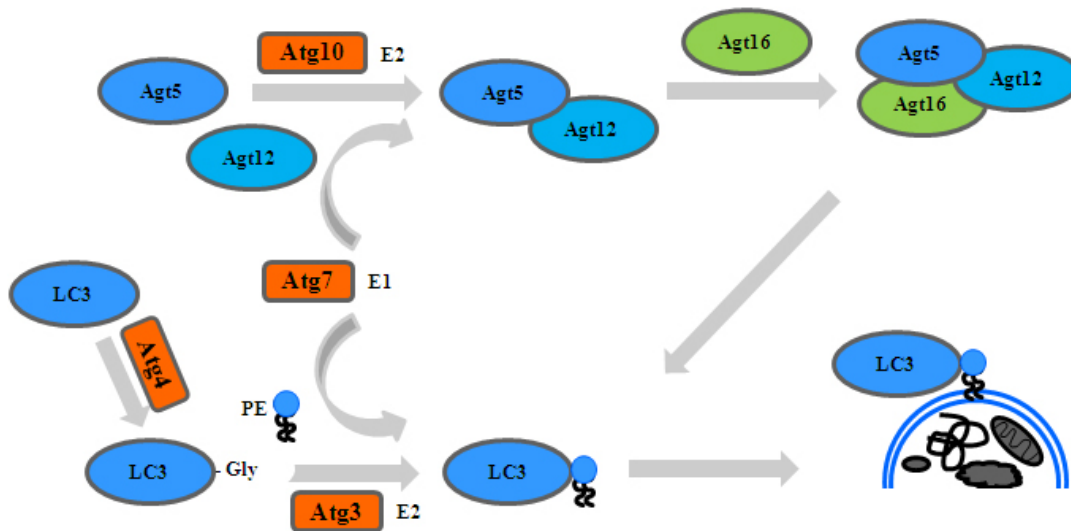
Figure 1.6: The two ubiquitin-like conjugation systems in autophagosome formation. The elongation and shape of the autophagosome are controlled by two conjugation pathways. In the Atg12 pathway. Atg12 is initially conjugated to Atg7 (an E1-activating enzyme) and then transferred to the E2-like conjugating enzyme ATG10, leading to the formation of the Atg12/Atg5 complex through an isopeptide bond. Eventually, the Atg12/Atg5 conjugate associates non-covalently with Atg16. The second pathway involves the conjugation of phosphatidylethanolamine (PE) to LC3/Atg8. Nascent LC3 is first processed by the protease Atg4 to a glycine-exposed form. LC3 is also activated by Atg7 and then transferred to Atg3 (an E2-like enzyme). Finally, LC3 conjugates with PE to form LC3-PE or LC3-II, which is anchored to the autophagosomal membrane. (Adapted from Maiuri et al (Maiuri et al., 2007b)).

The autophagosome is formed when the expanding phagophore membranes fuse. Completed autophagosomes are structures with around 400-900 nm diameters in yeast and 500-1,500 nm in mammalian cells (Stromhaug et al., 1998). This event triggers the Atg4-mediated cleavage of LC-PE to release cleaved LC3, and consequently Atg5/Atg12 and Atg16 complexes from the cytosolic surface of the completed autophagosome. The completed autophagosome is marked by the LC3-PE associated with its internal membrane, which is not accessible to be cleaved by Atg4. Many studies have suggested involvement of microtubules in the transport of the phagophore during expansion and/or maturation (Lang et al., 1998). Additionally, SNAREs [soluble N-ethylmaleimide-sensitive fusion (NSF) attachment protein receptors also play a role in autophagosome formation. Particularly, interaction between either endosomal Q/t-SNARE TIg2, the R/v-SNAREs Sec22 or Ykt6 with Sso1-Sec9 is required for normal Atg9 transport to provide lipids to autophagosome (Nair et al., 2011).

1.2.2.3. Autophagic fusion and degradation

Once the autophagosome is formed, it undergoes progressive maturation and finally fusion with lysosome to form an autolysosome. The lysosome membrane protein Lamp2, the GTP-binding protein Rab7 in humans; and SNARES vesicle-associated membrane protein 3 (VAMP3), VAMP7 and

Vtilb in yeast have been proposed to function in autophagic fusion (He and Klionsky, 2009; Moreau et al., 2013).

After fusion, the inner membrane as well as the luminal content of the autophagic vesicle are degraded by a series of lysosomal hydrolases that function optimally at acidic pH, including proteinases A and B (Epple et al., 2001; Teter et al., 2001); cathepsin B, D, and L (Tanida et al., 2005). Lysosomal permeases release the breakdown products (amino acids, lipids, nucleosides, and carbohydrates) into the cytosol, where they are used for synthetic and metabolic pathways. Atg22 is a putative amino acid efflux pump (Levine and Kroemer, 2008). Thus, autophagy plays an important physiological role in providing sufficient intracellular nutrients for cellular and organismal metabolism (Lum et al., 2005).

1.2.2.4. Regulation of autophagy

Autophagy is stimulated by many different intra- and extra-cellular factors. In response, a series of protein complexes composed of different members of the Atg family coordinate the formation of the autophagosome. The most well known key regulator of autophagy is mTOR. Nutrient starvation and rapamycin stimulate autophagy through inhibition of mTOR (Klionsky et al., 2012; Mizushima, 2007). The same mechanism was also observed with Torin 1 or KU-0063749 (Klionsky et al., 2012). In addition, interaction between Bcl-2/Bcl-XL and the BECN1/class III PI3K complex is also a key target to regulate autophagy.

Many other proteins are involved in regulation of autophagy. For example, the class I PI3K/Akt signaling molecules link receptor tyrosine kinases to mTOR activation in response to growth factor signals (Lum et al., 2005); 5'-AMP-activated protein kinase (AMPK) responds to low energy; the eukaryotic initiation factor 2α (eIF2α) responds to nutrient starvation, and endoplasmic reticulum (ER) stress; BH3-only proteins, death-associated protein kinases (DAPk) and c-Jun-N-terminal kinase disrupt the interaction between Bcl-2/Bcl-XL and the BECN1/class III PI3K complex; and so on (Criollo et al., 2007; Maiuri et al., 2007b; Meijer and Codogno, 2006; Rubinsztein et al., 2007). In addition, many pharmacological compounds target these proteins. Resveratrol activates AMPK, tunicamycin associates with ER stress, thapsingargin inhibits the sarcoplasmic/endoplasmic reticulum Ca^{2+} ATPase (SERCA), ABT-737 disrupts the BECN1/Bcl-2 interaction, or diallyl trisulfide and SP600125 activate and inhibit JNK1 activation, respectively (Bennett et al., 2001; Das et al., 2007; Klionsky et al., 2012; Maiuri et al., 2007a). In contrast, autophagic inhibitors including 3-MA, LY294002 and wortmannin inhibit the PI3K complex (class I as well as class III), and thereby suppress autophagosomal formation (Klionsky et al., 2012).

Moreover, autophagy can also be pharmacologically inhibited by targeting the autophagosome-lysosome fusion with vinblastine or thapsingargin; lysosomal proton pump inhibitor such as bafilomycin A1; lysosomal protease inhibitors such as leupeptin, E-64d, pepstatin A; or

lysosomotropic alkalines such as chloroquine or 3-hydroxychloroquine (Klionsky et al., 2012; Rubinsztein et al., 2007).

Besides the well-characterized phamarcological modulators described above, trehalose, a non-reducing dissacharide containing two D-glucose units, is also known as a mTOR-independent enhancer of autophagy (Sarkar et al., 2007). It has been reported to enhance the clearance of neurodegenerative disease-associated autophagic substrates like huntingtin aggregates, α-synuclein aggregates (Parkinson disease) (Casarejos et al., 2011; Sarkar et al., 2007), tau and phosphorylated-tau (AD) (Casarejos et al., 2011; Schaeffer et al., 2012). Trehalose also counteracted cellular prion infection (Aguib et al., 2009). However, the mechanism by which trehalose induces autophagosomal formation and promotes autolysosomal clearance is not well understood.

1.2.3. Autophagy and Alzheimer's disease

1.2.3.1. Alzheimer's disease-related proteins in the autophagic pathway

Aβ is generated in different cellular compartments such as ER, Golgi, endosomes and autophagic vacuoles (AVs) (Yu et al., 2005; Yu et al., 2004). Notably, autophagy is suggested as a major pathway for turn-over of APP and generation of intracellular Aβ (Li et al., 2010). This is supported by the detection of Aβ together with β- and γ-secretase in autophagic vacuoles (Yu et al., 2005; Yu et al., 2004). Moreover, modulation of autophagy altered Aβ production (Yu et al., 2005), indicating that autophagy is involved in the production of intracellular Aβ.

Autophagosomes can also fuse with the plasma membrane via endosomes leading to the release of the autophagosome-produced intracellular Aβ into extracellular fluids (Nilsson et al., 2013; Nixon, 2007), this demonstrates the involvement of autophagy in the secretion of extracellular Aβ. Thus, autophagy is also a potential pathway that is responsible for the increase of extracellular Aβ levels, which might contribute to extracellular Aβ deposition.

Moreover, various lysosomal proteases are involved in degradation of Aβ. The most extensively investigated and best characterized Aβ degrading protease is Neprilysin (NEP), which is present in endo-lysosomal compartments (Howell et al., 1995; Saido and Leissring, 2012). Particularly, levels of both Aβ40 and Aβ42 are twofold higher in NEP knock-out mice than in wild-type controls (Iwata et al., 2001), suggesting that NEP is an important endogenous regulator of Aβ. Supportively, a cross between the APP transgenic mice and NEP transgenic mouse that expresses eightfold higher levels of NEP resulted in a strong reduction in steady-state Aβ levels and the complete prevention of amyloid plaque formation (Leissring et al., 2003). Insulin-degrading enzyme (IDE) is also an important protease that degrades Aβ. Interestingly, IDE is also a lysosomal protease (Selkoe, 2001). Cathepsin D (Cat D), an aspartyl lysosomal protease that is highly activated in brain, also regulates Aβ levels. Accordingly, Cat D deletion led to a threefold increase of cerebral Aβ42 levels compared

to wild-type littermates, but did not affect Aβ40 levels, which leads to the increase of Aβ42/Aβ40 ratio (Saido and Leissring, 2012).

While numerous studies demonstrated tau as a proteasomal substrate, many lines of evidence revealed that the autophagic-lysosomal system also substantially contributes to the turn-over of tau (Brown et al., 2005; Feuillette et al., 2005). Indeed, modulation of autophagic-lysosomal activity by NH$_4$Cl, chloroquine, 3-methyladenine (3-MA), and cathepsin inhibitors, impaired tau degradation and enhanced the formation of high molecular weight tau species (Hamano et al., 2008; Wang et al., 2010). Additionally, mTOR is reported to regulate tau phosphorylation and degradation. Particularly, inhibition of mTOR by rapamycin ameliorates degradation of insoluble tau associated with autophagy and also protect against its toxicity in Drosophila (Berger et al., 2006; Caccamo et al., 2013).

In summary, tau is actively cleared through the ubiquitine-proteasome system (UPS) when it is in excess and soluble (Rubinsztein, 2006). Alternatively, when tau is monomeric, the UPS might be the more efficient and dominant process for tau degradation. However, aggregates of tau are likely to be inaccessible to the narrow proteasome opening, leading to a much higher dependency on the autophagy for degradation (Lee et al., 2013).

1.2.3.2. Autophagic dysfunction in Alzheimer's disease

As mentioned above, autophagy occurs at basal levels and plays an important role in intracellular protein homeostasis. The demand for basal autophagy differs among tissues; it is particularly important and active in the liver and non-dividing cells such as neurons and myocytes (Hara et al., 2006; Komatsu et al., 2007b; Nakai et al., 2007). Dysfunction in autophagy is implicated in the pathogenesis of many human diseases such as infection, cardial dysfunction, cancer and neurodegeneration (Kundu and Thompson, 2008). Recent studies have been focused on the role of autophagy in metabolism of neurodegeneration-associated misfolded protein aggregates and neuronal cell death (Martinez-Vicente and Cuervo, 2007; Nixon et al., 2008).

Defects of autophagy can occur at different steps and thereby affect cellular homeostasis differently. Failure in induction of autophagy results in accumulation of intracellular components or toxic molecules, including protein aggregates, nonfunctional mitochondria, deformed endoplasmic reticulum and lipid droplets (Hara et al., 2006; Komatsu et al., 2006).

Autophagic failure can also occur from inefficient cargo recognition. In this case, autophagosomes are still formed, but the bulk removal of randomly sequestered soluble components is impaired. Thus, the consequences of the failure are similar to those observed in failure of autopphagy induction (Martinez-Vicente et al., 2010).

Defects in autophagosome clearance has also been linked to a growing number of neurodegenerative disorders, including frontotemporal dementia, amyotrophic lateral sclerosis

(ALS), AD, Parkinson disease (PD), and Huntinton disease (HD) (Jaeger and Wyss-Coray, 2009). The distinctive feature of the affected neurons is an accumulation of autophagic vacuoles. Defects can result from impaired mobilization of autophagosomes towards endosomal-lysosomal compartments, decreased fusion between autophagosomal and endosomal-lysosomal membranes or decreased proteolysis of lysosomal constituents. Accordingly, changes in the properties and functions of microtubules, motor-associated proteins such as dynein, dynactin or tubulin deacetylases have been described to alter autophagy and thereby affect different neurodegenerative disorders. Defective proteolysis can result from changes in the lysosomal lumen such as impaired lysosomal acidification, accumulation of undigested by-products and decreased content or activity of lysosomal hydrolases (Wong and Cuervo, 2010). Recently, a defect in lysosomal acidification has been reported in presenilin deficient cells (Lee et al., 2010).

Dysfunction in autophagy has also been observed in Alzheimer's disease, but the contribution of autophagy to this disease may be more complicated than to other types of neurodegeneration. Autophagy is considered as an active pathway for turning over APP and generating Aβ peptides (Yu et al., 2005; Yu et al., 2004). The maturation of autolysosomes and their transport are impeded in AD, leading to a massive accumulation of autophagic vacuoles and degenerating neuritis. Thus, the defective clearance of Aβ-generating autophagic vacuoles is favorable for Aβ accumulation in AD (Mizushima et al., 2008). Additionally, many studies have indicated that PS1 may be necessary for normal lysosomal turnover of certain proteins (Esselens et al., 2004; Wilson et al., 2004) and that PS1-associated FAD mutations compromise autophagic turnover of proteins (Lee et al., 2010; Nixon, 2007). Thus, the mechanism by which PS mutants contribute to AD development might not only be the direct cleavage of APP to generate Aβ, but also involve altered trafficking of subcellular compartments, lysosomal pH regulation and disruption of other autophagy-dependent processes (Nixon, 2006).

1.3. Human stem cells-derived neurons – based model of Alzheimer's disease

1.3.1. Human pluripotent stem cells

Human pluripotent stem cells (hPSC) can self-renew indefinitely in culture while maintaining the ability to develop any cell type in the human body (Takahashi et al., 2007; Thomson et al., 1998; Yu et al., 2007). Today there are several methods to generate hPSC in cell culture. Embryonic stem cells (ESCs) are derived from the inner cell mass of the early blastocyst stage of embryonic development (Klimanskaya et al., 2006; Thomson et al., 1998). Yamanaka and colleagues successfully reprogrammed adult human fibroblasts into induced pluripotent stem cells (iPSC) via the retrovirus-mediated transfection of pluripotency-related transcription factors including OCT3/4, SOX2, KLF4, and c-MYC (Takahashi et al., 2007). Detailed characterization revealed close similarities between

human iPSC and ESC such as cell morphology, proliferation, gene expression, telomerase activity and other functions (Chin et al., 2010; Hawkins et al., 2010; Lowry et al., 2008). Human iPSC provide the possibility to model diseases by capturing the unique genetic background of the patients as well as using the generated cells for transplantation. They help avoid detrimental effects on histocompatibility or allografts faced by human ESC-based therapies (Faiz and Nagy, 2013).

The use of PSC has severeal advantages as compared to cells models from animal or human tissue in disease modeling. One reason is the genetic difference between humans and animals, which might prevent full recapitulation of human diseases in animal models. In addition, the availability of human tissue from neurodegenerative diseases is limited and represents only the later stages of disease. In contrast, stem cells can be used to model various stages of the disease at a large scale (Khandekar et al., 2012). Furthermore, differentiation of iPSC into disease-relavant cell types provides a potential tool for conducting biopsy-like experiments and assessing pathological development in vitro (Cundiff and Anderson, 2011).

1.3.2. Neuronal differentiation of ES and iPS cells

The ability to differentiate pluripotent stem cells into defined and homogenous cell types in vitro is critical for cell-based research and therapy. Recently, numerous protocols have been developed for deriving neural cell types from PSC, with the hopes of better understanding and alleviating neurodegenerative diseases (Faiz and Nagy, 2013).
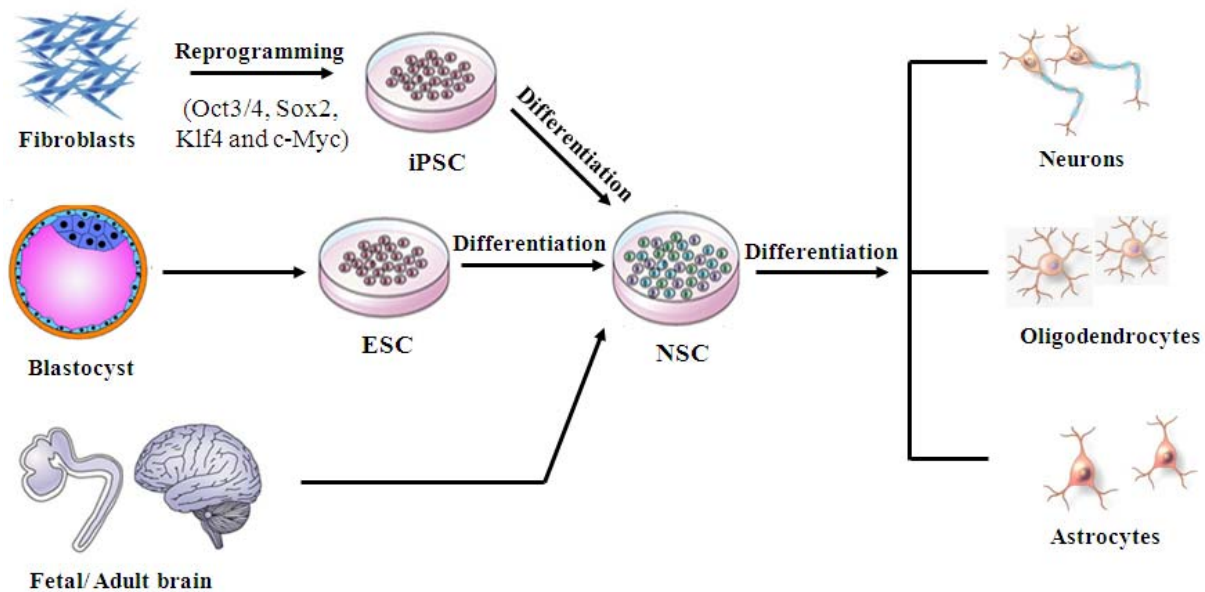
Figure 1.7: Neural stem cells (NSC) and their differentiation into cells in the central nervous system (CNS). NSC can be generated from from iPSC which are reprogrammed from somatic cells, ESC which are isolated from the inner cell mass of blastocysts, and from the fetal and adult brain. NSC can differentiate into CNS cells including neurons, astrocytes and oligodendrocytes. (Adapted from Conti *et al* (Conti and Cattaneo, 2010)).

Neurospheres and monolayer neural stem cell (NSC) lines can be generated from ESC, iPSC or the germinative areas of the fetal and adult brain. They are considered as tripotent cells as they can give rise to neurons, astrocytes and oligodendrocytes of the central nervous system (CNS). While the neurospheres are mixed cellular compositions with a small fraction of NSC cells, the monolayer NSC culture is more homogenous, resulting in higher neurogenic potential (Conti and Cattaneo, 2010). Fetal NSC are ubiquitous in the nervous system and can be isolated from different regions of the murine developing CNS (Conti et al., 2006). Their self-renewing proliferation in cell culture critically depends on FGF2 and EGF (Schultz and Lucas, 2006).

The NSC differentiation from ESC was established in both mouse (Brustle et al., 1997; Conti et al., 2005) and human (Koch et al., 2009; Lee et al., 2007). The ESC differentiation into the neural lineage begins with a "neutralization" process, which has been achieved by various approaches, including culturing embryoid bodies from ESC in the presence of retinoic acid (Bain et al., 1995), co-culturing ESC with stromal cells (Kawasaki et al., 2000; Perrier et al., 2004), and with monolayer culture of ESC to develop into neural precursors in serum- and feeder cell-free conditions in the absence of inhibitory bone morphogenetic protein signaling (Ying et al., 2003). Koch et al described the generation of a pure population of long-term self-renewing human ESC-derived neural stem cells (lt-NES) in a monolayer culture (Koch et al., 2009). In 2012 they published the generation of these lt-NES cells from iPSC. These lt-NES cells can be differentiated into standardized neuronal cultures, primarily GABAergic neurons (Koch et al., 2012). In general, the differentiation into a specific type of neurons can be achieved by the addition/inhibition of specific morphogens. For example, overexpression of the transcription factors Lmx1a and Msx1 led to the differentiation of ESC into dopaminergic neurons (Andersson et al., 2006).

Nowadays, a variety of protocols have been developed to directly differentiate pluripotent stem cells into neurons or somatic cells into NSC. The direct differentiation of ESC into neurons was established for mouse (Okabe et al., 1996) as well as for human ESC (Zhang et al., 2001). For example, mimicking signaling in cortical development, mouse ESC have been differentiated into cortical-specific neurons (Gaspard et al., 2009; Gaspard et al., 2008). Additionally, it has been shown that induction of Brn2, Sox2, and FoxG1 directly converted fibroblasts to induced neural precursor cells at very high efficiency (Lujan et al., 2012).

Moreover, a number of recent studies have shown the direct conversion of fibroblasts to specific neuronal subtypes using sets of neuronal differentiation specific transcription factors. For example, expression of three factors, Ascl1 (Mash1), Brn2, and Mytl, converts mouse embryonic fibroblasts into functional neurons (induced neurons or iNs) (Vierbuchen et al., 2010). However, they represent a heterogeneous population of neurons (glutamatergic and GABAergic). Alternatively, various combinations of different transcription factors have directly generated glutamatergic, dopaminergic or motor neurons from mouse and human fibroblasts (Caiazzo et al., 2011; Kim et al., 2011;

Pfisterer et al., 2011; Qiang et al., 2011; Son et al., 2011). For example, viral cotransduction of a combination between a larger set of forebrain transcription regulators (Brn2, Myt1l, Zic1, Olig2, and Ascl1); and a set of neuronal survival factors including brain-derived neurotrophic factor (BDNF), neurotrophin-3 (NT3), and glial-conditioned media (GCM), generated mainly glutamatergic neurons (Qiang et al., 2011). However, the efficiency of transdifferentiation was very low. Recently, Ladewig and colleagues presented an efficient conversion from postnatal human fibroblasts into functional neurons (mainly GABAergic and glutamatergic neurons) by combining two-factor neuronal reprogramming with small molecule–based inhibition of glycogen synthase kinase-3β and SMAD signaling (Ladewig et al., 2012). One advantage of this direct conversion protocol is to reduce time-consuming and potentially mutagenic iPSC reprogramming process; the disadvantage is that it does not generate a self-renewing, stable progenitor population therefore the obtained cell number is limited (Young and Goldstein, 2012).

1.3.3. Human stem cells - based model of Alzheimer's disease

Investigating the pathogenesis of AD has been restricted to the use of post-mortem human tissue or non-neuronal cell systems of animal models. In fact, the access to biopsies of brain tissues of affected patients is not feasible and the obtained cells do not fully recapitulate in vitro all key events during development of the disease, whereas mouse models for sporadic AD are not available so far (Boissart et al., 2013; Young and Goldstein, 2012). Additionally, the overexpression of AD-related proteins in vertebrate and non-vertebrate models of AD might cause abnormal phenotypes and does not recapitulate all of human AD pathology (Duff and Suleman, 2004). Furthermore, mouse and human neurons are post mitotic cells, which will limit the amount of biological resources needed for molecular mechanism studies and pharmacological screening (Boissart et al., 2013).

With the developed iPSC technology it is possible to investigate the different AD phenotypes by maintaining their endogenous genome and transcriptional control mechanisms (Byers et al., 2012). Recently, iPSC were successfully reprogrammed from skin fibroblasts of sporadic and familial AD patients, and then differentiated into functional neurons. Importantly, these neurons have demonstrated similar biological properties associated with the disease (Israel et al., 2012; Mertens et al., 2013). To test whether differentiated neurons recapitulate AD phenotypes, the Aβ levels have been assessed (Mertens et al., 2013; Qiang et al., 2011).

In addition, new advanced techniques were introduced for direct conversion of fibroblasts from AD patient to functional neurons (Qiang et al., 2011). The success of generating neurons from somatic mature cells of incurable disease patient like AD is a promising approach to recapitulate disease phenotype, study disease mechanisms and drug screening (Young and Goldstein, 2012).

Initial approaches in generating PSC-derived AD models produced several positive findings in neuronal modeling. Firstly, the described FAD mutations did not influence the neuronal

differentiation ability of the parental cell types. Secondly, disease markers like Aβ peptides and especially tau as a neuronal protein could be detected in neurons while they are under detectable levels in fibroblasts and many other cell types. Thirdly, the Aβ levels could be modulated by different pharmacological modulators such as nonsteroidal anti-inflammatory drugs which act as γ-secretase modulators, indicating that this system provides a promising model for screening pharmacological compounds (Young and Goldstein, 2012).

In addition to disease modeling, many studies have shown successful application of NSC in cell-based therapies. For example, transplanted NSC into the hippocampus of aged triple transgenic mice (3xTg-AD) rescued the spatial learning and memory deficits (Qu et al., 2001). Moreover, a coincident increase in axonal outgrowth and synaptic density with high levels of BDNF were also observed, indicating that transplanted NSC-derived BDNF is essential for the cognitive benefits (Blurton-Jones et al., 2009). NSC were also used for differentiation of specific types of neurons that have clinical applicability such as cholinergic neurons, which are especially vulnerable in AD (Kar and Quirion, 2004; Weiss et al., 1994).

Besides transplantation studies with NSC, astrocytes known as supportive cells for neurons, were effective in AD treatment after transplantation (Glat and Offen, 2013). Astrocytes phagocytose cell debris, secrete neurotrophic factors, uptake glutamate, and maintain the balance and regulation of potassium and calcium ions (Lian and Stringer, 2004; Ridet et al., 1997; Schousboe and Waagepetersen, 2005). Engele and coworkers also showed that astrocytes improve neuronal differentiation, maturation, and synapse formation in rodents (Engele et al., 1991). The addition of astrocytes or conditioned media enhanced the in vitro survival of hNSC-derived cholinergic neurons (Jordan et al., 2008). In addition, activated glia was accumulated around Aβ plaques, demonstrating the function in Aβ clearance and supporting the idea of prevention of AD pathology by using glia cells (Haga et al., 1989; Pihlaja et al., 2008).

1.4. Aims of the study

AD is the most common form of neurodegenerative diseases. Many studies have been focused on understanding the mechanisms leading to proteolytic cleavage of APP and amyloid plaque deposition, but less is known about mechanisms that control general intracellular protein metabolism and secretase independent APP metabolism during the pathogenesis of AD. Autophagy plays an important role in intracellular protein quality control, especially of long-lived, misfolded and aggregated proteins (Nixon et al., 2008). Dysfunction of autophagy is implicated in the pathogenesis of AD-associated neurodegeneration (Kundu and Thompson, 2008). Based on these observations, regulation of autophagic activity may affect the metabolism of AD-related proteins and thereby Aβ generation.

Modulation of Amyloid Precursor Protein metabolism by autophagy

γ-Secretase cleavage of APP-CTFβ generates Aβ peptides. Thus, metabolism of APP-CTF is crucial for amyloid plaque deposition. Many studies have implicated the presence of γ-secretase subunits as well as Aβ and APP-CTF in autophagic vesicles (Yu et al., 2005; Yu et al., 2004). As the consequence, autophagy could have an important impact in regulating autophagic degradation of APP-CTF and Aβ peptides. One important aim of this study was to elucidate how modulation of autophagy affects the metabolism of full-length APP, its derivative APP-CTFs. To modulate autophagy, different nutritional (amino acid and growth factor deprivation medium, lipids) and pharmaceutical approaches were applied to target different stages of autophagy. Subsequently, APP metabolism upon autophagic modulation was assessed by molecular cell biological and biochemical methods.

Famillial Alzheimer's disease-associated mutations in presenilin-1 impair autophagy

Besides the well known feature as the catalytic subunit of γ-secretase to cleave APP and increase the generation of the toxic Aβ42 relative to Aβ40 (Shen and Kelleher, 2007), it is unclear how FAD-linked PS mutations affect autophagic activity and intracellular protein metabolism. The second aim of the work was to dissect the role of PS1 mutants in the autophagic process. In particular, the roles of PS1 mutants in regulation of autophagic initiation and flux have been investigated, and the potential contribution to cytopathological processes characteristic for AD. Since autophagy is very important to control intracellular protein metabolism in non-dividing cells like neurons, advanced iPSC- and ESC-derived neuronal models carrying FAD-associated and artificial PS1 mutations have been investigated in comparison to conventional fibroblast models.

2. Materials and Methods

2.1. Materials

2.1.1. Cell lines

Cell	Source
Induced pluripotent stem cells-derived neurons (iPSC-DN)	Prof. Dr. Oliver Brüstle, University of Bonn, Germany (Mertens et al., 2013)
Human embryonic stem cells-derived neurons (hESC-DN). The human ESC were obtained according to regulation of the ethical committee.	Prof. Dr. Oliver Brüstle, University of Bonn, Germany (Koch et al., 2012)
Human neuroglioma H4	ATCC
H4-C99GFP	AG Walter
H4-mCherry-GFP-LC3	AG Walter
MEF-WT and MEF-PS1/PS2 double knock-out (MEF-PSdKO)	Prof. Dr. Bart De Strooper, VIB, Belgium (Nyabi et al., 2002)
NPC1$^{-/-}$ null Chinese hamster ovary (CHO) cells and parental CHO cells	Ruđer Bošković Institute, Croatia

2.1.2. Plasmids

Plasmid	Source
pcDNA3.1/Hygromycin + C99GFP	Gift from Dr. Christoph Kaether, Fritz Lipmann Institute, Germany (Kaether et al., 2006)
pcDNA3.1/Zeocin + PS1WT	AG Walter
pcDNA3.1/Zeocin + PS1D257A	AG Walter
pcDNA3.1/Zeocin + PS1D385N	AG Walter
pcDNA3.1/Zeocin + PS1L166P	AG Walter
pcDNA3.1/Zeocin + PS1A79V	AG Walter
pcDNA3.1/Zeocin + mRFP-LC3	Gift from Dr. Christoph Kaether, Fritz Lipmann Institute, Germany
pBABE-puro mCherry-EGFP-LC3	Gift from Prof. Dr. Jörg Höhfeld, University of Bonn, Germany
pLVX-Tight-Puro	Clontech
pLVX-Tet-ON-Advanced	Clontech
psPAX2	Prof. Dr. Oliver Brüstle, University of Bonn, Germany
pMD2.G	Prof. Dr. Oliver Brüstle, University of Bonn, Germany
pLenti-EF1α-PS1	Prof. Dr. Oliver Brüstle, University of Bonn, Germany
pLVXEP-Lmx1a-Flag	Prof. Dr. Oliver Brüstle, University of Bonn, Germany

2.1.3. Antibiotics

Antibiotic	Source
Ampicilin	Sigma Aldrich
Blasticidin	InvivoGen
Doxycycline	Sigma Aldrich
Hygromycin	Invitrogen
Kanamycin	Sigma Aldrich
G418 (Geneticin)	Invitrogen
Puromycin	InvivoGen
Penicilin-Streptomycin	Invitrogen
Zeocin	InvivoGen

2.1.4. Antibodies

Primary antibodies

Target	Source	WB dilution	IF dilution
β-Actin	Sigma Aldrich	1:5000	-
APP-CT (C1/6.1)	Covance	1:1000	1:1000
APP-NT (5313)	AG Walter	1:1000	1:100
APP-CT (AB140)	AG Walter	1:1000	1:100
Bcl-2	Santa Cruz	1:500	-
p-Bcl-2 (Ser70)	Santa Cruz	1:250	-
BECN1	Cell Signaling	1:1000	-
Cathepsin D (mouse specific)	Gift from Prof. Dr. Stefan Höning, Cologne, Germany	1:500	1:500
Cathepsin D (human specific)	Gift from Prof. Dr. Stefan Höning, Cologne, Germany	1:500	1:500
Lamp2 (mouse specific)	Iowa Hybridoma Bank	1:500	1:250
Lamp2 (human specific)	Iowa Hybridoma Bank	1:500	1:250
LC3	MBL International Corporation	1:1000	-
LC3	Cell Signaling	1:1000	1:500
LC3	NanoTools	-	1:250
p62	Sigma Aldrich	1:2000	1:1000
PS1-CT (3109)	AG Walter	1:500	-
PS1-NT (3111)	AG Walter	1:500	-
β-III-tubulin	Covance	1:3000	1:3000

Secondary antibodies

HRP-coupled		
Species	**Source**	**Dilution**
Anti-goat	Sigma Aldrich	1:25000
Anti-mouse	Sigma Aldrich	1:50000
Anti-rat	Sigma Aldrich	1:50000
Anti-rabbit	Sigma Aldrich	1:50000

Fluorophore-coupled			
Species	**Fluorophore**	**Source**	**Dilution**
Anti-Rabbit	Alexa 488	Invitrogen	1:750
Anti-Mouse	Alexa 488	Invitrogen	1:750
Anti-Rat	Alexa 488	Invitrogen	1:500
Anti-Rabbit	Alex 546	Invitrogen	1:1000
Anti-Mouse	Alex 546	Invitrogen	1:1000
Anti-Mouse	Alexa 350	Invitrogen	1:250
Anti-Goat	Alexa 350	Invitrogen	1:250

2.1.5. RT-PCR primers

Target	Identification	Sequence (5' → 3')
hLC3	Fw	AAGACCTTCAAGCAGCGCC
	Rv	GAGCTGTAAGCGCCTTCTA
mLC3	Fw	AAGACCTTCAAGCAGCGCC
	Rv	GCTGCAAGCGCCGTCTGAT
hGAPDH	Fw	GAAGGTGAAGGTCGGAGTC
	Rv	GAAGATGGTGATGGGATTTC
mGAPDH	Fw	TGCACCACCAACTGCTTA
	Rv	GGATGCAGGGATGATGTTC

2.1.6. Compounds and reagents

Compound and reagent	Source
Bafilomycin	Enzo Life Sciences
BCA Protein Assay Reagent	Thermo Scientific
BSA	Roth
B27 supplement	Invitrogen
Chloroquine	Sigma Aldrich

Complete Protease Inhibitor Cocktail Tablets	Roche
DAPI (4',6-Diamidino-2-phenyindole)	Sigma Aldrich
DAPT	Sigma Aldrich
DMEM high glucose	Invitrogen
DMEM/F12	Invitrogen
DMSO	Sigma Aldrich
DNaseI	Fermentas
DNA ladder (100 bq)	Invitrogen
dNTPs	Fermentas
EBSS	Invitrogen
ECL select (Western blotting detection reagent)	GE Healthcare
FCS	PAN Biotech
Ganglioside mixture	MERCK
Glucose	Sigma Aldrich
HBSS	Invitrogen
HEPES	Invitrogen
Leupeptin	Enzo Life Sciences
[^{35}S] L-methionine/Cysteine	Hartmann Analytic
L-methionine	Applichem
Lysosensor Yellow/Blue DND-160	Invitrogen
Lipofectamine® 2000	Invitrogen
Maltose	Sigma Aldrich
Neurobasal medium	Invitrogen
Neurobasal-A medium	Invitrogen
NucleoBond Xtra Maxiprep kits (or columns)	Macherey-Nagel
NuPAGE 4-12% Bis-Tris electrophoresis gel	Invitrogen
Opti-MEM® Medium	Invitrogen
PageRuler Unstained protein ladder	Thermo Scientific
PageRuler Prestained protein ladder	Thermo Scientific
PhosStop phosphatase inhibitor cocktail tablets	Roche
Poly-L-Lysin	Sigma Aldrich
Rapamycin	Enzo Life Sciences
RNA easy kit	Qiagen
Scintillation cocktail	Hidex
SeeBlue prestained protein ladder	Invitrogen

SDS	Roth
Trehalose	Sigma Aldrich
Tripsin/EDTA	PAN Biotech

2.1.7. Instruments

Blotting chamber	Amersham Pharmacia
Chemiluminescence Imager (ChemiDoc XRS)	Bio-Rad
Cell culture hoods	Thermo Scientifc
Centrifuge	Eppendorf
Cloning cylinders	DUNN Labortechnik
CO_2 incubator 37°C	Binder
Cooling system	Lauda
DNA electrophoresis chamber	Thermo Scientific
Heating block	Stuard Scientific
Hamilton syringe	Hamilton
Liquid scintillation counter	Hidex
Magnetic stirrer	Velp scientifica
Microcentrifuge	Eppendorf
Microscope	Nikon
Microscope (Fluorescence)	Zeiss
Microwave	LG
Nanophotometer	IMPLEN
Nitrocellular membrane	Whatman
NuPAGE® Novex® 4-12% Bis-Tris Gels	Invitrogen
Orbital shaker	Stuart Scientific
Overhead rotor	Scientific Industries
PAGE/blot chamber	Amersham Pharmacia
PAGE/blot power supply	Amersham Pharmacia
PCR cycler	Eppendorf
pH meter	Mettler Toledo
Photoimager	Fuji
Photometer	Thermo Scientific
Micropipette (10, 100 and 1000 µL)	Eppendorf
Pipetteboy	Accu-Jet
PVDF membrane	Whatman
Refrigerator	AEG Electrolux

Spectra Max Gemini	Thermo Fisher Scientific
Thermomixer	Eppendorf
Trans-UV illuminator	Syngene
Ultrasonic bath	MERCK
Vortex Genie	Scientific Industries
Vortex shaker	IKA
Warm incubator	Binder
Water bath	Medigen
Weighing balances	Mettler Toledo
XCell SureLock Electrophoresis cell	Invitrogen
X-ray films	Kodak

2.1.8. Softwares

Program	Manufacturer
ApE - A Plasmid Editor 1.17	M. Wayne Davis
AxioVision 4.8	Zeiss
Excel 2007	Microsoft
Image J 1.44p	NIH
Photoshop 7.0	Adobe
Prism 6.0	Graphpad
Quantity One 4.6.9	Bio-Rad
Word 2007	Microsoft

2.2. Methods

2.2.1. Buffers and solutions

Ammonium persulphate (APS): APS 1 g, H_2O 10 ml. Store at 4^oC

Blocking solution (for ICC): PBS 90%, FCS 10%, Triton X-100 0.1% (optional for intracellular staining)

Blotting buffer: Tris 5 mM, Glycine 200 mM, methanol 10 % for nitrocellulose membrane (or 20 % for PVDF membrane), dH_2O. Store at 4^oC

Chase medium: Basic DMEM medium with 0.3 mg/ml L-methionine

Citrate Buffer: Sodium citrate 150 mM, dH_2O, adjust pH to 6.4 with citric acid

Freezing medium (for cell lines): FCS 90%, DMSO 10%

Ganglioside mixture: GM1 21%, GD1a 40%, GD1b 16%, GT1b 19% and other gangliosides. The mixture was dissolved in H_2O to 5 mg/ml stock, store at -20^oC.

Hypotonic buffer D: Tris HCl 10 mM pH 7.5, NaCl 10 mM, EGTA 0.1 mM, Glycerol 2-Phosphate 25 mM and DTT 1 mM. Store at 4^oC. Protease and phosphatase inhibitors were added prior to use.

Labeling Medium: Stavation medium + 2 µCi/ml [^{35}S] – Methionine/Cysteine label

Laemmli sample buffer (5x): Glycerin 50 % (v/v), SDS 7.5% (w/v), DTT 0.1 M, Bromophenol blue instacking gel buffer 0.025 mg/ml.

Laminin coating solution: Laminin in PBS 1 ug/ml, H_2O

Luria-Bertani (LB) medium: Tryptone 10 g, Yeast extract 5 g, NaCl 5 g, NaOH solution (1 M) 1 ml, H_2O 1000 ml, autoclaved and stored at 4^oC.

LB Agar: Agar 7 g, LB medium 1000 ml, autoclaved and selection antibiotics added (ampicillin 100 µg/ml or kanamycin 50 µg/ml).

Lower-Tris (4x): Tris 1.5 M, SDS 0.4% (w/v), dH_2O, pH 8.8

MES (2-(*N*-morpholino)ethanesulfonic acid) buffer: NaCl 5 mM, KCl 115 mM, $MgSO_4$ 1.3 mM, MES 25mM

Paraformaldehyde (PFA) fixation solution 4%: PFA 40 g, H_2O to 1000 ml, heat to dissolve, filter, pH 7.4. Freeze at -20^oC.

Phosphate Buffered Saline (PBS): NaCl 140 nM, Na_2HPO_4 10 mM, KH_2PO_4 1.75 mM, dH_2O, pH 7.4

PBS-T: PBS, Tween20 0.05 %, pH 7.4

Permibilization solution: Triton X-100 0.1 ml, PBS 100 ml

Poly-L-Lysine coating medium: Poly-L-lysine 100 µg/ml, PBS

Poly-L-ornitine coating medium: Poly-L-ornitine 1.5 µg/ml, H_2O

Radiolabeled amino acids (Hartmann Analytic): [^{35}S] – Methionine (70%)/Cysteine (25%), ~10 mCi/ml, ~370 MBq/ml

RIPA lysis buffer: NaCl 150 mM, Tris pH 8.0 10 mM, NP-40 (Igepal CA-630) 1%, Na-DOC 0.5%, SDS 0.1% and EDTA 5 mM. Store at 4^oC. Protease and phosphatase inhibitors were added prior to use.

SDS running buffer 1x: Tris 25 mM, Glycine 200 mM, SDS 0.1 % (v/v), dH_2O

Sodium deoxycholate (Na-DOC) 2%: Na-DOC 2 g, dH_2O 100 ml

Starvation Medium: DMEM (Gibco #21013) contains 4.5 g/L D-glucose; without L–glutamine, Sodium pyruvate, L-Methionine and L–Cysteine.

Trichloroacetic acid (TCA) 100 %: Prepare 100% (w/v) solution by dissolving 2.2 g of TCA in 1 ml of H_2O. Freshly make prior to use.

Tris Buffered Saline-Tween 20 (TBS-T): Tris 10 mM, NaCl 150 mM, Tween20 0.1%, dH_2O, pH 7.5

Upper-Tris (4x): Tris 500 mM, SDS 0.4% (w/v), dH_2O, pH 6.8

2.2.2. Molecular biological techniques

2.2.2.1. Transformation of bacteria and storage

Transformation of E. coli (DH5α) competent cells was performed according to the manufacturer's instructions (Invitrogen). Briefly, 1-10 ng of plasmid were mixed with 50 µl of competent *E.coli* DH5α and incubated on ice for 30 min. The bacteria were subjected to a heat shock at 42°C for 1 min and subsequently put back on ice for 2 min. The cells were then added to 950 µl warm (37°C) LB-medium and incubated in thermomixer at 37°C with shaking at 225 rpm for 1 h. The suspension was then centrifuged at 13,200 rpm for 1 min to collect the pellet, which was re-suspended in 100 µl of LB medium and then streaked on an LB-plate. After overnight incubation at 37°C, colonies were picked, transferred to 2 ml LB medium and incubated at 37°C. Next morning, the bacterial cultures were transferred to 100-300 ml of fresh LB medium for a large-scale culture to harvest DNA. LB-plates and medium for bacterial culture always contained the respective selection antibiotics.

For cryoconservation, 0.8 ml of bacterial culture were mixed with 0.4 ml conservation medium (70% glycerol) in a safe-lock tube. The mixture was gently inverted and frozen at -80°C. For re-use of frozen transformed bacteria, the cells were picked up from frozen stock and subcultured in 3-5 ml of LB medium containing selection antibiotic. The cell suspension was incubated at 37°C overnight in a thermomixer with 225 rpm shaking.

2.2.2.2. Extraction of DNA from transformed bacteria

DNA plasmids were extracted either on larger scale by using the QIAGEN Plasmid Maxi Kit (QIAGEN) or on small scale by using the PureYield™ Plasmid Miniprep System (Promega). The extractions were performed as described in the manufacturers' instructions. DNA concentration was measured by Nanophotometer at 260 nm according to the manufacturer's instructions.

2.2.2.3. Semi-quantitative reverse transcriptase PCR analysis (RT-PCR)

Total RNA was purified with Quiagen RNeasy kit and reversely transcribed into cDNAs (Biorad iScript cDNA synthesis kit). PCR reactions were performed with Taq DNA Polymerase (Invitrogen) and loading control was assessed via GAPDH mRNA expression levels. Primers are listed in 2.1.5 section. PCR products were separated by agarose gel electrophoresis in TAE buffer.

2.2.2.4. Quantitative RT-PCR analysis (qRT-PCR)

For quantitative analysis, RNAs were incubated with Quiagen QuantiTect SYBR$^{®}$ Green PCR Kits for two-step RT-PCR. Quantitative RT-PCR was performed in triplicates on a Biorad-iCycler using the SYBR-green detection method. Data were normalized to GAPDH and Actin mRNA levels. Analysis used the CtDD method.

2.2.3. Cell biological techniques

2.2.3.1. Cell culture

Medium for H4 cells and mouse embryonic fibroblasts (MEF)

DMEM High Glucose containing 2 mM L-glutamine, 10% heat inactivated FCS, 50 U/ml penicillin and 50 μg/ml streptomycin. FCS was inactivated by heating at 57°C for 30 min.

MEF expressing PS1 variants were selected and kept with respective antibiotics.

Medium for CHO and NPC1$^{-/-}$ cells

DMEM/F12 medium containing 2 mM L-glutamine, 0.5 mM Na-pyruvate, 10% FCS, 50 U/ml penicillin and 50 μg/ml streptomycin.

2.2.3.2. In vitro differentiation of human pluripotent stem cells into neuronal cultures

Neuronal cultures were generated in the lab of Prof. Dr. Oliver Brüstle, Institute of Reconstructive Neurobiology, University of Bonn.

To investigate effects of FAD-associated PS1 mutants on autophagy in human neurons, mature neuronal cultures differentiated from human pluripotent stem cells (hPSC)-derived homogenous neural stem cells were used. The protocol for neuronal differentiation was described previously (Mertens et al., 2013). Briefly, fibroblasts from an AD patient carrying the endogenous FAD-linked PS1 A79V mutant (named as AD-1 in (Mertens et al., 2013)), and from two healthy control donors (named as Ctrl-1 and Ctrl-2 in (Mertens et al., 2013)) were reprogrammed into induced pluripotent stem cells (iPSC) and then differentiated into homogenous long-term self-renewing rosette-type neural stem cells (lt-NSC), which were eventually differentiated into mature human neuronal cultures according to the established protocols (Falk et al., 2012; Koch et al., 2009b). Besides the neurons carrying endogenous PS1 mutant derived from iPSC, the studies also used neurons overexpressing human PS1 variants derived from human embryonic stem cells (hESC). Initially, Lt-NES were originally differentiated from human ESC line I3 by using the same differentiation protocol with iPSC (Koch et al., 2009b). Subsequetly, the lt-NES were lentivirally transduced with PS1 wild-type (PS1WT); catalytically inactive variant D385N (PS1DN); and FAD-associated PS1 mutants PS1 L166P (PS1LP) and PS1 A79V (PS1AV). Eventually, PS1-transgenic lt-NSC were further harnessed to generate differentiated neurons (Koch et al., 2012). For autophagy studies, neurons derived from lt-NES were allowed to mature in culture for 4 weeks.

2.2.3.3. Lipid supplementation and autophagic modulation

Cells were treated with media containing GSLs and autophagic modulators. Control cells were treated with media containing the respective solvents. Treatment conditions were as follows: gangliosides 50 ng/ml for 48 h; bafilomycin A1 50 nM for 12 h; chloroquine 50 μM for 12 h;

leupeptin 20 µM for 24 h; rapamycin 10 µg/ml for 24 h; trehalose 100 mM for 24, 48 and 96h; maltose 100 mM for 24.

For starvation, cells were properly washed with PBS to remove remaining serum and subsequently add either EBSS or Neurobasal-A medium to MEF or neurons, respectively.

2.2.3.4. Cell transfection and transduction

2.2.3.4.1. Transfection and generation of stably expressing cell clones

Cell transfection was done with Lipofectamine 2000 reagent according to manufactures' instructions (Invitrogen). Briefly, transfection was performed when cells were grown approximately 80% confluence. DNA and Lipofectamine were separately mixed with Opti-MEM in two tubes and incubated for 5 min at room temperature (RT). After that, the content of the two tubes was mixed and incubated for 15-20 min at RT. Eventually, the mixture was added in cell dishes containing Opti-MEM medium. The transfected medium was changed to normal DMEM medium after 4-5 h transfection and the cells were incubated for another 24 h at 37°C and 5% CO_2.

For single-cell cloning: 24 h after transfection, cells were split at dilutions of 1:500, 1:250, 1:100, 1:50 and 1:10 in 10 cm dishes. Subsequently, they were cultured in the selection medium containing the respective antibiotic for 2-3 weeks. After 2-3 weeks of antibiotic selection, cell colonies were grown up to 5-10 mm in diameter. Dishes were washed with PBS and and clones were isolated with plastic cloning cylinders. Colonies were trypsinised and transferred to 96-well plate and then expanded to bigger plates. To confirm the expression of transfected protein, colonies were screened by microscopic fluorescence, western blot or RT-PCR.

For pooled colony cultures: 24 h after transfection cells were cultured in selection medium for 2-3 weeks. Colonies were trypsinized, pooled and then cultured under constant presence of the respective antibiotics. The expression of desired protein in growing cells was confirmed by microscopic fluorescence, western blot or RT-PCR.

2.2.3.4.2. Transduction of cells with lentivirus

Production of lentiviral particles was performed as described previously (Koch et al., 2012). Briefly, HEK-293FT cells were co-transfected with the packaging plasmid psPAX2, the envelop plasmid pMD2.G and the respective lentiviral vector plasmid. Viral particles were enriched by centrifugation and used to transduce into human ESC-derived lt-NSC.

2.2.3.5. Lysosomal pH measurement

Lysosomal pH was determined by using Dextran conjugated Lysosensor Yellow/Blue DND-160. Cells were grown to approximately 80-90% confluency. Cells were then trypsinized, loaded (1x10^6 cells/ml) with 2 µl of 0.05 mg/ml Lysosensor-Dextran and incubated at 37°C with 5% CO_2 for 1 h. Subsequently, cells were washed three times in Hank's Balanced Salt Solution (HBSS) and aliquoted

with each 100 µl into a Greiner Black 96-well plate. The standard curve was generated by incubating cells in 10 µM monensin and 10 µM nigericin in MES buffer (5 mm NaCl, 115 mm KCL, 1.3 mm MgSO4, 25 mm MES), with the pH adjusted to within the range 3.0–8.0 for 7–10 min prior to lysosensor addition. Samples were read in a Spectra Max GEMINI with excitation at 355 nm and emission at 440 nm, and ratios of emission 440/355 nm calculated for each sample. The pH values were determined from the linear standard curve generated via the pH calibration samples.

2.2.3.6. Immunocytochemsitry

Neurons and other cell lines were cultured in polyornithin/laminin-coated plastic dishes and poly-L-lysine–coated coverslips, respectively. After fixation with 4% PFA for 20 min, cells were blocked with blocking solution at RT for 1 h. Subsequently, cells were incubated with primary antibodies at 4°C overnight or at RT for 1-2 h, and then with secondary antibodies for 1 h at RT. The details of the protocol were previously described (Koch et al., 2012; Tamboli et al., 2011a). Cells were imaged with Carl Zeiss Axio Imaging 2 ApoTome Fluorescence Microscope for optical sectioning. Signal intensity and co-localization was analyzed by using AxioVision software in randomly selected images.

2.2.4. Biochemical methods

2.2.4.1. Cell lysis, cell fractionation and isolation of membranes

Total cell lysates were obtained by lysing cells in RIPA buffer supplemented with 1% protease and phosphatase inhibitors for 15 minutes and then centrifuged at 13,200 rpm for 15 minutes to get the supernatant.

For cell fractionation and isolation of membranes, cells were resuspended in hypotonic buffer D supplemented with 1% protease and phosphatase inhibitors on ice for 10 minutes. Cells were then homogenized by using 21 gauche needles and centrifuged at 1000 rpm for 10 minutes to get nuclear pellets. The supernatant was further centrifuged at 13,200 rpm for 30 minutes to obtain the cytosolic fraction in the supernatant and the membrane fraction in the pellet.

2.2.4.2. Estimation of protein concentration

Extracted proteins were measured by BCA Protein Assay Kit according to manufacturer's instructions. Briefly, standard BSA protein was diluted to different concentrations for the generation of a standard curve. Protein standards and samples were pipetted into 96-well plate and then the mixture of the kit reagents was added. After incubation for 30 min at 37°C, protein concentration was measured by the absorption at 562 nm and calculated according to the standard curve.

2.2.4.3. Sodium dodecyl sulfate polyacrylamide gel electrophoresis (SDS-PAGE)

Depending on molecular weight of desired proteins, proper gels were chosen for protein separation according to the recipe in the table 2.1. Separation gel was firstly casted in 1.5 mm gel caster. When it was polymerized, stacking gel was casted on top. Protein samples were prepared by mixing 20-30 µg cellular protein lysates with 5x Laemmli sample buffer and boiled at 95°C for 5 min. After stacking gel was polymerized, 20-30 µg proteins were loaded in the gel pockets. PageRuler™ unstained or prestained protein ladder was loaded on the gel for the protein markers. Electrophoresis was performed in SDS running buffer at 25-30 mA/gel and maximum voltage.

Table 2.1: Composition of the SDS-PAGE gels

	Separation gel			Stacking gel
	12 %	10 %	7 %	4 %
dH$_2$O	7 ml	8.3 ml	10.3 ml	6.2 ml
Acrylamide/Bisacrylamide	8 ml	6.7 ml	4.7 ml	1.3 ml
Lower-Tris	5 ml	5 ml	5 ml	-
Upper-Tris	-	-	-	2.5 ml
APS	50 µl	50 µl	50 µl	25 µl
TEMED (Roth)	50 µl	50 µl	50 µl	25 µl
Total	20 ml	20 ml	20 ml	10 ml

For Urea SDS-PAGE stacking and separation gels**:** H$_2$O was replaced by Urea 8 M for the recipe in the table 2.1.

Alternatively, pre-casted gradient 4-12% Bis-Tris polyacrylamide gels were also used to get better separation for proteins from small- to medium-sized. Electrophoresis was performed according to the instructions from manufacturer.

2.2.4.4. Western-Immunobloting

After separation by gel electrophoresis, proteins were transferred to nitrocellulose or PVDF membrane. Blotting was performed at 120 V, 400 mA for 2 h in cooled blotting buffer. Membranes were blocked in 5% non-fat milk in TBS-T for 1 h to reduce unspecific antibody binding. The blocked membrane was then incubated with primary antibody in TBS-T solution either at 4°C overnight or at RT for 1-2 h. Subsequently, membranes were washed three times with TBS-T and incubated with respective HRP-conjugated secondary antibodies for 1 h. After washing three times with TBS-T, membranes were sprayed with enhanced chemiluminescence (ECL) substrate to detect proteins by emitted signal in chemiluminescence imager.

2.2.4.5. Metabolic radiolabeling and autoradiography

For metabolic labeling, cells were starved in serum-free, methionine/cysteine-free medium for 1 h and then pulse-labeled with 2 μCi/ml [^{35}S]-methionine/cysteine (hereafter called [^{35}S]-methionine) for 1 h at 37^{0}C. Cells were then washed 3 times with PBS and chased in normal culture medium supplemented 10% FCS and 0.3 mg/ml unlabeled methionine for the time periods indicated in the respective experiments. Subsequently, cells were washed with cold PBS and lysed with RIPA buffer supplemented with 1% phosphatase protease inhibitors on ice for 10 minutes. Lysates were collected by centrifugation at 13,200 rpm for 30 minutes and subsequently loaded equally on 4-12% Bis-Tris gel for separation. Proteins were eventually transferred to nitrocellulose membrane, dried and exposed to X-ray film for autoradiography. Quantitative analyses were performed by densitometry using the Quantity One software package.

2.2.4.6. Scintillation counting

After radiolabeling with [^{35}S]-methionine, cells were lysed with RIPA lysis buffer. Lysates were cleared by centrifugation and proteins in the supernatant were precipitated with trichloroacetic acid (TCA) as mentioned in 2.2.4.7. After sedimentation of precipitates by centrifugation at 13,200 rpm for 30 minutes, pellets were collected and dissolved in 20 μL buffer containing 1% SDS and 50 mM Tris supplemented with 1 μL Tris 1 M. Subsequently, the suspension was mixed with the scintillation cocktail and the measurement was performed according to instructions from the counter's manufacturer.

2.2.4.7. Protein precipitation by Trichloro acetic acid

Cleared protein lysates (400 μl) were mixed with 2% Na-DOC (0.02 % final concentration). The mixture was kept on ice for 15 min. Subsequently 100% TCA (10% final concentration) was added and samples kept at RT for 30 min. Precipitated proteins were collected by centrifugation at 13,200 rpm at 4°C for 30 min. Pellets were washed with cold acetone twice. Finally, pellets were dried in air and re-suspended in 20 μL buffer containing 1% SDS and 50 mM Tris supplemented with 1 μL Tris 1 M. If the mixture turned to yellow color due to residual TCA, solution was titrated with 1 N NaOH or 1M Tris HCl pH 8.5 until samples turned blue.

2.2.4.8. In vitro assay of γ-secretase activity

Cells were lysed in hypotonic buffer D and membrane isolated as described under 2.2.4.1. The membrane pellet was then re-suspended in Citrate buffer supplemented with 1% protease/phosphatase inhibitors and incubated in the absence or presence of γ-secretase modulators at 37$^{°}$C for 2 h as indicated in the respective experiments. Samples were centrifuged at 13,200 rpm for 1 h, the pellet and supernatant were separated by SDS-PAGE. Proteins were detected by Western-immunoblotting.

2.2.4.9. Aβ measurement

Secretion of Aβ peptides in conditioned medium and cell lysates were quantified by a sandwich immunoassay using the Meso Scale Discovery Sector Imager 2400 (Meso Scale Discovery Sector, Gaithersburg, MD) as previously described (Tamboli et al., 2011a). The concentrations of Aβ peptides were normalized to total cellular protein concentration of corresponding cell pellets.

2.2.5. Statistical analysis

ECL signals of immunoblotting were measured and analyzed by chemiluminescence imaging and Quantity One software package. Statistical analyses were carried out by calculation of standard deviation (SD) or standard error of the mean (SEM) and Student's t test. Significance is indicated by asterisks as follows: * for $p<0.05$, ** for $p<0.01$, *** for $p<0.001$ and NS: non-significant.

3. Results

3.1. Modulation of autophagic and lysosomal APP metabolism

First, the metabolism of APP was characterized under different nutritional conditions (lipid storage and amino acid deprivation) and pharmacological modulation of autophagy. These results are parts of one manuscript in preparation and two published papers (Tamboli et al., 2011a; Tamboli et al., 2011b).

3.1.1. Lipid accumulation impairs degradation of APP-CTFs

Lysosomal capacity or autophagy has been shown to be impaired in certain lysosomal storage diseases (LSDs) (Settembre et al., 2008b; Takamura et al., 2008), which are caused by accumulation of membrane lipids such as cholesterol, sphingolipids (SLs) and glyosphingolipids (GSLs) (Settembre et al., 2008a). Several LSDs share pathological similarities with AD (Auer et al., 1995; Jeyakumar et al., 2003; Rojo et al., 2008) and have an impact on the metabolism of APP (van Echten-Deckert and Walter, 2012; Walter and van Echten-Deckert, 2013). Thus, LSDs-regulated autophagy might play an important role in the metabolism of APP.

In order to investigate the involvement of membrane lipids in APP metabolism, APP expression levels were assessed upon an addition of different lipids. To partly recapitulate LSDs in vitro, H4 neuroglioma cells were incubated without (Ctr) or with 50 ng/µl GSLs purified bovine brain gangliosides for 48 h. The study initially analyzed autophagy via changes in the amount of autophagosomes as measured by the metabolism of the microtubule-associated protein 1 light chain 3/MAP1LC3LC3 (shortly LC3). As described in the introduction, LC3 is a widely used marker for autophagosomes as it is converted from a cytosolic form (LC3-I) to a phosphatidylethanolamine-conjugated form (LC3-II) and recruited to the autophagosomal membrane during autophagosomal synthesis (Yang and Klionsky, 2010). The treatment with GSLs did not alter levels of LC3-I, but significantly increased LC3-II levels (Fig. 3.1 A), leading to elevated LC3-II/LC3-I ratio (Fig. 3.1 B). However, because autophagy is a dynamic process, the increase of LC3-II/LC3-I ratio could be due to enhanced autophagosomal synthesis (conversion from LC3-I to LC3-II) or/and decreased autophagosomal clearance (LC3-II degradation). Importantly, while APP-full length (APP-FL) levels were unchanged, APP-C terminal fragments (APP-CTFs) levels were strongly elevated in GSLs-treated cells as compared to controls (Fig. 3.1 A), resulting in a significant increase of APP-CTFs/APP-FL ratio, which indicates a selective accumulation of APP-CTFs (Fig. 3.1 C). Therefore, it was assumed that APP-CTF accumulation in GSLs-treated cells is caused by impairment of autophagic pathway.
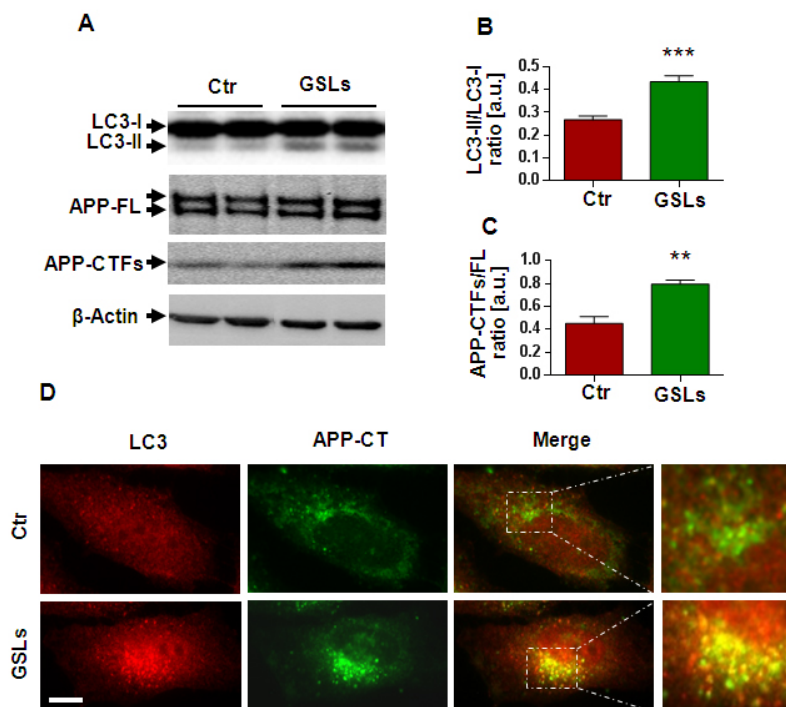
Figure 3.1: Accumulation of APP and its derivatives APP-CTFs upon cell treatment with glycosphingolipids. A, H4 cells were incubated in the absence (Ctr) or presence of 50 ng/ml glycosphingolipids (GSLs) for 48 h. After lysis in RIPA buffer, cell lysates were separated by SDS-PAGE and proteins were transferred to nitrocellulose membranes. The indicated proteins were detected by immunoblotting and visualized by ECL imaging. β-Actin was used as loading control. B-C, Quantification of the indicated proteins was done by densitometry. The graphs show the ratios of LC3-II/LC3-I (B) and APP-CTFs/APP-FL (C). Values are means of three independent experiments (n=6) ± S.D. D, Immunocytochemistry of LC3 and APP in H4 cells. After incubation with or without GSLs (see A), cells were fixed and co-stained with primary antibodies against LC3 and the C-terminus of APP (C1/6.1). Primary antibodies were detected with Alexa Flour 546- and Alexa Flour 488-conjugated secondary antibodies, respectively. Scale bar represents 10 µm.

To test this hypothesis, the subcellular localization and expression levels of LC3 and APP were analyzed by fluorescence microscopy. H4 cells were incubated in the presence or absence of 50 ng/µl GSLs for 48 h and stained with LC3 and APP-CTF antibodies. Double-immunofluorescence labeling with LC3 and APP-CTF antibodies revealed the accumulation of APP in LC3-positive vesicles in GSLs-treated as compared to control cells (Fig. 3.1 D). Since autophagy is defective in LSDs (Pacheco and Lieberman, 2008; Settembre et al., 2008b; Takamura et al., 2008), these findings suggest that dysfunction of GSLs-regulated autophagy causes APP-CTF accumulation in autophagic vesicles.
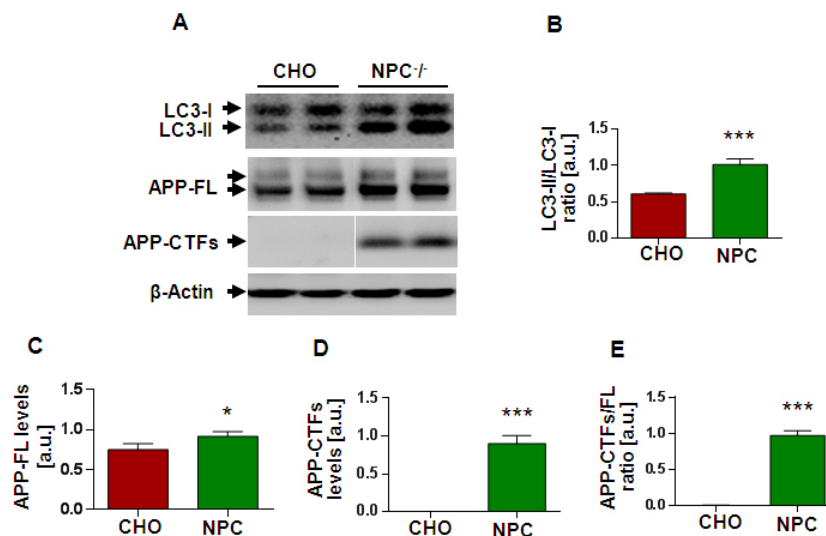
Figure 3.2: Accumulation of APP-FL and APP-CTFs in a genetic model of lipid storage disease. A, Western immunoblot of LC3 and APP in lysates of NPC1^{-/-} null CHO cells and parental CHO wild-type cells. B-E, Densitometric quantification of (A) by ECL imaging. The graphs show LC3-II/LC3-I ratio (B), APP-FL levels (C), APP-CTF levels (D) and APP-CTFs/APP-FL ratio (E). Values are means of two independent experiments (n=6) ± S.D.

Niemann-Pick type C (NPC) disease is a fatal autosomal recessive neurodegenerative disorder, characterized by abnormal accumulation of cholesterol and GSLs in the liver, spleen, and central nervous system (Bauer et al., 2013; Karten et al., 2009). Therefore, a cell model of NPC (NPC1^{-/-} null CHO cells) was used to assess effects of lipid storage on APP metabolism. LC3-I levels were similar in NPC1^{-/-} and CHO cells, whereas LC3-II levels were strongly increased in NPC1^{-/-} cells (Fig. 3.2 A), resulting in an increased ratio of LC3-II/LC3-I (Fig. 3.2 B). Interestingly, while WT cells showed predominantly APP-FL and very low APP-CTF levels, NPC1^{-/-} cells had a slight increase in APP-FL levels (Fig. 3.2 A, C), and a marked increase in APP-CTF levels (Fig. 3.2 A, D), resulting in an elevated APP-CTFs/APP-FL ratio (Fig. 3.2 E). Thus, the data from the effects of GSL supplementation on APP metabolism (Fig. 1) were recapitulated in the genetic lipid storage NPC1^{-/-} cell model, indicating impaired autophagic degradation of APP-CTFs under lipid storage conditions.

3.1.2. Regulation of APP-CTF accumulation by autophagic modulation

To further confirm that APP-CTFs are degraded during autophagy, this pathway was modulated by targeting different stages of the process. The amino acid and growth factor deprived medium Earle's Balanced Salt Solution (EBSS) is known to activate autophagic initiation by suppression of the mammalian target of rapamycin (mTOR) complex actitivity, and enhances lysosomal activity (Zhou et al., 2013). Accordingly, H4 cells were subjected to EBSS medium for 0, 0.25, 0.5, 1 and 6 h. Starvation from 0 to 1 h increased the LC3-II/LC3-I ratio, which might suggest an enhanced conversion from LC3-I to LC3-II at early stages of starvation-induced autophagy or that the rate of autophagosomal synthesis is higher than the autophagosomal clearance after 1 h starvation. In

contrast, starvation from 1 to 6 h decreased the LC3-II/LC3-I ratio, suggesting an elevated autophagosomal clearance as compared to the sysnthesis (Fig. 3.3 A, B). Interestingly, the APP-CTFs/APP-FL ratio was unchanged after 0.25 h and then decreased in time dependent manner during EBSS-induced starvation (Fig. 3.3 C). Thus, these data demonstrate that APP-CTFs undergo starvation-induced autophagic degradation.
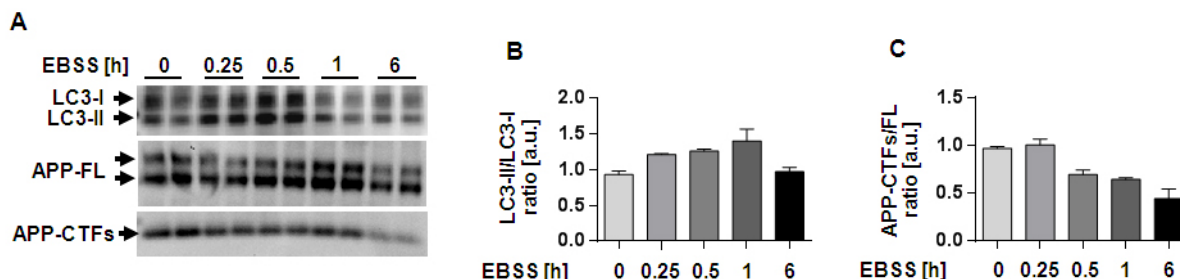
Figure 3.3: Starvation-induced autophagy affects APP metabolism. A, Western immunoblot of LC3 and APP after incubation of H4 cells in EBSS medium for the indicated time periods. B-C, Densitometric quantification of the LC3 and APP levels. The graphs show the ratios of LC3-II/LC3-I (B) and APP-CTFs/APP-FL (C). Bar graphs show means of two values from the blot (A) ± S.D.

By extension, autophagic degradation of APP-CTFs was also investigated in inhibition of lysosomal activity. H4 cells were treated with different lysosomal inhibitors including 20 µM leupeptin for 24 h, 50 nM bafilomycin A1 (Bafi) for 12 h, or 50 µM chloroquine (Chlo) for 12 h. Leupeptin is an inhibitor of cysteine, serine and threonine proteases thereby blocking lysosomal protein degradation (Klionsky et al., 2012). Bafilomycin A1 is a specific inhibitor of the vacuolar-type H(+)-ATPase, which inhibits acidification and therefore protein degradation in lysosomes (Yoshimori et al., 1991). Chloroquine is a lysosomotropic compound that elevates/neutralizes the lysosomal/vacuolar pH (Klionsky et al., 2012). The inhibition of lysosomal function was firstly assessed by the processing of Cathepsin D (Cat D), which is an abundant aspartic endopeptidase, and plays major role in protein proteolysis in lysosomes (Benes et al., 2008; Metcalf and Fusek, 1993). Importantly, Cat D processing is affected by lysosomal acidity and cysteine proteases (Gieselmann et al., 1985). As expected, treatment with leupeptin, bafilomycin and chloroquine increased the levels of full-length Cat D (Cat D-FL) (precursor and intermediate forms) and markedly reduced the levels of the mature or active form of Cat D (Cat D-active) as compared to control (Fig. 3.4 A), leading to a decrease of the Cat D-active/Cat D-FL ratio (Fig. 3.4 B) or an impairment of Cat D processing. Thus, the data confirm of the inhibition of lysosomal acidification by bafilomycin and chloroquine treatments; and cysteine protease activity by leupeptin treatment.

In addition, the treatment with these lysosomal inhibitors slightly changed the LC3-I levels, but markedly increased the LC3-II levels as compared control (Fig. 3.4 A), resulting in an increase of the LC3-II/LC3-I ratio (Fig. 3.4 C). Collectively, the data confirm inhibited autophagic degradation upon these lysosomal inhibitors. Importantly, the tested lysosomal inhibitors also increased the APP-CTF

levels (Fig. 3.4 A, D), demonstrating an increased APP-CTF accumulation upon the inhibition of autophagic-lysosomal clearance.

All together, the present data indicate that APP-CTFs are substrates for autophagic-lysosomal degradation.
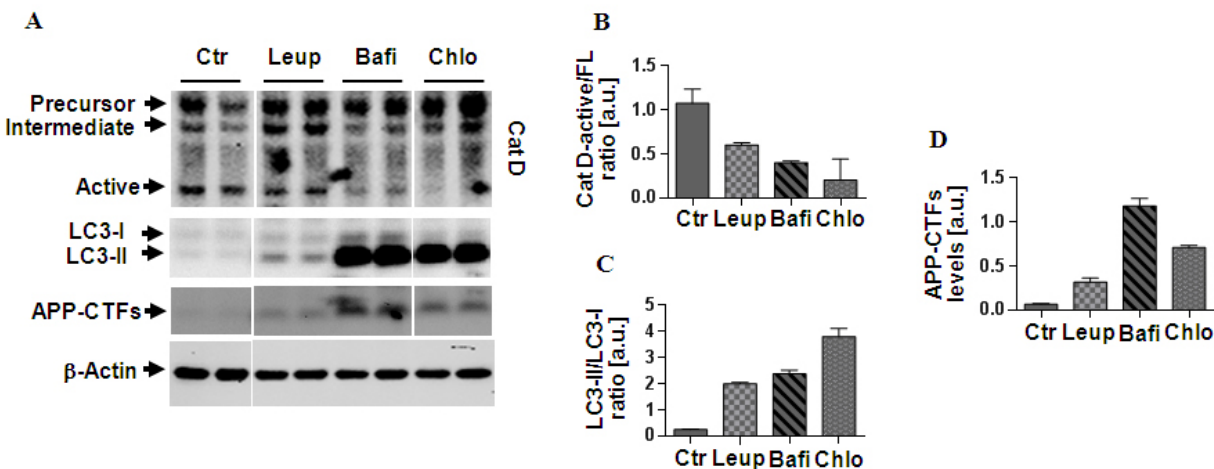
Figure 3.4: Inhibition of lysosomal activity affects APP metabolism. A, Western blot of Cathepsin D (Cat D), LC3, and APP in H4 cells after treatment with 20 µM leupeptin (Leup) for 24 h, 50 nM bafilomycin A1 (Bafi) for 12 h, or 50 µM chloroquine (Chlo) for 12 h. B-D, Densitometric quantification of the Cathepsin D (Cat D), LC3, and APP bands from (A) (n=2). The graphs show the ratio of Cat D-active/full length (FL = precursor + intermediate) (B), LC3-II/LC3-I ratio (C) and expression levels of APP-CTFs (D). Bar graphs show means ± S.D.

3.1.2.1. Trehalose inhibits the degradation of APP-CTFs

The disaccharide trehalose is characterized as an autophagic activator, but the mechanism of action is unknown (Aguib et al., 2009; Casarejos et al., 2011; Sarkar et al., 2007; Schaeffer et al., 2012). It was initially tested whether trehalose treatment could enhance the degradation of APP-CTFs.

Surprisingly, trehalose treatment led to a strong increase of the both APP-FL and APP-CTF levels already after 24 h (Figure 3.5 A, B). However, longer trehalose treatment had no additional effect on the APP-FL and APP-CTF levels (Fig. 3.5 A, B). Similar to APP, both LC3-I and LC3-II levels were also increased over time by trehalose treatment (Fig. 3.5 A). However, LC3-II levels were strongly increased until 48 h and then saturated until 96 h treatment of trehalose (Fig. 3.5 A), resulting in elevated LC3-II/LC3-I ratios for all tested time points (Fig. 3.5 C). Thus, the combined accumulation of LC3-II and APP-CTFs rather suggests an impaired than stimulated autophagic degradation upon trehalose treatment. To further assess lysosomal function, processing of Cat D was analyzed. Interestingly, Cat D processing was impaired upon cell treatment with trehalose in a time-dependent manner, demonstrated by elevated Cat D-precursor and intermediate forms, with concurrent decrease in the active form of Cat D (Fig. 3.5 A). Accordingly, ratios of Cat D-active/ Cat D-FL were strongly reduced upon cell incubation with trehalose (Fig. 3.5 D), indicating a reduction of lysosomal capacity upon trehalose treatment. To support the above findings, the subcellular

localization of APP and LC3 was analyzed by fluorescence microscopy. Acquired images showed an increase in LC3 and APP-CTF positive vesicles and partial co-localization of both proteins upon trehalose treatment compared to control cells (Fig. 3.5 E).

Altogether, these data demonstrate an impairment of autophagic degradation of APP-CTFs upon trehalose treatment.
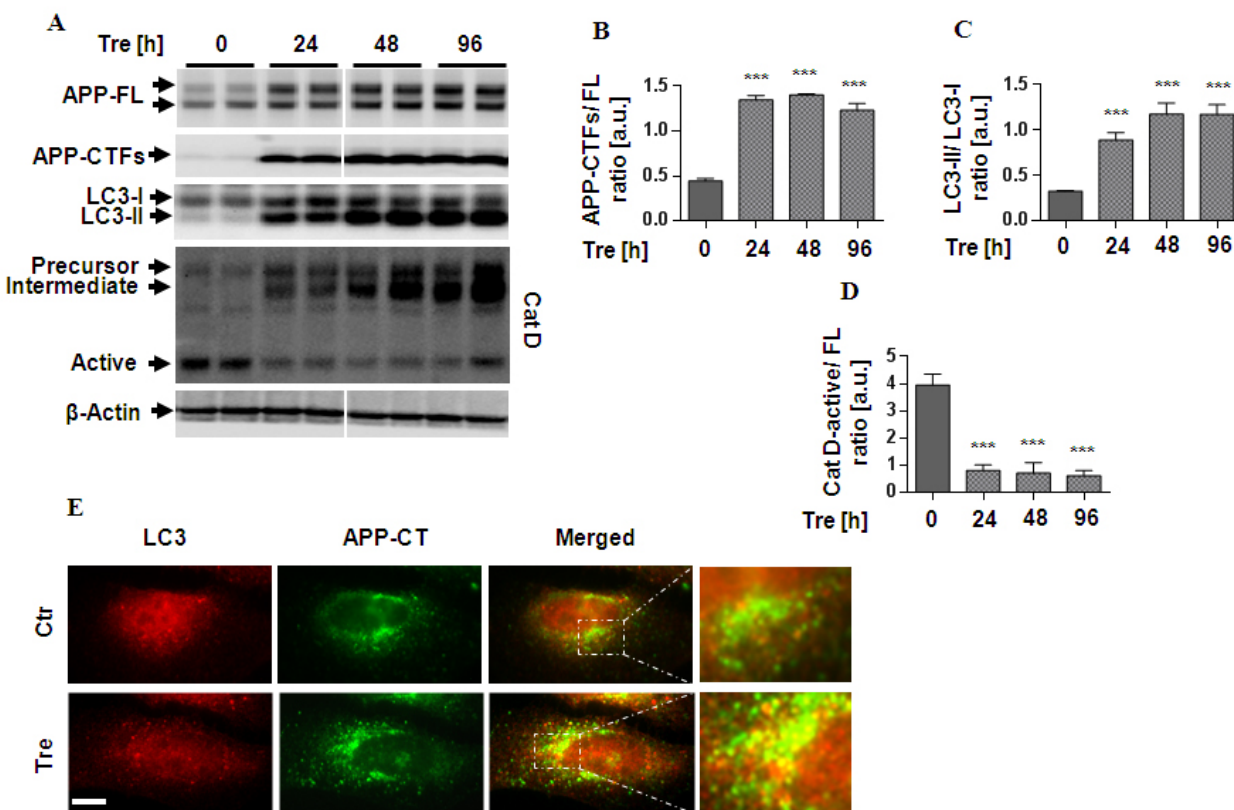
Figure 3.5: Trehalose impairs the metabolism of APP. A, Western immunoblot of APP, LC3 and Cat D from lysates of H4 cells after treatment with 100 mM trehalose (Tre) for the indicated time periods. B-D, Quantification of APP (B), LC3 (C) and Cat D (D) by ECL imaging. Values represent means of two independent experiments (n=6) ± S.D. E, Immunocytochemistry of LC3 and APP after cell treatment with 100 mM trehalose for 24 h. Cells were co-stained with anti-LC3 and anti-APP C-terminal specific (C1/6.1) primary antibodies; and Alexa Flour 546 and Alexa Flour 488-coupled secondary antibodies; respectively. Scale bar represents 10 µm.

3.1.2.2. Trehalose-induced accumulation of APP-CTFs independent of γ-secretase

Given that APP-CTFs are cleaved by the γ-secretase complex to generate AICD, the accumulation of APP-CTFs upon trehalose treatment might result from a decrease of γ-secretase activity. To test this hypothesis, γ-secretase in vitro assay was performed with purified membranes of H4 cells. After incubation, membranes were centrifuged to separate pellets and supernatants for the detection of APP-CTFs and AICD, respectively. The ratio of AICD/APP-CTFs was used to assess the γ-secretase activity. As expected, the pharmacological inhibition of γ-secretase by the specific inhibitor DAPT led to a stabilization of APP-CTFs and reduction of AICD production as compared to control cells

(Fig. 3.6 A, B). Importantly, trehalose incubation did not change the AICD/APP-CTFs ratio as compared to control (Fig. 3.6 A, B), indicating that γ-secretase activity is not affected by trehalose.
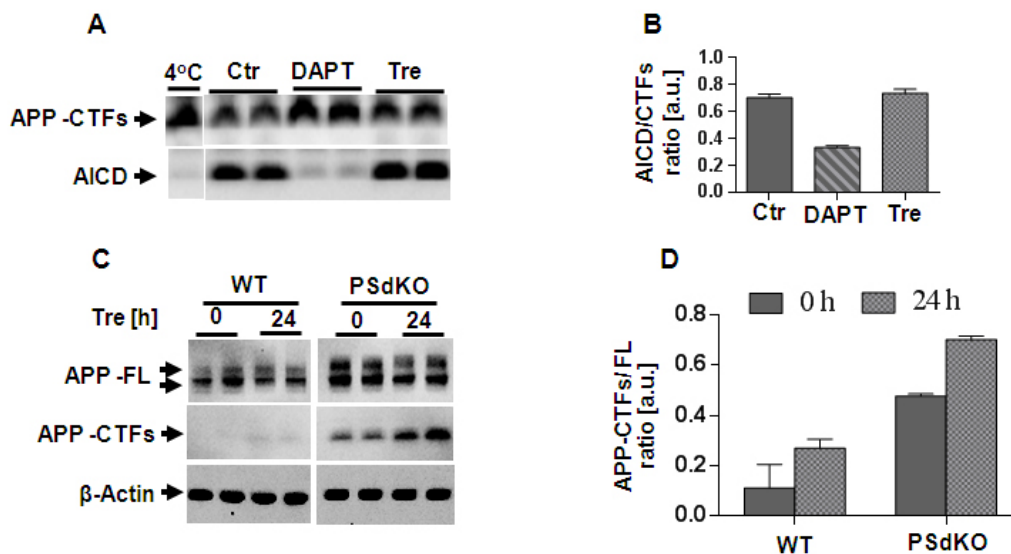
Figure 3.6: Trehalose decreases the degradation of APP-CTFs independent on γ-secretase. A, γ-Secretase in vitro assay in H4 cells. Isolated membranes of H4 cells were incubated in citrate buffer supplemented with either 10 μM DAPT or 100 mM trehalose at 37°C for 2 h and then centrifuged to separate pellets and supernatants. The proteins of the pellets and supernatants were separated by SDS-PAGE and blotted for APP-CTFs and the APP intracellular domain (AICD) detection, respectively. B, Quantification of the AICD/APP-CTFs ratio from the blot (A) (n=2). C, Immunoblotting of APP in MEF wild-type (WT) and MEF presenilin 1 and 2 double knock out (PSdKO) lysates after treatment with 100 mM trehalose for 24 h. D, Quantification of the APP-CTFs/APP-FL ratio from (C) (n=2). Bar graphs represent mean ± S.D.

To further confirm this observation, MEF wild-type (PSWT) and MEF PS1/2 double knock-out (PSdKO) were treated with 100 mM trehalose for 0 and 24 h. As expected, the basal levels of APP-CTF were much higher in PSdKO than in PSWT cells (Fig. 3.6 C, D). Importantly, trehalose treatment led to a marked increase of APP-CTF levels in both WT and PSdKO cells after 24 h (Fig. 3.6 C), as demonstrated by increased APP-CTFs/APP-FL ratios (Fig. 3.6 D). Thus, APP-CTF accumulation upon trehalose treatment is not caused by γ-secretase inhibition. Collectively, trehalose has been shown to stabilize APP-CTFs independent of γ-secretase activity. These findings further support the notion that trehalose inhibits autophagic degradation of APP-CTFs.

3.1.2.3. Trehalose regulates autophagic degradation of APP-CTFs in a glucose independent manner

The intracellular pathways by which trehalose is metabolized and regulates cell signaling are still unknown. Since trehalose is a disaccharide composed of two D-glucose monosaccharides, it was tested whether glucose is involved in trehalose-regulated autophagic degradation of APP-CTFs. Therefore, H4 cells were treated with 100 mM trehalose or 150 mM glucose for 24 h. Notably, the medium of H4 cells already contains 150 mM glucose. While trehalose treatment led to strong

accumulation of LC3-II/LC3-I ratio as observed previously, glucose treatment did not change LC3-II/LC3-I ratio (Fig. 3.7 B, C). Thus, addition of glucose does not alter autophagy. Importantly, APP-CTFs/APP-FL ratio was increased selectively upon treatment with trehalose, but not with additional glucose (Fig. 3.7 B, D). Together, the data indicate that the trehalose-induced autophagy is glucose-independent.
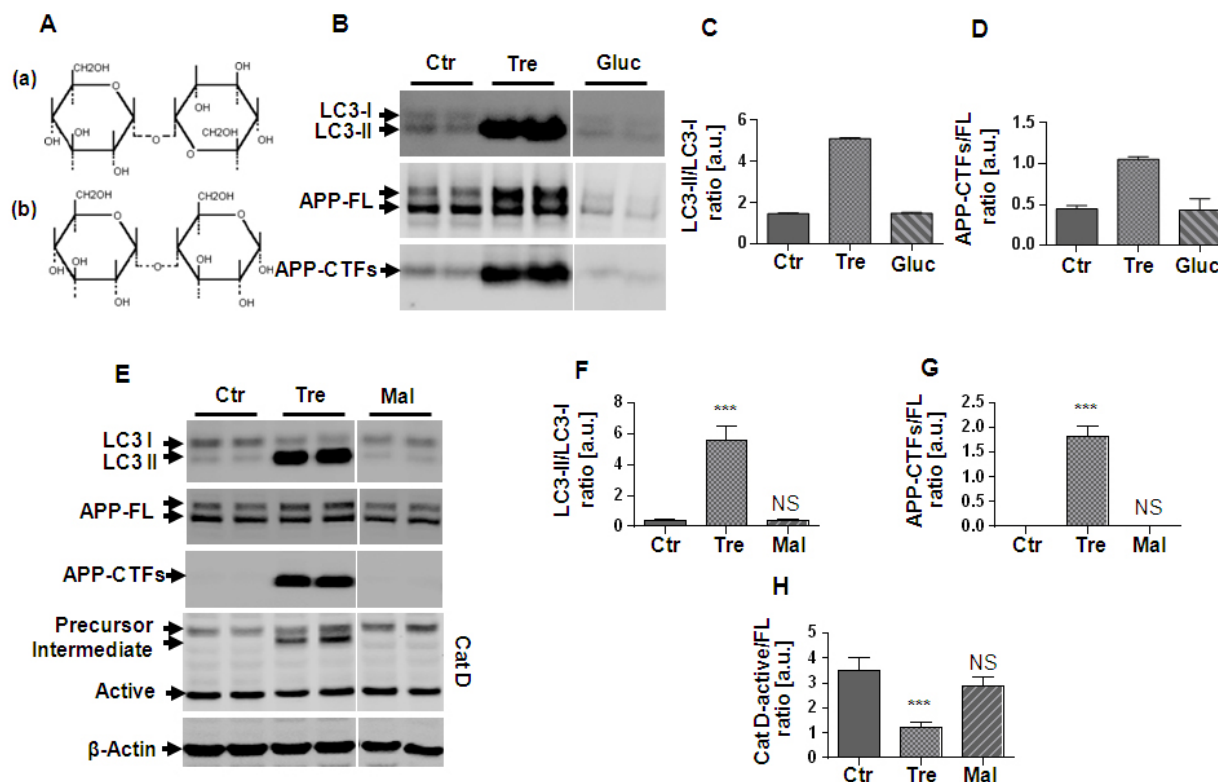
Figure 3.7: Trehalose inhibits degradation of APP-CTFs in a glucose independent manner. A, Molecular structures of Tre, characterized by an α-1,1 glycosidic linkage between two glucose (Gluc) molecules (a) and maltose (Mal), characterized by an α-1,4 linkage between two glucose molecules (b) (Magazu et al., 2007). B, H4 cells were treated with 100 mM trehalose or 150 mM glucose for 24 h, and LC3 and APP were detected by immunoblotting. C-D, Quantification of LC3 (C) and APP (D) from the blot (B) (n=2). E, H4 cells were treated with 100 mM trehalose or 100 mM Mal for 24 h. LC3, APP and Cat D were immunobloted from cellular lysates. F-H, Quantification graphs from the LC3 (F), APP (G) and Cat D (H) blots from (A) (n=3). Bar graphs show mean ± S.D.

In addition, maltose is a disaccharide similar to trehalose that is also composed of two glucose molecules. The difference between these two disaccharides is the type of the glycosidic bond linking the two glucoses. While the glucose molecules in maltose are coupled by an α-1,4 linkage, they are coupled by an α-1,1 glycosidic linkage in trehalose (Venables et al., 2008) (Fig. 3.7 A). Therefore, to test whether trehalose-regulated autophagic degradation of APP-CTFs is generally affected by disaccharides, H4 cells were treated with 100 mM maltose or 100 mM trehalose. However, in contrast to trehalose, maltose had no effect on LC3 and APP levels (Fig. 3.7 E-G). To further confirm differences in autophagic activity between trehalose and maltose, Cat D processing

was assessed. Consistent with previous observations, Cat D processing was impaired upon trehalose treatment as indicated by decreased Cat D-active/Cat D-FL ratio, whereas it was not affected by maltose treatment (Fig. 3.7 E, H). Altogether, these findings indicate that the inhibiton of autophagy is specific for trehalose, and not observed with the other dissacharide maltose or the monosaccharide glucose.

3.1.2.4. Trehalose alters lysosomal acidification
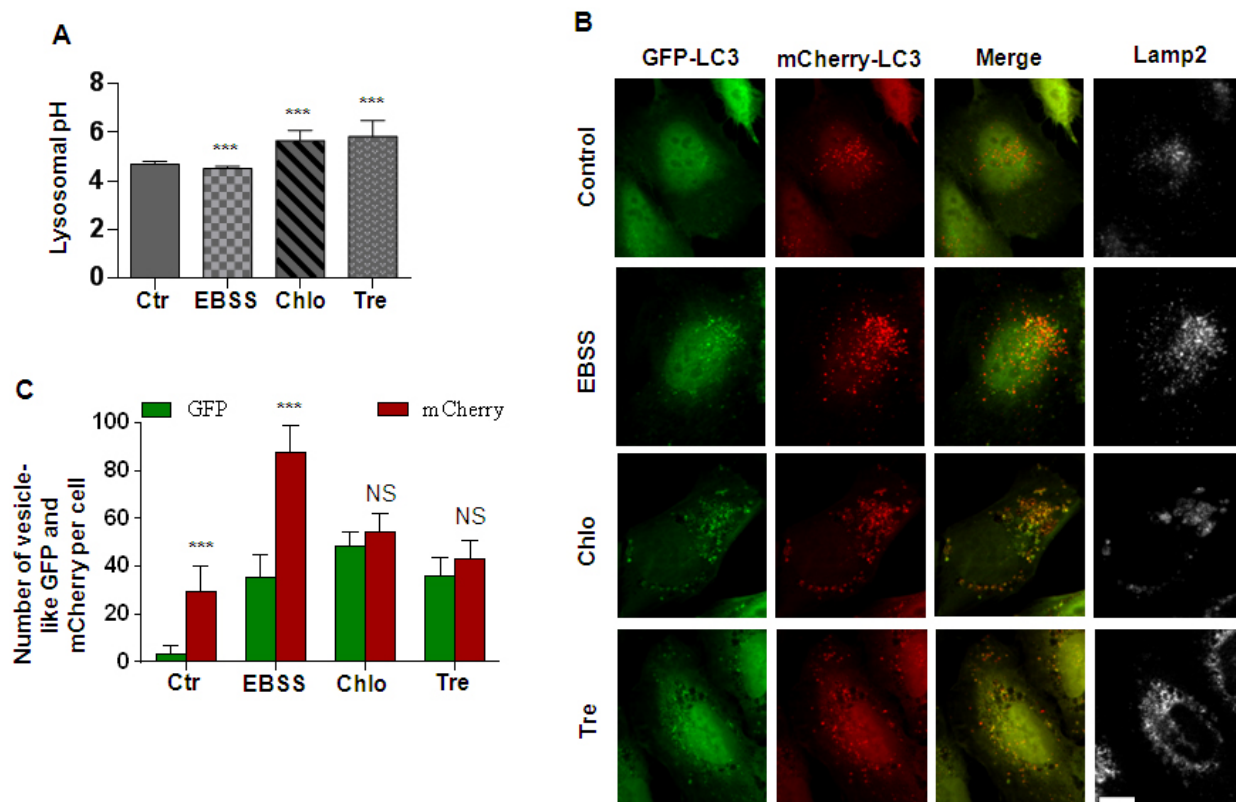
Figure 3.8: Autophagic modulation alters lysosomal acidification. A, H4 cells were subjected into EBSS medium for 3 h, 50 µM chloroquine-containing medium for 12 h or 100 mM trehalose-containing medium for 24 h. Lysosomal pH was measured ratiometrically using LysoSensor yellow/blue DND-160–Dextran. B, H4 cells stable expressing mCherry-GFP-LC3 were treated with EBSS medium, chloroquine (Chlo) or trehalose (Tre) as described in (A). After fixation, cells were stained for lysosomal marker Lamp2 primary antibody and Alexa fluor 350 secondary antibody. Representative maximum-intensity layers of Apotome optical sections are shown. Co-localization panels show overlapping mCherry–LC3 and GFP-LC3 signals. Scale bar 10 µm. C, Autolysosome acidification in H4-mCherry-GFP-LC3 cells upon these treatments was quantified by quenching of GFP-LC3 signals. GFP and mCherry positive punctae was counted in random two 150 µm^2 boxes per cell (n=10). Bar graphs show mean ± S.D. NS represents non-significant.

The described data showed an involvement of trehalose and other autophagic/lysosomal modulators (EBSS starvation medium and chloroquine) in APP-CTF metabolism and Cat D processing. Since proper acidification is crucial for lysosomal function (Mindell, 2012), it was initially tested whether the lysosomal pH is affected by cell treatment with trehalose. Accordingly,

lysosomal pH measurement was performed in H4 cells upon treatment with 100 mM trehalose for 24 h. As chloroquine neutralizes lysosmal pH (Klionsky et al., 2012) and cell starvation has been reported to promote lysosomal acidification (Ni et al., 2011; Zhou et al., 2013), H4 cells were subjected in EBSS medium for 3 h or 50 μM chloroquine-containing medium for 12 h for the positive controls. Measurement of lysosomal pH by a LysoSensor (LysoSensor yellow/blue DND-160-Dextran) revealed that the average lysosomal pH value in control cells was approximately 4.7. Cell incubation with EBSS medium significantly decreased the lysosomal pH to 4.5, while chloroquine significantly increased it to approximately 6.0. Interestingly, the lysosomal pH in trehalose-treated cells was comparable to the chloroquine-treated cells, approximately 6.0 (Fig. 3.8 A). These data indicate that trehalose interferes with lysosomal acidification. Thus, the observed effects on protein accumulation in trehalose-treated cells likely involve improper regulation of the lysosomal pH.

GFP-LC3 is being widely used as a fluorescent marker of autophagosomes. However, GFP is acid-sensitive, and thus its fluorescence decreases in acidic compartments, i.e. when GFP-LC3-anchored autophagosomes fuse with endosomes and lysosomes (Pankiv et al., 2007). In contrast, a monomeric red fluorescent protein mCherry is acid-stable. Therefore, a tandem fusion of an acid-insensitive red fluorescent protein (mCherry) and an acid-sensitive green fluorescent protein (GFP) at the N-terminus of LC3 will be a useful tool to alternatively assess lysosomal acidification. Accordingly, H4 cells stably expressing mCherry-GFP-LC3 were generated. The expression of the double-tagged fusion proteins was confirmed by immunoblotting and fluorescent microscopic analyses (data not shown). Subsequently, H4-mCherry-GFP-LC3 cells were cultured in EBSS medium, chloroquine or trehalose-containing medium as described previously. Counting fluorescent structures from the acquired images revealed that control cells showed predominantly mCherry punctae, but very few GFP punctae (Fig. 3.8 B). Quantification indicated that the number of mCherry punctae was approximately ten-time higher than GFP punctae (Fig. 3.8 C). This could be explained that under basal conditions, GFP fluorescence is efficiently quenched in the acidic milieu of the lysosomes when mCherry-GFP-LC3 is sequestered into lysosomes. Upon incubation in EBSS for 3 h, both mCherry and GFP punctae were increased as compared to control cells. Importantly, the number of mCherry punctae was approximately three-time higher than the number of GFP-LC3 positive punctae (Fig. 3.8 B, C). One possible explanation would be that EBSS starvation enhanced induction of autophagy, which increased the number of both mCherry positive-autophagic vesicles; and promoted lysosomal acidity, which led to efficient quenching of GFP punctae as compared to mCherry punctae. In contrast to EBSS treatment, chloroquine treatment increased the numbers of both mCherry and GFP positive punctae as compared to control cells (Fig. 3.8 B, C). Moreover, there was a large overlap in mCherry and GFP fluorescence (Fig. 3.8 B, C), indicative for inefficient quenching of the GFP signals. These observed effects are due to neutralized lysosomal pH upon chloroquine treatment (Klionsky et al., 2012). Interestingly, trehalose treatment affected autophagy in the same way like chloroquine. Indeed, trehalose treatment increased the number of both

mCherry and GFP punctae as compared to control, with a large overlap of both fluorescent proteins (Fig. 3.8 B, C). This could further support an increase in the lysosomal pH by the treatment with trehalose. Thus, alteration of lysosomal acidification upon autophagic modulation, as shown by the quenching of the GFP signal, was consistent with the measurement of lysosomal pH. Additionally, chloroquine and trehalose treatment led to distribution in aggregate-like structures of mCherry and GFP punctae (Fig. 3.8 B). This might be explained by changes in autolysosomal morphology upon inhibition of the lysosomal function. To confirm this, the cells were stained with Lamp2 antibody to visualize lysosomal and autolysosomal structures. Interestingly, the staining showed the Lamp2-positive signals in aggregate-like structures upon chloroquine and trehalose treatment (Fig. 3.8 B).

Altogether, by different approaches, the data indicate that trehalose treatment decreases lysosomal acidification. Furthermore, the data also demonstrate changes in lysosomal morphology and/or distribution upon trehalose treatment.

3.2. Famillial Alzheimer's disease-associated mutations in presenilin-1 impair autophagy

Recently, Presenilin (PS) proteins have been linked to lysosomal function or autophagic activity in blastocysts and fibroblasts (Coen et al., 2012; Lee et al., 2010; Neely et al., 2011; Zhang et al., 2012).

In this part of the project, the role of PS1 in the regulation of autophagy was investigated in neuronal cell models. The study was mainly conducted with human induced pluripotent stem cells-derived neurons (iPSC-DN), and human embryonic stem cells-derived neurons (ESC-DN). The project was carried out in collaboration with the group of Prof. Dr. Oliver Brüstle, Institute of Reconstructive Neurobiology, University of Bonn.

3.2.1. Characterizations of the FAD-associated PS1 mutant cell models

iPSC were created by reprogramming of primary fibroblasts derived from an AD patient carrying the FAD-linked PS1A79V mutation in one allele of the PS1 gene (Larner and Doran, 2006) and from two healthy individuals, Ctr1 and Ctr2, carrying PS1 wild-type (details were described in the method 2.2.3.2). One clone of each control iPSC and two clones of AD iPSC were subsequently differentiated into homogenous lt-NSC according to established protocols (Falk et al., 2012; Koch et al., 2009) and further into mature neuronal cultures. The generation and characterization of the obtained iPSC clones, lt-NES and neuronal populations have been described in detail previously (Mertens et al., 2013). The PS1 genotypes were verified by sequencing of genomic DNA at the lt-NES stage. The efficiency of neuronal differentiation was evaluated by staining with neuronal markers β-III-tubulin and Map2ab. The staining showed that 75-85% of cells were positive for the neuronal markers. Furthermore, the development of functional properties was also confirmed in differentiated

neurons (Falk et al., 2012; Koch et al., 2009; Mertens et al., 2013). Overall, control and AD neurons showed similarities in neuronal morphology, basic electrophysiological function, and differentiation efficiency (Mertens et al., 2013). Since FAD-linked PS1 mutants have been reported to increase Aβ42/Aβ40 ratio (Sisodia and St George-Hyslop, 2002), a measurement of secreted Aβ42 and Aβ40 species was performed in iPSC-DN. Of note, the measurement showed an elevated Aβ42/Aβ40 ratio in AD neurons, which was caused by selectively lowering Aβ40 levels (Mertens et al., 2013). As Aβ40 is the major peptide generated from γ-secretase cleavage of APP-CTFβ (Jarrett et al., 1993), the data also indicated the partially loss-of-function of γ-secretase as implicated in previous studies (Kelleher and Shen, 2010; Moehlmann et al., 2002). Thus, iPSC-DN originating from healthy individuals and an AD patient carrying PS1AV mutant demonstrate neuronal features and recapitulate disease phenotypes of a FAD-linked PS1 mutant.
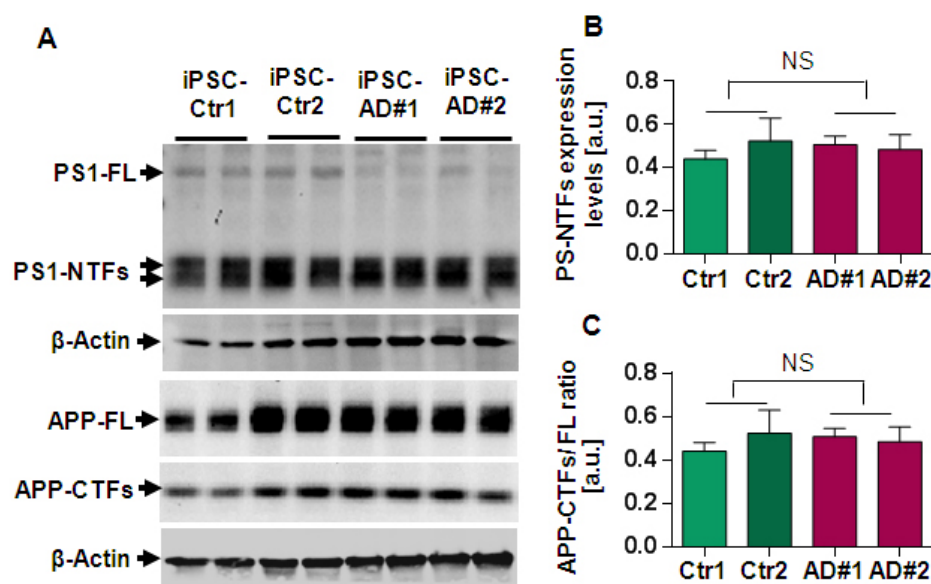
Figure 3.9: Endogenous expression of PS1 and APP in human iPSC-DN. A, Western immunoblot of PS1 and APP in 4-week old neurons generated from skin fibroblasts of healthy individuals (Ctr1 and Ctr2) and one AD patient carrying PS1 A79V mutant (two clones: AD#1 and AD#2). B-C, Quantification of PS1 (B) and APP blots (C) by ECL imaging. The graphs show expression levels of PS1 N-terminal fragments (NTFs) (B) and the ratio of APP-CTFs/APP-FL (C). Bar graphs represent means of duplicate values quantified from the blot (A) ± S.D. NS represents non-significant.

Next, PS1 expression in the different clones was assessed after neuronal differentiation. Cellular membranes were isolated and subjected to Western immunoblotting. Antibody 3111 raised against an N-terminal fragment predominantly detected a 30 kDa protein, representing an N-terminal fragment of PS1 derived from endoproteolytic processing (Fig. 3.9 A). Consistent with previous results (Ratovitski et al., 1997; Thinakaran et al., 1996; Walter et al., 1997), levels of full-length PS1 were much lower. Importantly, levels of PS1-NTF were comparable between control and AD neurons (Fig. 3.9 A, B). Additionally, to determine whether the A79V mutation alters γ-secretase-

mediated processing of protein substrates, the cleavage of the C-terminal fragments (CTFs) of APP was measured. APP was detected as a full-length (FL) protein and C-terminal fragments (CTFs). Both APP-FL and APP-CTF levels varied between the two control clones, but were relatively similar in the two clones of the AD patient (Fig. 3.9 A). Importantly, the ratio of APP-CTFs/APP-FL ratio was not significantly different between control and AD neurons (Fig. 3.9 A, C).
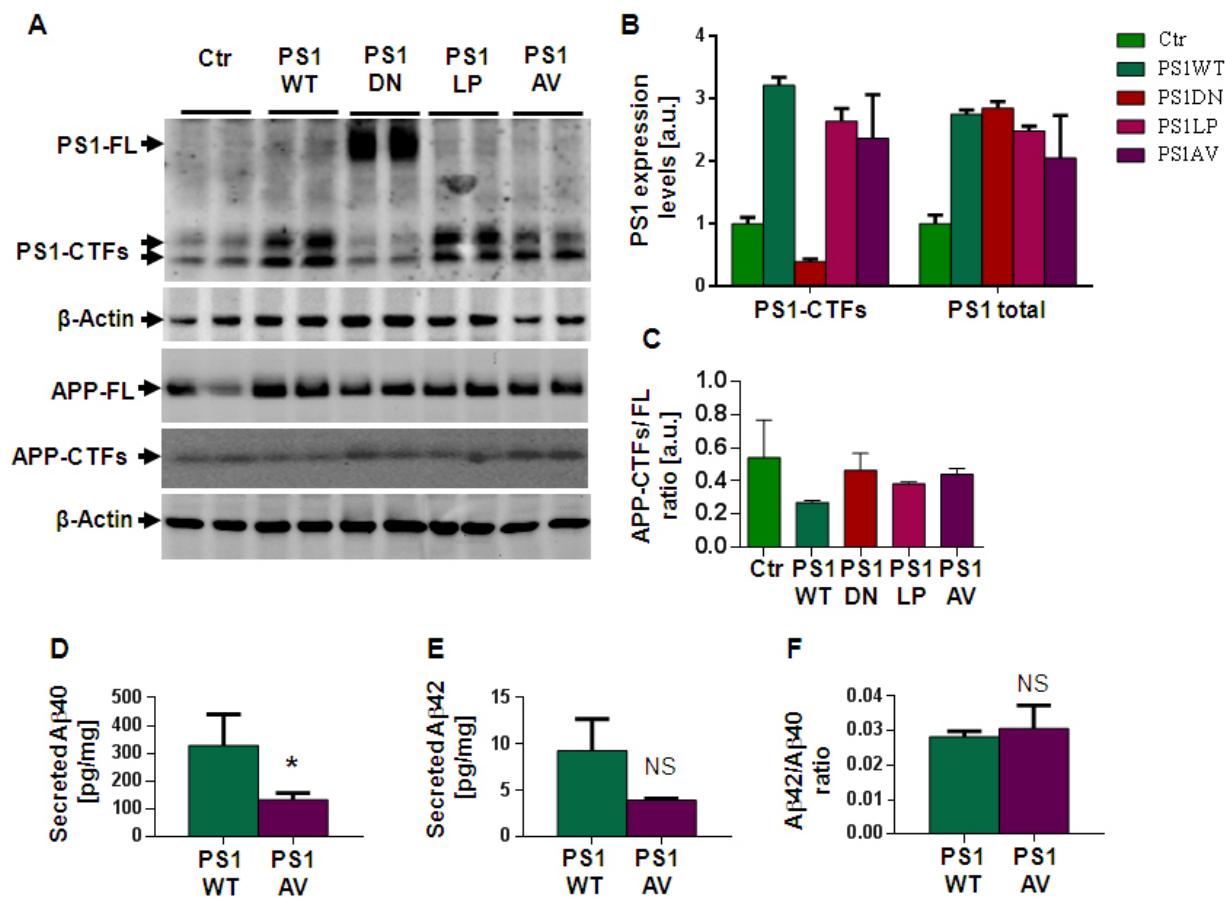
Figure 3.10: Characterization of human ESC-DN overexpressing PS1 variants. A, Western immunoblot of PS1 and APP in 4-week old neurons overexpressing different human PS1 variants: PS1 wild-type (PS1WT), PS1 catalytically inactive variant D385N (PS1DN), and two FAD-linked PS1 mutants PS1 L166P (PS1LP) and PS1 A79V (PS1AV). B-C, Quantification of the PS1 (B) and APP blots (C) by ECL imaging (n=2). The graphs show expression levels of PS1 C-terminal fragments (CTFs) and total PS1 (B), and the ratio of APP-CTFs/APP-FL (C). D-F, Measurement of secreted Aβ40 (D) and Aβ42 peptides (E), and the ratio of Aβ42/Aβ40 (F). The measurement was performed in biological triplicates.

Due to limited number of FAD-associated PS1 mutants in iPSC and potential clonal variations, the study was extended to human ESC. To specifically assess the function of γ-secretase and PS1 in this cellular model system, the ESC-derived lt-NSC were lentivirally transduced with different human PS1 variants including PS1 wild-type (PS1WT), the catalytically inactive D385N variant of PS1 (PS1DN), and two FAD-linked PS1 mutants L166P (PS1LP) and A79V (PS1AV). The PS1-transgenic lt-NSC were subsequently differentiated into mature neuronal cultures. Neuronal differentiation of the lt-NSC

clones was previously verified by expression of beta-III tubulin in almost 80% of the cells. Additionally, the neuronal cultures also demonstrated expression of neuronal-specific APP695 variant and secretion of Aβ peptides (Koch et al., 2012).

In this study, the transgenic expression of the different PS1 variants was analyzed by Western immunoblotting. Different pattern of PS1 expression were observed in the individual clones due to endoproteolytic processing. PS1WT, PS1LP and PS1AV cells expressed predominantly PS1-CTFs, while PS1-FL was hardly detectable (Fig. 10A, B). In contrast, PS1DN cells showed a strong accumulation of the PS1-FL and suppressed endogenous PS1-CTFs as compared to control cells (Fig. 3.10 A, B). This result is consistent with no endoproteolysis of the catalytically inactive PS1DN variant and a dominant-negative effect on endogenous PS1 incorporation into the γ-secretase complex (Wolfe et al., 1999). In addition, total PS1 levels in PS1 overexpressing cells were significantly elevated as compared to control (Fig. 3.10 A, B). As estimated by densitometry, PS1 overexpressing cells had approximately three times more PS1 than control cells (Fig. 3.10 B). Next, endogenous APP processing was assessed by detection of APP-FL and APP-CTFs. As expected, PS1WT overexpressing cells showed low levels of APP-CTFs due to increased γ-secretase activity (Fig. 10A, C). In contrast, PS1DN cells displayed an accumulation of APP-CTF levels due to the expression of inactive PSDN and the suppression of endogenous γ-secretase activity. PS1LP and PS1AV expressing cells also displayed an accumulation of APP-CTF levels, but this effect was lower as compared to the PS1DN expressing cells (Fig. 3.10 A, C). Since FAD-linked PS1 mutants are well known to increase the Aβ42/Aβ40 ratio, the expression of PS1 variants in ESC-DN was further evaluated by a measurement of secreted Aβ isoforms. Previous characterization has indicated a reduced secretion of both Aβ40 and Aβ42 in PS1DN cells, and an increased Aβ42/Aβ40 ratio in PS1LP cells due to selective reduction in the Aβ40 secretion (Koch et al., 2012). This indicates a partial loss-of-γ-secretase function of PS1LP cells. However, the measurement in PS1AV cells revealed unchanged Aβ42/Aβ40 ratio (Fig. 3.10 F) although the secretion of Aβ40 were significantly reduced compared to PS1WT overexpressing cells (Fig. 3.10 D, E). In general, the increased Aβ42/Aβ40 ratio in FAD-linked PS1 mutants might be caused by either increased Aβ42 and/or decreased Aβ40 production (Larner and Doran, 2006; Repetto et al., 2007; Selkoe, 2011; Shen and Kelleher, 2007; Sisodia and St George-Hyslop, 2002). Thus, the decrease of Aβ40 and Aβ42 (in trend) production in PS1AV overexpression demonstrate a strong loss-of-function of γ-secretase. Together, human ESC-DN could be modeled to express different PS1 variants to allow further investigations on their role in neuronal metabolism.
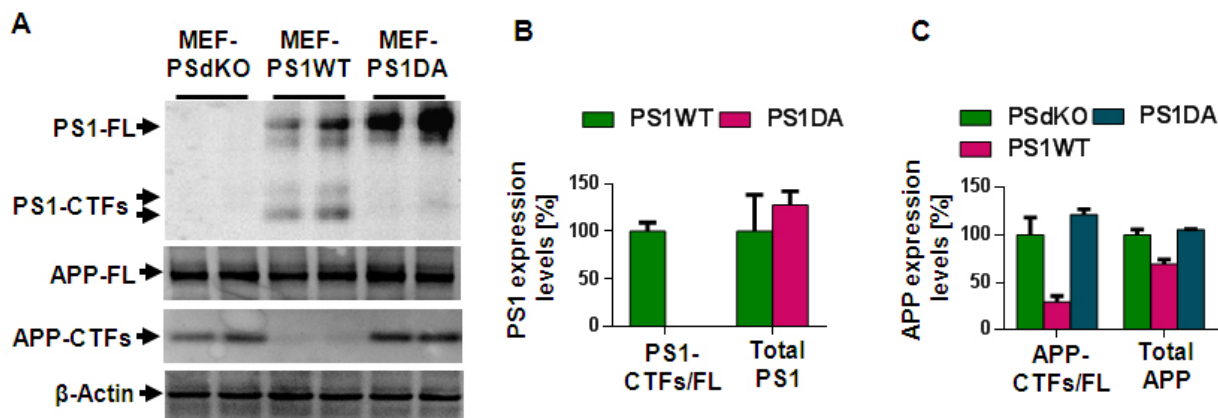
Figure 3.11: Characterization of mouse embryonic fibroblasts (MEF) carrying PS1 variants. Parental fibroblasts with PS1, PS2 double knock-out (PSdKO) were reconstituted with human PS1WT or PS1 catalytically inactive form D257A (PS1DA). A, Western immunoblot of PS1 and APP. B-C, Quantification of the PS1 (B) and APP blots (C) by ECL imaging. Bar graphs represent means of duplicate values from the blot (A) ± S.D.

To allow assessment of cell type-specific and cell type independent effect of PS1, mouse embryonic fibroblasts (MEF) were also included in this study. MEF from mice lacking endogenous expression of PS1 and PS2 (PS1/2 double knock-out - PSdKO) were transduced with active human PS1WT or the catalytically inactive PS1 D275A (PS1DA) variant and selected for stable expression. The expression of PS1WT and PS1DA was demonstrated by western immunoblotting (Fig. 3.11 A, B). Indeed, while PS1WT cells showed both the FL and CTF forms, PS1DA revealed only the FL form due to inactivated autoproteolysis (Fig. 3.11 A). Densitometric quantification showed that total PS1 levels were comparable between PS1WT and PS1DA cells (Fig. 3.11 B). To confirm the PS-dependent γ-secretase activity in MEF expressing PS1 variants, APP processing was assessed by immunoblotting. As compared to PSdKO cells, the expression of PS1WT resulted in strongly decreased levels of APP-CTFs, while levels of APP-FL were similar. Thus, the data demonstrate increased activity of γ-secretase upon re-expression of PS1WT, resulting in higher cleavage of APP-CTFs. In contrast, the expression of PS1DA showed very similar expression of both APP-FL and APP-CTFs as compared to PSdKO cells (Fig. 3.11 A, C). Together, the successful expression of active (PS1WT) and inactive (PS1DA) variants in a PSdKO background allows not only to investigate role of PS1 (between PSdKO cells and reconstituted PS1WT cells), but also to differentiate between potential effects dependent or independent of the enzymatic activity of γ-secretase.

3.2.2. PS1 mutants and PS deficiency impair the metabolism of long-lived proteins

To assess whether PS proteins play a role in neuronal protein metabolism, pulse chase experiments were initially performed in iPSC-DN with control expressing endogenous PS1WT and AD neurons expressing PS1AV mutant. Cells were radiolabeled with [^{35}S] L-methionine for 1 h and chased for 0, 4 and 16 h. Autoradiography of total protein extracts revealed no significant differences in the

global protein turn-over between control and AD clones until 4 h of chase (Fig. 3.12 A, B), indicating that the degradation of short-lived proteins is not altered by the PS1AV mutant in AD neurons. Interestingly, a significant difference was observed in the degradation of proteins after 16 h of chase, which are considered as long-lived (Fig. 3.12 A, C). Particularly, while control neurons turned-over about 59 % (Ctr1: ~ 58 %, Ctr2: ~ 61 %) of radiolabeled proteins after 16 h of chase, AD neurons only degraded about 44 % of radiolabeled proteins. Interestingly, very similar results were also obtained in independent experiments by scintillation counting of radiolabeled proteins after precipitation with trichloro acetic acid (Fig. 3.12 C). Thus, these findings demonstrate that the global turn-over of long-lived proteins is significantly reduced in neurons expressing one allele of the FAD-associated PS1AV mutant. This is consistent with previous findings indicating that the turn-over of long-lived proteins in human fibroblasts carrying different FAD-linked PS1 mutants was lower than in wild-type fibroblasts (Lee et al., 2010).
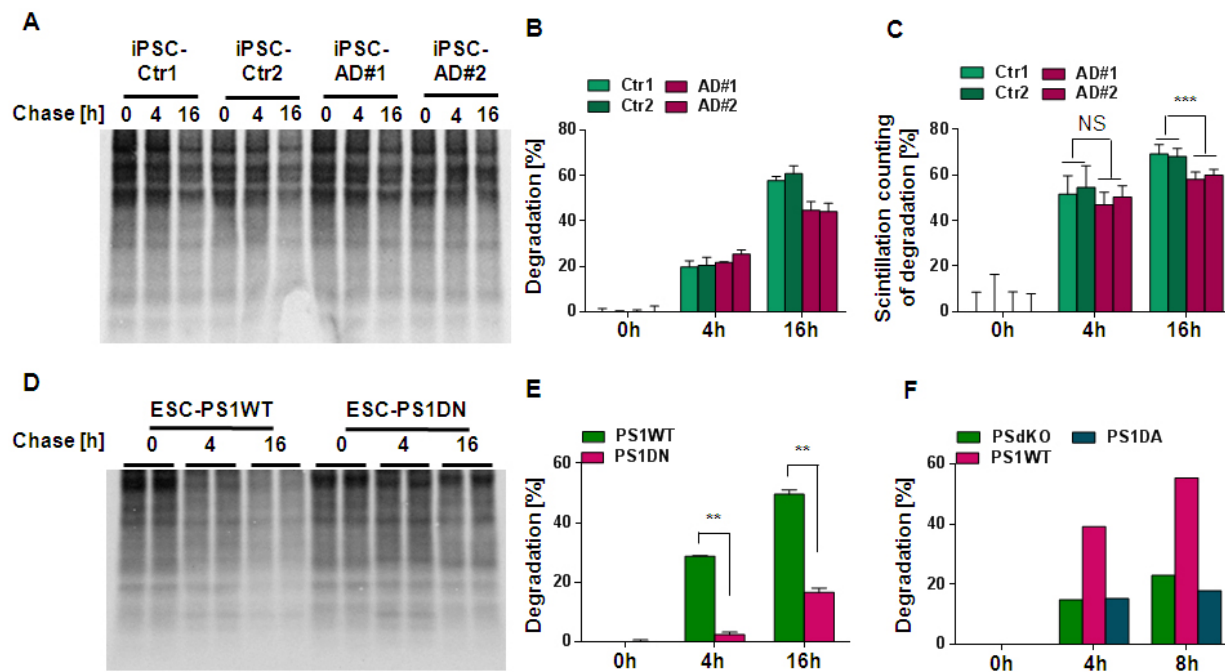
Figure 3.12: Altered proteolysis of long-lived proteins in PS1 mutant and PS deficient cells. iPSC-DN (A-C), ESC-DN (D-E) and MEF (F) expressing PS1 variants were labeled with [S^{35}] L-methionine for 1 hour and then chased for the indicated times. Protein lysates of iPSC-DN (A) and ESC-DN (D) were separated by 4-12% Bis-Tris gels, transferred to nitrocellulose membranes and protein degradation was measured by autoradiography. B, Quantification of autoradiography (A) (n=2). C, Scintillation counting of TCA-insoluble factions from lysates of iPSC-DN normalized to cellular protein concentrations. The measurement was performed from a triplicate experiment. E, Quantification of autoradiography (D) from two duplicate experiments. F, Quantification of autoradiography from MEF (n=1) (data not shown). The quantification graphs show percentages of radiolabeled protein degradation + SEM. NS represents non-significant.

To verify this effect of PS1 in the global protein metabolism in an independent neuronal model, human ESC-DN overexpressing PS1WT and PS1DN were subjected to pulse-chase experiments.

Interestingly, the neurons overexpressing the catalytically inactive PS1DN also showed a significant reduction of the general protein degradation as compared to neurons overexpressing PS1WT. Thus, consistent with a complete loss of γ-secretase activity, we observed significantly decreased protein degradation at 4 h and 16 h of chase (Fig. 3.12 D, E).

In addition, to verify the effect of γ-secretase activity on the overall metabolic turn-over in a non-neuronal model, MEF expressing PS1 variants were subjected to the same pulse-chase experiment. Interestingly, consistent with the findings obtained from both human ESC-DN, re-expression of PS1WT in PSdKO MEF strongly increased protein degradation, whereas the re-expression of the inactive PS1DA variant did not restore metabolic activity (Fig. 3.12 F). Thus, these results demonstrate that the observed effects were dependent on the catalytic activity of the γ-secretase complex.

Taken together, these findings demonstrate that FAD-associated PS1 mutants or a complete loss of γ-secretase function impair global protein metabolism.

3.2.2.1. Impaired induction of autophagy in PS1 mutant cells
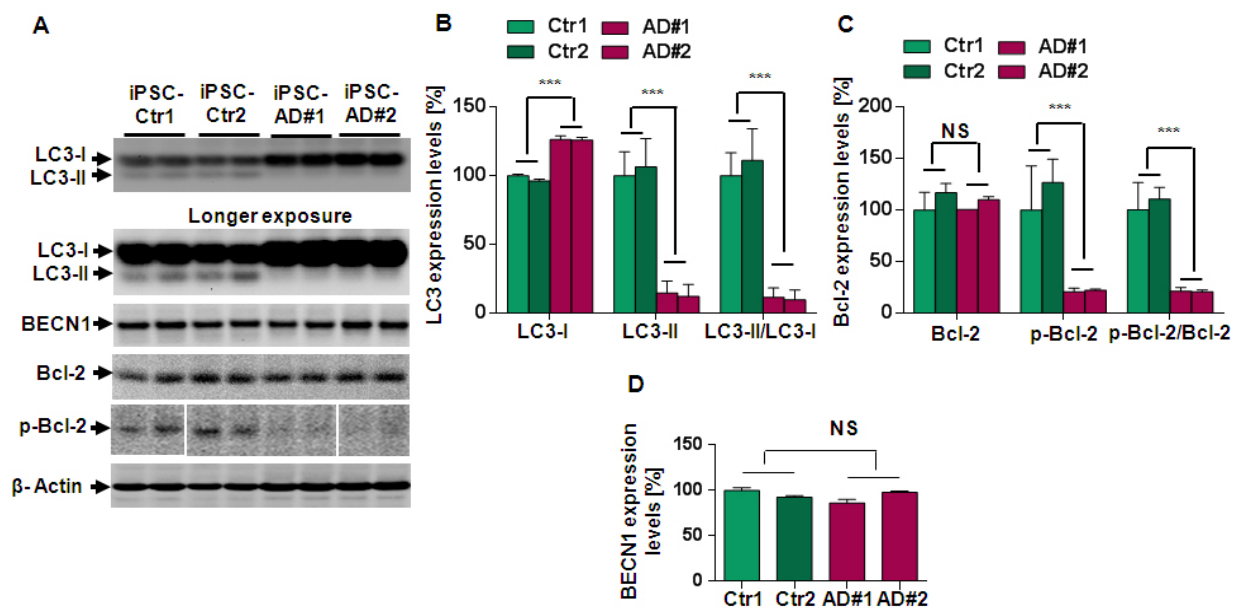
Figure 3.13: Alterations in autophagic marker proteins in PS1 mutant iPSC-DN. A, Western immunoblot of LC3, Bcl-2 and Beclin-1 (BECN1) in iPSC-DN from two healthy individuals (Ctr1 and Ctr2) and one AD patient carrying PS1A79V mutant (two clones: AD#1 and AD#2). B-D, Quantification of LC3 (B), Bcl-2 (C) and BECN1 blots (D) by ECL imaging. Bar graphs represent means of two independent experiments (n=4) ± S.D. NS: non-significant.

Given that the metabolism of long-lived proteins is a means to assess general autophagic capacity (Levine and Kroemer, 2008; Nixon et al., 2008), it was wondered what steps in the autophagic process are affected by PS1 mutations. Consequently, autophagy was monitored in cells expressing

different PS1 variants. Immunoblot analyses of key autophagy-related proteins in iPSC-DN revealed prominent expression of LC3-I and lower levels of LC3-II in controls (Fig. 3.13 A). Notably, levels of LC3-II were strongly decreased in AD neurons, while LC3-I was increased as compared to control neurons, resulting in a significant decrease in the ratio of LC3-II/LC3-I (Fig. 3.13 A, B). This suggests a reduced conversion from LC3-I to LC3-II or a decreased autophagosomal synthesis, rather than enhanced autophagic flux in AD cells. Based on this observation, the expression of proteins involved in early steps of autophagy such as Bcl-2 and BECN1 was investigated next. Bcl-2 and BECN1 are involved in regulation of the autophagosome formation as described in introduction. In mammalian cells, Bcl-2 binds to BECN1 during non-starvation conditions and thereby inhibits autophagy. Upon starvation, Bcl-2 is phosphorylated at residues T69, S70, and S87 of the nonstructured loop, leading to its dissociation from BECN1 and initiation of the autophagosomal formation. Notably, Bcl-2 and BECN1 levels were very similar in control and AD neurons (Fig. 3.13 A, C, D). Interestingly, the phosphorylation of Bcl-2 at S70 was strongly reduced in AD neurons as compared to control neurons (Fig. 3.13 A, C), resulting in decreased p-Bcl-2/Bcl-2 ratio in AD cells (Fig. 13C). Together, the data so far indicate a reduction of autophagic initiation in iPSC-DN carrying FAD-linked PS1AV mutant.
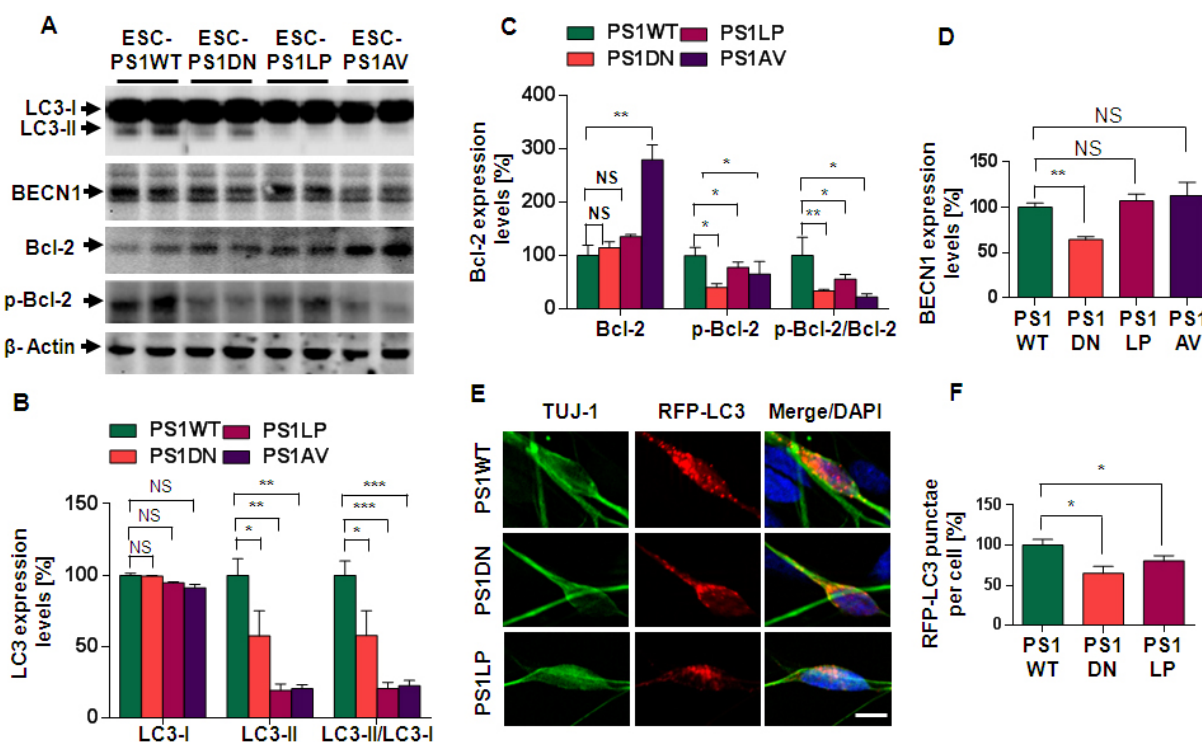
Figure 3.14: Analyses of autophagic marker proteins in human ESC-DN. A, Western immunoblot of LC3, Bcl-2 and BECN1 in ESC-DN overexpressing PS1WT, PS1DN, PS1LP and PS1AV. B-D, Quantification of LC3 (B), Bcl-2 (C) and BECN1 blots (D) by ECL imaging. Bar graphs represent means of two duplicate experiments (n=4) ± S.D. E, Lentiviral transduction of RFP-LC3 to visualize autophagic vesicles in ESC-DN. Neuronal morphology was confirmed by β III- tubulin (TUJ-1) and nuclei were stained by DAPI. Scale bar represents 10 µm. F, Quantification of RFP-LC3 punctae in neurons (n> 20), LC3 positive punctae were counted in 100 µm^2 box per cell. Bar graphs represent means ± S.D. NS prepresents non-significant.

To proof these findings in an independent neuronal model, autophagy was next investigated in human ESC-DN overexpressing different PS1 variants. Importantly, while LC3-I levels were comparable between overexpressed PS1 variants, LC3-II levels were significantly reduced in PS1DN, PS1LP and PS1AV expressing cells as compared to PS1WT expressing cells, resulting in decreased LC3-II/LC3-I ratio in PS1 mutant cells (Fig. 3.14 A, B). Interestingly, although Bcl-2 levels were increased in cells expressing PS1 mutants, phosphorylation of Bcl-2 (S70) was significantly decreased as compared to PS1WT expressing cells resulting in a decreased p-Bcl-2/Bcl-2 ratio in PS1 mutant cells (Fig. 3.14 A, C). In addition, BECN1 levels were unchanged in cells expressing PS1 FAD mutants (PS1LP and PS1AV), but significantly decreased in PS1DN expressing cells as compared to PS1WT expressing cells (Fig. 3.14 A, D). This suggests an involvement of γ-secretase activity in BECN1 expression.

Given the strong decrease in LC3-II in the PS1 mutant cells, autophagosomes were visualized to determine whether this molecular change induces a concomitant decrease in autophagosomal formation. Next, ESC-DN overexpressing PS1 variants were co-stained with antibodies against LC3 and neuronal marker TUJ-1. However, the number of observed autophagic vesicles was very low (data not shown), consistent with the low levels of autophagosome-associated LC3-II as compared to soluble LC3-I in western blot analysis (see Fig. 3.14 A). Therefore, the human ESC-derived lt-NSC were transduced with a lentivirus encoding RFP-LC3 and subsequently differentiated into neurons. The overexpression of RFP-LC3 was confirmed by immunobloting (data not shown). Consistent with immunobloting data, quantification of acquired images by counting red fluorescent punctae revealed a decrease in number of LC3 positive punctae in PS1-FAD mutant and PS1DN as compared to PS1WT overexpressing cells (Fig. 3.14 E, F).

Collectively, these data provide strong evidence that autophagic induction is decreased upon partial loss of γ-secretase activity by PS1-FAD associated L166P and A79V or by the dominant-negative PS1DN in both human iPSC- and ESC-DN.
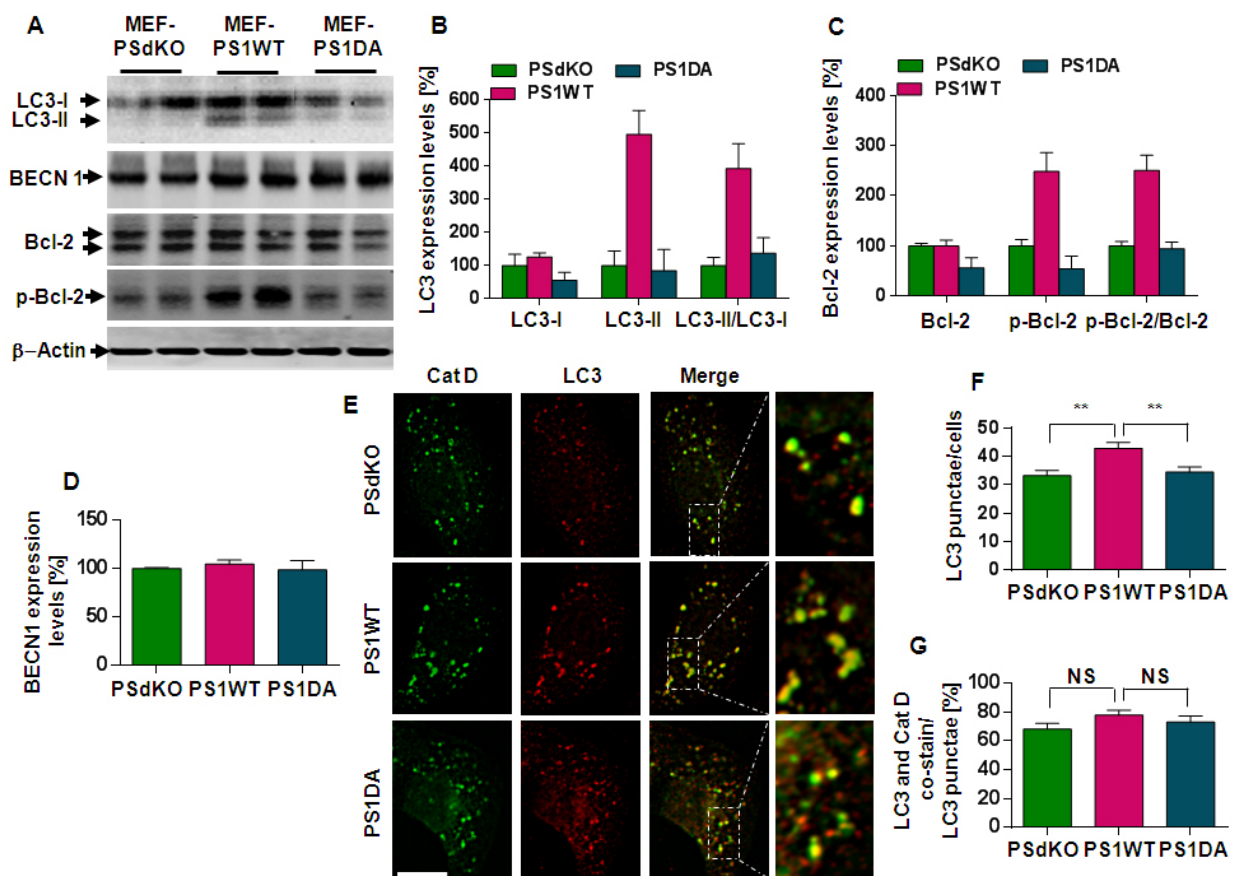
Figure 3.15: Analyses of autophagic marker proteins in MEF expressing different PS1 variants. A, Western immunoblot of LC3, Bcl-2 and BECN1 in MEF PSdKO, PS1WT and PS1DA. B-D, Quantification of LC3 (B), Bcl-2 (C) and BECN1 blots (D) by ECL imaging (n=2). E, MEF were stained with primary antibodies LC3 and Cat D; and fluorophore-coupled secondary antibodies Alexa 546 and 350, respectively. Scale bar represents 10 μm. F, Quantification of LC3 positive punctae per image (n>20). G, Efficiency of autophagosome-lysosome fustion was quantified by percentage of LC3 punctae in co-localization with Cat D punctae per total LC3 punctae (n>20). Bar graphs show means ± S.D. NS represents non-significant.

To extend these observations in a non-neuronal cell model, the role of PS proteins and γ-secretase activity in autophagy was also investigated in MEF carrying PSdKO, PS1WT and PS1DA. Notably, PS deficient (PSdKO) MEF displayed predominantly LC3-I and less LC3-II. While expression of PS1WT in PSdKO cells did not affect LC3-I, but elevated LC3-II levels (Fig. 15A); expression of the catalytically inactive PS1DA variant in PSdKO cells resulted in no obvious change in both LC3-I and LC3-II levels (Fig. 3.15 A, B). Furthermore, the role of PS1/γ-secretase activity in BECN1/Bcl-2 interaction was also assessed. Notably, levels of Bcl-2 and BECN1 were comparable in all PS1 variants (Fig. 3.15 A-C). Interestingly, phosphorylation of Bcl-2 (S70) was selectively increased in PS1WT, but not in PS1DA expressing cells as compared to PSdKO cells (Fig. 3.15 A, C).

In addition, the biochemical analysis of LC3 by fluorescence microscopy was also performed. MEF PSdKO, PS1WT and PS1DA cells were stained with primary antibodies against LC3 and the lysosomal

protease Cat D, and Alexa Fluor 546 and 350-labeled secondary antibodies, respectively (Fig. 3.15 E). Quantification from acquired images revealed a significantly increased number of LC3 positive punctae in PS1WT cells upon the expression in PSdKO cells. In contrast, PS1DA cells revealed no change in the number of LC3 positive punctae as compared to PSdKO cells (Fig. 3.15 F). Thus, these data are consistent with the observations in the immunoblotting analyses. Since PS1 and γ-secretase components have been shown to localize to the lysosomal membrane (Pasternak et al., 2003), the role of PS1/γ-secretase in autophagosome-lysosome fusion was assessed by co-staining of LC3 and Cat D positive punctae. However, the result revealed no significant difference in percentage of LC3 in colocalization with Cat D per total LC3 punctae between PS1 variants, suggesting that fusion of autophagosomes and lysosomes is comparable in all PS1 variant cells (Fig. 3.15 E, G). This finding implies that autophagosome and lysosome fusion is not affected by γ-secretase activity.

In summary, the data indicate reduced induction of autophagy in cells expressing FAD-associated PS1 mutants or a complete loss of γ-secretase activity.

3.2.2.2. Modulation of autophagy in cells expressing different PS1 variants

Given the involvement of PS1 in the initiation of autophagy under basal conditions, next experiments were designed to further assess the role of PS1 under modulation of autophagic activity. As described previously, one of the major regulators of autophagy induction is mTOR. Autophagy can be induced by rapamycin treatment or nutrient starvation medium via inhibition of mTOR complex. Therefore, control and AD iPSC-DN were cultured in neuronal starvation medium Neurobasal-A for 3 h or 10 µg/ml rapamycin-containing medium for 24 h. However, although the reduction of autophagic initiation was confirmed in AD neurons, the incubation of control and AD neurons with either Neurobasal-A or rapamycin-containing medium did not cause a remarkable change in the conversion of LC3-I to LC3-II or in the LC3-II/LC3-I ratios as shown in the representative data (Fig. 3.16 A, B). This suggests an unchanged autophagosomal synthesis upon starvation and rapamycin treatment in AD neurons. This observation could be due to already high basal autophagic activity in neurons as described previously (Boland et al., 2008; Komatsu et al., 2007). For further confirmation, the same experiment was also performed in human ESC-DN overexpressing different PS1 variants. Consistently, both Neurobasal-A and rapamycin treatment did not change the levels of both LC3-I and LC3-II in neurons overexpressing PS1 variants (data not shown).
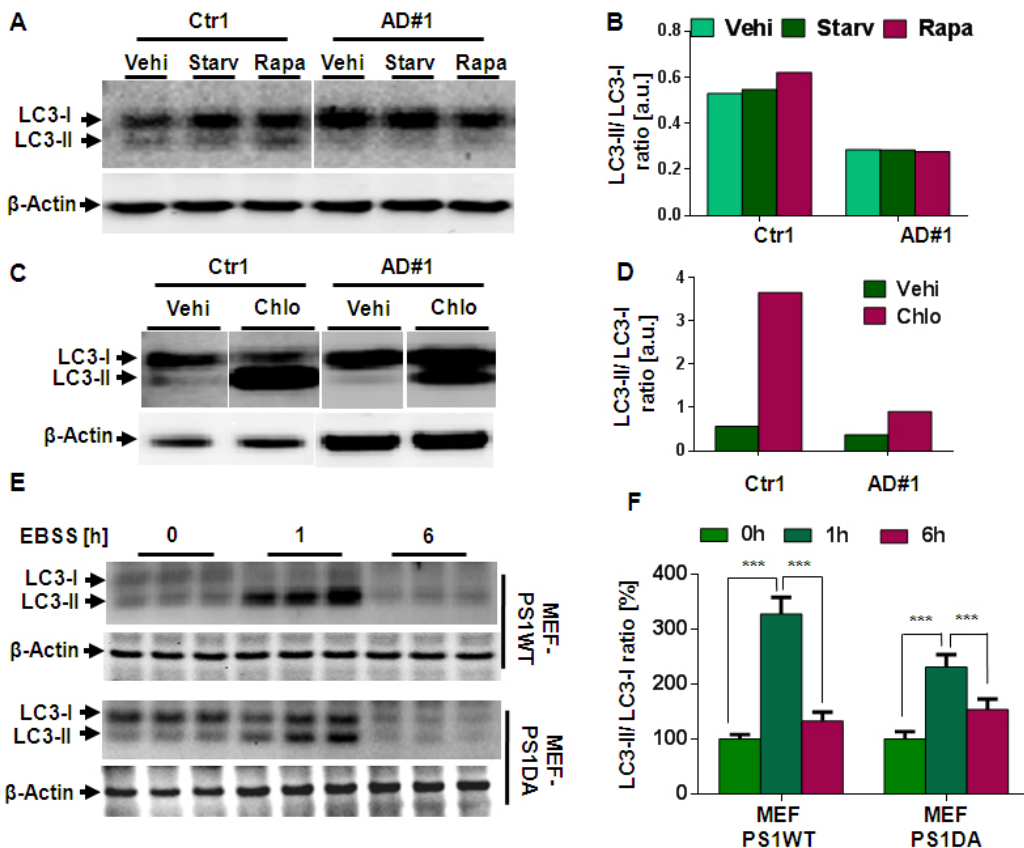
Figure 3.16: Stimulation of autophagy in PS1 mutant cells. A-D, Western immunoblot of LC3 in iPSC-DN Ctr1 and AD#1 upon autophagic modulation: vehicle treatment (Vehi), neuronal starvation Neurobasal-A medium (Starv) for 3 h, 10 µg/ml rapamycin (Rapa) for 24 h or 50 µM chloroquine (Chlo) for 12 h. B and D, Quantification of the blots (A) and (C), respectively. Bar graphs represent the ratio of LC3-II/LC3-I (n=1). E, Immunoblot of LC3 in MEF expressing PS1WT and PS1DA after starvation with EBSS medium for 1 and 6 h. F, Quantification graph of the ratio LC3-II/LC3-I from the blot (E). The bar graphs show mean of the triplicate values ± S.D.

Since starvation in neurons did not obviously change the conversion from LC3-I to LC3-II, the role of FAD-linked PS1 mutant in autophagic induction was alternatively assessed upon chloroquine treatment. The rationale behind is that chloroquine inhibits LC3-II degradation in lysosomes, and allows to compare LC3-II generation between treatment conditions. Therefore, control and AD iPSC-DN were treated with 50 µM chloroquine for 12 h. Chloroquine treatment led to a strong accumulation of LC3-II levels in both control and AD neurons as compared to vehicle treatment (Fig. 3.16 C, D). However, the increase of LC3-II accumulation upon chloroquine treatment in AD neurons was much lower than in control neurons (Fig. 3.16 D), indicating that the PS1AV mutant impairs the conversion of LC3-I to LC3-II, rather than promoting LC3-II degradation in neurons.

Additionally, since the iPSC-DN and ESC-DN showed no change in the LC3-II/LC3-I ratio in response to starvation or rapamycin treatment, likely due to a high rate of basal autophagy in these cells, MEF expressing PS1WT and PS1DA were also analyzed to assess PS1-regulated autophagic response

to nutrient starvation. Incubation of PS1WT cells in EBSS medium for 1 h strongly decreased LC3-I levels and increased LC3-II levels, suggesting an efficient conversion of LC3-I to LC3-II. After 6 h starvation, both LC3-I and LC3-II levels were strongly reduced suggesting an efficient conversion from LC3-I to LC3-II and clearance of LC3-II (Fig. 3.16 E, F). In contrast, PS1DN cells showed strongly reduced conversion of LC3-I to LC3-II after one hour starvation and impaired LC3-II degradation after six hours starvation (Fig. 3.16 E, F), suggesting an impaired autophagic capacity of cells with no γ-secretase activity upon starvation.

Altogether, the data so far uncover the novel findings that FAD-associated PS1 mutants and the catalytically inactive variant PS1DN impair autophagic induction. Importantly, the data also imply the involvement of γ-secretase activity in autophagic degradation capacity.

3.2.2.3. Impaired lysosomal activity in PS1 mutant cells

Recently, PS proteins have been linked to lysosomal acidification or autophagic activity in blastocysts and fibroblasts (Coen et al., 2012; Lee et al., 2010; Neely et al., 2011; Zhang et al., 2012). However, the results were not consistent in the different studies. Here, we also took advantage of the human iPSC- and ESC-DN to specifically assess the effect of PS1 mutants on lysosomal function. Since Cat D is an abundant aspartic endopeptidase, and its processing is affected by lysosomal acidity and cysteine proteases (Benes et al., 2008; Gieselmann et al., 1985; Metcalf and Fusek, 1993), Cat D processing was analyzed in cells expressing PS1 variants. Both control and AD iPSC-DN expressed predominantly the active form of Cat D, whereas the levels of the precursor and intermediate forms of Cat D were very low (Fig. 3.17 A). Importantly, the levels of the active Cat D in AD neurons were much lower than in control neurons (Fig. 3.17 A). Quantification from the blot revealed a significant decrease of Cat D active levels in AD neurons (Fig. 3.17 B), indicating an impaired maturation of Cat D into the catalytically active fragment in AD neurons. Additionally, sequestosome 1 (SQSTM1) or p62 protein is also commonly used as the marker for lysosomal degradation. p62 is involved in substrate sequestration during autophagy, but also cleared during autophagic flux (Bjorkoy et al., 2005). Consistent with impaired activity of lysosomes, levels of p62 were increased in AD neurons (Fig. 3.17 A, C). By extension, the reduction of Cat D processing in AD neurons was investigated upon treatment of control and AD neurons with chloroquine. The treatment led to a strong impairment of Cat D processing in control neurons as indicated by a markedly reduced Cat D-active/Cat D-FL ratio, but only slightly reduced in AD neurons as compared to vehicle treatment (Fig. 17D, E). This finding demonstrates efficient processing of Cat D in control neurons. Thus, these data indicate an impairment of autolysosomal degradation activity in AD neurons carrying FAD-associated PS1AV mutant.
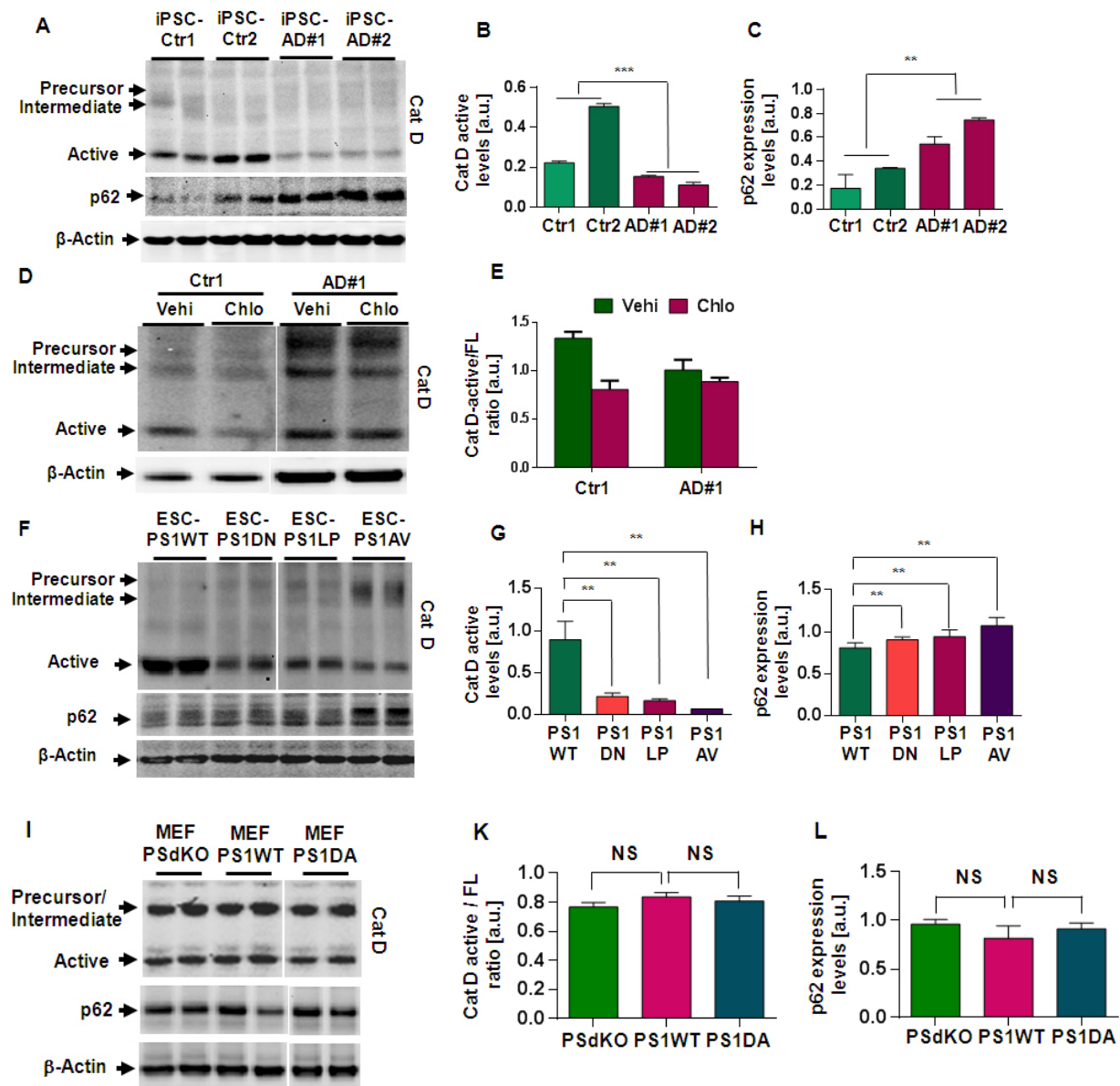
Figure 3.17: Impaired maturation of cathepsin D and decreased clearance of p62 in PS1 mutant neurons. A, Western immunoblot of Cat D and p62 in iPSC-DN. B and C, Quantification graphs of the Cat D-active and p62 expression levels of the blot (A) (n=4). D, Immunoblot of Cat D in iPSC-DN after treatments with vehicle (Vehi) or 50 μM choloroquine (Chlo) for 12 h. E. Quantification graph of the Cat D-active/FL ratio from the blot (D) (n=2). F, Immunoblot of Cat D and p62 in ESC-DN overexpressing PS1 variants. G and H, Quantification graphs of the Cat D-active (G) and p62 expression levels (H) of the blot (F) (n=4). I, Immunoblot of Cat D and p62 in MEF PSdKO, PS1WT and PS1DA. K and L, Quantification graphs of the Cat D-active/FL ratio (K) and p62 expression levels (L) from the blot (I) (n=3). Bar graphs represent means ± S.D.

Consistent with findings in iPSC-DN, the ESC-DN overexpressing PS1 variants also expressed predominantly the active form of Cat D, while precursor and intermediate forms were very low (Fig. 3.17 F). Importantly, cells expressing the FAD-linked PS1 mutants and the inactive variant PS1DN revealed the low levels of Cat D active form as compared to cells expressing PS1WT (Fig. 3.17 F, G).

Moreover, p62 levels also accumulated in neurons expressing FAD-linked PS1 mutants and PS1DN as compared to neurons overexpressing PS1WT (Fig. 3.17 F, H). Thus, the accumulation of p62 further supports a decreased clearance capacity of PS1 mutant neurons.

To extend these observations to the MEF model, Cat D and p62 were detected by immunoblotting in lysates of PSdKO, PS1WT and PS1DA cells. However, the blots revealed that Cat D processing (Cat D-active/FL ratio) and p62 levels were comparable between all PS1 variants of MEF cells (Fig. 3.17 I-L), suggesting cell-type specific effects of PS1 mutations on autophagy and lysosomal activity.

4. Discussion

Many lines of evidence suggest that autophagy is a potential therapeutic pathway for treatment of human disorders, including neurodegenerative diseases (Choi et al., 2013; Nilsson et al., 2013; Son et al., 2012; Yang et al., 2011; Zhou et al., 2013). Thus, understanding the molecular mechanisms in autophagy, as well as the underlying regulatory pathways is necessary for future therapeutical and preventive approaches (Lamb et al., 2013).

4.1. Modulation of autophagic and lysosomal APP metabolism

The Aβ peptides, which aggregate and accumulate in the AD brain, are derived by proteolytic cleavage of the APP-CTFβ by γ-secretase. It has been well established that the expression of FAD-associated mutations in APP increases the intracellular accumulation of potentially amyloidogenic and neurotoxic APP-CTFs in neurons (McPhie et al., 1997). Additionally, APP-CTFs can also trigger inflammation, astrocytosis (Bach et al., 2001; Chong, 1997) and eventually neurodegeneration (Yankner, 1996). Especially, the overexpression of APP-CTFs in the brain of transgenic mice is detrimental and develops AD-like features (Chang and Suh, 2005). Therefore, the metabolism of APP-CTFs might play an important role in AD development. In this study, the role of autophagy in the metabolism of APP-CTFs was characterized.

4.1.1. Lipid accumulation impairs degradation of APP-CTFs

Recent studies indicated similarities between LSDs and AD, including the dysregulation of autophagy, which could contribute to the development of these disorders (Boland et al., 2008; Nixon, 2007; Pacheco and Lieberman, 2008). Additionally, LSDs are known to affect APP processing(van Echten-Deckert and Walter, 2012; Walter and van Echten-Deckert, 2013). This raised the possibility that the dysfunction of autophagy in LSDs has an impact on APP metabolism. Initial in vitro experiments to mimic LSDs by GSLs treatment revealed an elevation in the autophagosomal marker LC3-II and APP-CTFs, as well as colocalization of both proteins. However, the accumulation of LC3-II could indicate either enhanced formation of autophagosomes or/and impaired autophagosomal clearance. To verify this effect, the studies were further extended by analysis of an authentic NPC disease cell model. Consistent with the observations upon GSLs treatment, NPC1$^{-/-}$ cells also revealed an increase of LC3-II and APP-CTF levels. The deficiency of NPC1 is linked to lysosomal dysfunction (Pacheco and Lieberman, 2008; Sarkar et al., 2013; Settembre et al., 2008; Takamura et al., 2008). Thus, these findings imply an impaired autophagic degradation of APP-CTFs in models of lipid storage disorders and such conclusion is indeed in agreement with earlier reports demonstrating that autophagosomes and lysosomes contribute to both generation and degradation of APP-CTFs (Haass et al., 1992; Nixon, 2007; Tamboli et al., 2011a; Tian et al., 2014; Yu et al., 2005).

Since APP-CTFs are cleaved by γ-secretase, increased APP-CTF accumulation might also result from a reduced γ-secretase activity. However, it has been reported that GSLs rather stimulate γ-secretase

activity and thus increase Aβ peptide generation (Tamboli et al., 2011b). Thus, the present data rather suggest a decreased degradation of APP-CTFs by autophagy upon GSLs treatment.

The targeting of APP and its derivatives to the lysosomes is well-established. APP has previously been shown to be transported and processed to Aβ within the secretory pathway. In addition, unprocessed APP can be endocytosed and degraded in lysosomes (O'Brien and Wong, 2011). However, very little is known about how APP-CTFs are transported to autophagosomes. Recently, it has been reported that the adaptor-related protein complex 2 (AP2) and phosphatidylinositol binding clathrin assembly protein (PICALM) play a role in transport of APP-CTFs from endosomes to autophagosomes via their fusion (Tian et al., 2014). Particularly, AP2 and PICALM play critical role in clathrin-mediated endocytosis (Ohno et al., 1995; Tebar et al., 1999). While the subunit AP2M1 is responsible for the recognition and selection of the cytosolic region of type I transmembrane proteins like APP during endocytosis (Ohno et al., 1995), PICALM binds to clathrin, phosphatidylinositol, and AP2 to aid in the formation of clathrin-coated pits (Tebar et al., 1999). Accordingly, AP2 cross-links LC3 to APP-CTFs and mediates endosome-autophagosome fusion, suggesting that the AP2/PICALM complex functions as an autophagic cargo receptor for the recognition and shipment of APP-CTFs from the endocytic pathway to the LC3-marked autophagosomes. Additionally, in this context, it is noteworthy to mention that autophagosomes are supposed to be derived from the ER (Axe et al., 2008; Hamasaki et al., 2013; Hayashi-Nishino et al., 2009; Yla-Anttila et al., 2009). Therefore, this can also be a potential route for targeting APP and its derivatives into autophagosomes.

Since Aβ peptide generation is mediated by cleavage of APP-CTFβ, the accumulation of APP-CTFβ in autophagic-lysosomal dysfunction in LSDs potentially promotes the generation and persistence of Aβ, leading to elevated intracellular Aβ levels. Recent data suggest that intracellular Aβ causes neurodegeneration by increased ER stress, endosomal/lysosomal leakage and dysfunctional mitochondria (Umeda et al., 2011). Additionally, constitutive autophagy selectively degrades dysfunctional mitochondria to maintain mitochondrial quality (Kim et al., 2007). Therefore, reduced autophagic flux results in the persistence of dysfunctional mitochondria, leading to increased generation of reactive oxygen species, which subsequently could trigger apoptotic and inflammatory processes (Green et al., 2011; Terman et al., 2010).

4.1.2. Regulation of APP-CTF metabolism by autophagic modulation

Given that APP-CTFs are degraded via autophagy, the present data further confirmed that modulation of autophagic activity affects APP-CTF metabolism. Initially, autophagy was activated by subjecting cells into EBSS, a glucose-containing medium that is devoid of amino acids and other growth factors. As the consequence of autophagic activation, the increased LC3-II/LC3-I ratio after 1 h and decreased LC3-II/LC3-I ratio after 6 h starvation suggest an enhanced autophagosomal synthesis after 1 h and then efficient consumption of autophagosomes after 6 h. Interestingly, APP-

CTFs also decreased in time-dependent manner of the starvation, indicating the selective degradation of APP-CTFs upon stimulation of autophagy.

In search of the molecular mechanisms underlying the enhanced autophagy upon starvation, many studies have clearly demonstrated the involvement of mTOR complex. mTOR is a negative regulator of autophagy. The inhibition of mTOR during starvation leads to increased autophagosomal formation (Mizushima, 2010; Russell et al., 2014). However, mTOR is also required for the reformation of lysosomes upon starvation-induced autophagy (Yu et al., 2010). Particularly, mTOR is reactivated by prolonged starvation; leading to attenuation of autophagy and regeneration of functional lysosome from autolysosome (Yu et al., 2010). Additionally, the mTOR complex 1 activity on lysosomal membranes was recently reported to directly phosphorylate the transcriptional factor EB (TFEB), leading to inhibition of TFEB activity (Settembre et al., 2012). Thus, the suppression of mTOR complex 1 upon starvation activates TFEB and consequently upregulate lysosomal function in the course of autophagy (Zhou et al., 2013). Importantly, a very recent study provided evidence that starvation enhances lysosomal acidification associated with increased Cat B and L enzyme activity, leading to increased lysosomal capacity (Zhou et al., 2013). Thus, amino acid and growth factor deprivated medium (EBSS) exerts dual effects on the autophagic-lysosomal pathways, including increased autophagosomal formation and enhanced lysosomal activity. Therefore, EBSS increases autophagic degradation of APP-CTFs.

Importantly, blockage of autophagosome-lysosome fusion has been shown to inhibit lysosomal acidification and cathepsin activity, suggesting that lysosomal activity is dependent on efficient fusion with autophagosomes (Zhou et al., 2013).

Since APP-CTFs can be cleaved by γ-secretase, the decrease of APP-CTF levels upon starvation might not only be caused by inhibition of lysosomal degradation, but also involve stimulation of γ-secretase activity. In fact, it has been shown that starvation-induced autophagy leads to a translocation of the γ-secretase complex from endosomes and/or ER to autophagic vesicles. This makes autophagic vesicles to become an important cellular pool of γ-secretase during starvation, resulting in increased cleavage of APP-CTFs and Aβ production upon starvation (Yu et al., 2005).

Next, to further confirm the role autophagy in APP-CTF metabolism, lysosomal function or autophagy was inhibited by treatments with leupeptin, bafilomycin or chloroquine. Interestingly, all the inhibitors led to a strong accumulation of the autophagosomal marker LC3-II and APP-CTF levels, indicating the degradation of APP-CTFs in autolysosomes.

Taken together, the present data demonstrate an important role of autophagic capacity in the metabolism of APP-CTFs, the major process leading to Aβ peptide generation. Thus, understanding the regulation of autophagic activity has important implications in biomedicine and AD research in particular. Our findings are also consistent with earlier reports in which BECN1-regulated basal

autophagy plays a role in the degradation of APP. Particularly, in cells stably expressing APP wild-type, BECN1 knockdown lead to the accumulation of APP, APP-CTFs and Aβ peptides; whereas induction of autophagy via BECN1 overexpression decreases APP, APP-CTF and Aβ levels (Jaeger et al., 2010). Supportingly, reduced BECN1 levels together with increased Aβ levels are observed in AD patients (Pickford et al., 2008). Additionally, genetic reduction of BECN1 expression in APP transgenic mice increased both intraneuronal and extracellular Aβ deposition (Pickford et al., 2008). Notably, increased BECN1 expression rescued these amyloid pathologies (Jaeger et al., 2010; Pickford et al., 2008), indicating that stimulation of autophagy could be beneficial in AD therapy and prevention.

4.1.2.1. Trehalose inhibits the autophagic degradation of APP-CTFs

The experiments with trehalose showed a strong accumulation of APP-CTFs. This was very surprising, because trehalose is well described as an mTOR-independent enhancer of autophagy (Sarkar et al., 2007). Trehalose has been shown to promote the clearance of neurodegenerative disease-associated proteins such as huntingtin (HD), α-synuclein (PD) (Casarejos et al., 2011; Sarkar et al., 2007), tau and phosphorylated-tau (AD) (Casarejos et al., 2011; Kruger et al., 2012; Schaeffer et al., 2012). However, these are cytosolic proteins, which can be degraded by either UPS and/or in lysosomes. In contrast, APP is an intergral membrane protein, which is transported to the plasma membrane from where it undergoes rapid endocytosis. APP is then recycled back to the cell surface or targeted to endosomal-lysosomal compartments (Walter et al., 2001). Moreover, our previous results demonstrated APP-CTFs as the substrates of autophagic-lysosomal pathways. Notably, cell treatment with trehalose also strongly increased autophagosomal marker LC3-II. However, previous studies have attributed this observation to activation of autophagy (Aguib et al., 2009; Casarejos et al., 2011; Sarkar et al., 2007; Schaeffer et al., 2012). To determine if trehalose treatment indeed enhances autophagy, lysosomal function has been assessed. Surprisingly, the data indicated an impaired processing of the major lysosomal hydrolase Cat D, indicating an inhibitory effect of trehalose on lysosomal function. Thus, in contrast to previous conclusions of other studies, our data imply an inhibitory effect of trehalose on autophagy.

Although trehalose treatment leads to increased LC3-II levels, very little is known how it regulates the autophagic machinery. Our study focused on well known upstream events regulating autophagosomal formation, such as the mTOR and the class III PI3K complexes (Laplante and Sabatini, 2009; Levine and Kroemer, 2008). However, BECN1, Bcl-2 phosphorylation, and mTOR phosphorylation remained constant upon trehalose treatment, implying that trehalose is not involved in autophagosomal formation. Altogether, it is likely that trehalose rather decreases lysosomal activity.

Next, the study investigated the involvement of trehalose in γ-secretase activity. By using γ-secretase in vitro assay and MEF PSdKO treated with trehalose, the data indicated that trehalose

has no effect on γ-secretase activity. This further supports that the accumulation of APP-CTFs and LC3-II is caused by impaired autophagic clearance.

Trehalose is a disaccharide composed two D-gluclose molecules linked by an α-1,1 glycosidic linkage (Venables et al., 2008). Therefore, to test whether potential metabolites of trehalose affect autophagy, glucose was added into cell medium that already contains 150 mM glucose. In addition, the effects of maltose, another disaccharide with α-1,4 glycosidic linkage were also investigated. However, neither addition of glucose nor maltose had overt effects on lysosomal function, as indicated by unchanged levels of autophagosomal marker LC3-II and APP-CTFs. Altogether, the data indicate that the observed effects are specific for trehalose, and not due to increased supply with glucose.

4.1.2.2. Trehalose alters lysosomal acidification

It is indeed striking that trehalose treated cells showed accumulation of autophagosomes and APP-CTFs, together with impaired Cat D activation. To gain further insights, the lysosomal pH was measured upon trehalose treatment and compared to the effect of known pH modulators, including EBSS medium and chloroquine. As expected, cell incubation in EBSS medium significantly reduced lysosomal pH to approximately 4.5 compared to pH 4.7 of control cells, whereas chloroquine treatment raised the lysosomal pH to approximately 6.0 as it functions to neutralize/elevate lysosomal pH (Klionsky et al., 2012). Importantly, trehalose also significantly raised lysosomal pH to approximately 6.0. Thus, the pH measurement has revealed an effect of trehalose on lysosomal pH regulation.

This notion was further supported by additional experiments using a fusion protein of the pH-insensitive red fluorescent protein (mCherry) and a pH-sensitive green fluorescent protein (GFP) at the N-terminus of LC3. Consistent with the pH measurements, the tandem fusion mCherry-GFP tagged LC3 also revealed significant changes in lysosomal acidification upon trehalose treatment. Notably, while control cells showed predominantly mCherry punctae due to quenching of GFP in efficiently acidified autolysosomes, trehalose treatment increased mCherry and GFP colocalization, indicating an inefficient lysosomal acidification. In addition, aggregate-like structures of the mCherry and GFP positive punctae were observed upon trehalose treatment, further indicating aberrant morphology of autolysosomal compartments. Visualization of the lysosomal structure by immunocytochemistry with Lamp2 antibody has revealed the distribution of Lamp2-positive signals in aggregate structures upon trehalose treatment. This further supports a dysfunction of lysosome in trehalose-treated cells.

Taken together, multiple lines of evidence in the study established that defective autophagy upon trehalose treatment principally reflects a failure in lysosome/autolysosome acidification. However, the underlying causes of this effect remain unknown. It has been well established that the

glycosylation of the V0a1 subunit of the vacuolar ATPase (V-ATPase) and its proper targeting to lysosomal membrane are essential for proton translocation and lysosomal acidification (Lee et al., 2010; Zhang et al., 2012). Addtitionally, the master transcriptional regulator of lysosomal biogenesis and autophagy, termed TFEB, is also well established to be involved in control of lysosomal function (Settembre et al., 2011; Zhou et al., 2013). TFEB is regulated by a signaling mechanism that is sensitive to nutrient and growth factors (Settembre et al., 2011; Zhou et al., 2013). Thus, trehalose might affect the proper function of V-ATPase and/or TFEB and therefore leading to lysosomal impairment.

In summary, this study re-examined the role of trehalose, known as mTOR-independent autophagic activator, in the autophagic metabolism of APP-CTFs. Surprisingly, and in contrast to the well-established degradative role of trehalose in neurodegeneration-related protein aggregates, we found that trehalose prevented autophagic degradation of APP-CTFs. Since neurodegeneration-associated protein aggregates, such as phosphorylated tau, huntingtin and α-synuclein mutants are considered to be primarily degraded in autophagy, the underlying mechanisms of these contradictory effects of trehalose on intracellular protein clearance are unclear. A possible explanation might emerge from a recent study that demonstrates the involvement of unconventional secretion of aggregated α-synuclein through exophagy in cases of impaired autophagosome-lysosome fusion or lysosomal function (Ejlerskov et al., 2013). Particularly, aggregated α-synuclein is engulfed into autophagosomes, which is further fused with endosomes to form amphisomes. Under conditions that block amphisome-lysosome fusion or lysosomal function, amphisomes do not fuse with lysosomes, but with the plasma mebrane to release their content by exophagy (Ejlerskov et al., 2013). Supportively, recent study has shown that a combination of starvation and lysosomal inhibition increase tau secretion in primary neurons, which is likely caused by the release of autophagosomal contents into extracellular space (Mohamed et al., 2014). Although still speculative, this mechanism might underlie the decrease of neurodegeneration-associated proteins upon trehalose treatment since trehalose inhibits lysosomal function. Therefore, trehalose-induced autophagy dysfunction might trigger both impaired APP-CTF degradation in lysosomes and enhanced exophagy to release neurodegeneration-associated protein aggregates. However, further experiments are needed to confirm enhanced exophagy of protein aggregates by trehalose.

An alternative explanation for decreased levels of neurodegeneration-associated protein aggregates upon trehalose treatment would be the involvement of the other major degradation pathway in eukaryotic cells, UPS. Tau, huntingtin or α-synuclein is cytosolic protein and accumulating evidence indicates an involvement of UPS in the reduction of these protein aggregates. For example, inhibition of proteasome by epoxomicin increased the levels of α-synuclein and hyperphosphorylated tau, and such increase correlated with enhanced cell death

(Casarejos et al., 2011). Moreover, both inhibition of autophagy with 3-MA and of proteasome with lactacystin increased mutant huntingtin EGFP-HDQ74 aggregates and their toxicity (Sarkar et al., 2007). Thus, although autophagy is considered as the major pathway to degrade protein aggregates, a role of proteasome in reduction of aggregate-prone proteins thereby affecting their aggregate is not excluded. Furthermore, trehalose can also act as a chemical chaperone and influence protein folding through direct protein-trehalose interactions, as demonstrated by decreased aggregation of polyglutamine (polyQ)[3] and lowered toxicity upon treatment of a mouse model of HD with trehalose. This protective effect is likely caused by trehalose binding to expanded polyQ and stabilizing the partially unfolded mutant protein (Sarkar et al., 2007).

Although its actions in the metabolism of intracellular proteins are largely unknown, trehalose has shown beneficial effects in animal models and primary fibroblast from patients of neurodegenerative disorders by decreasing the levels of toxic protein aggregates and improving clinical symptoms and survival (Fernandez-Estevez et al., 2014; Sarkar and Rubinsztein, 2008; Schaeffer et al., 2012). Especially, trehalose is under investigation for a number of medical applications including the treatment of AD and HD (Luyckx and Baudouin, 2011). Additionally, it is widely used in the food industry, the biopharmaceutical preservation of labile protein drugs and in the cryopreservation of human cells (Luyckx and Baudouin, 2011). Therefore, effects of trehalose on cellular mechanisms should be further investigated to evaluate the implications for therapeutical applications.

4.2. Famillial Alzheimer's disease associated mutations in presenilin-1 impair autophagy

Several conflicting results as to how PS1 protein affects autophagic-lysosomal function have been reported so far. FAD-linked mutations of PS1 have been reported to increase lysosomal pathology in both mouse models and humans (Cataldo et al., 2004). This was further validated as PS1 deficiency and FAD mutants impaired autophagic turnover of long-lived proteins (Lee et al., 2010; Neely et al., 2011). Particularly, Lee et al provided evidence that PS1 deficiency impairs V-ATPase function and lysosomal acidification (Lee et al., 2010). However, Coen and colleagues has recently challenged this mechanism by showing that PS1 deficiency affects lysosomal Ca^{2+} homeostasis instead of lysosomal acidification, thereby impairing lysosomal fusion capacity (Coen et al., 2012). In contrast, Zhang and colleagues recently showed that both the turnover of autophagic substrates and lysosomal acidification are unchanged in PS1 deficient cells (Zhang et al., 2012). The reasons for these discrepancies remain unclear, but could be due to the use of different methodologies, and cell lines. Nevertheless, how FAD-linked mutations in PS1 regulate autophagy in human differentiated neurons has never been addressed. Therefore, the project used advanced protocols of neuronal

differentiation from human pluripotent stem cells to investigate the effects of PS1-FAD mutants on autophagy.

The results of this study revealed essential roles of PS1 in the regulation of autophagic initiation and lysosomal activity, which could be relevant to the mechanism how PS1 mutations induce and/or accelerate the pathogenesis of AD.

4.2.1. Characterization of the FAD-associated PS1 mutant cell models

This study used neuronal cultures differentiated from iPSC and ESC. iPSC were generated from one woman with familial AD (two clones), who carries an A79V substitution in one allele of the PS1 gene that results in autosomal-dominant AD (Larner and Doran, 2006). The age of biopsy was 65 and the patient had advanced stage of AD already several years before. Ctr1 and Ctr2 were generated from two healthy men with the ages of biopsy were 34 and 33 (Mertens et al., 2013). The protocols of neuronal differentiation and characterization of neuronal cultures were described previously (Falk et al., 2012; Koch et al., 2009b; Mertens et al., 2013). Particularly, the established iPSC lines indicated sustained silencing of the reprogramming transgenes, maintained a normal karyotype, expressed the pluripotency-associated markers alkaline phophatase AP, OCT4, TRA1-60 and TRA1-81, and could develop teratomas (ectodermal, mesodermal and endodermal lineages) upon in vivo transplantation (Mertens et al., 2013). In neuronal cultures, the efficiency of neuronal differentiation was comparable between control and AD neurons as shown by positive stainings with β-III-tubulin and Map2ab in 75-85% of cells. Additionally, the expressions of neuronal-specific APP695 variant, β- and γ-secretase complex-associated genes were similar between control and AD neurons. Moreover, the properties of functional neurons and maturation were also confirmed (Falk et al., 2012; Koch et al., 2009b; Mertens et al., 2013). Overall, the differentiation was similar between control and AD neurons in the morphology, basic electrophysiological function, and differentiation efficiency (Mertens et al., 2013).

Further immunoblot analysis revealed comparable expression levels of characteristic PS1-NTF between control and AD neurons. Additionally, PS1-dependent γ-secretase activity was elucidated via the processing of APP-CTFs. Notably, the expression levels of APP-CTFs were similar between control and AD neurons. Importantly, previous study with the same cell models has shown an increased Aβ42/Aβ40 ratio due to a decreased Aβ40 levels in AD neurons (Mertens et al., 2013), indicating a partial loss of γ-secretase activity in PS1AV mutant as shown in other PS1-FAD mutations. Collectively, the neuronal cultures originated from fibroblasts of healthy individuals and an AD patient carrying PS1AV mutant show neuronal features and recapitulate disease phenotypes of FAD-linked mutations of PS1.

Nowadays, our knowledge of Alzheimer's disease pathogenesis is seemingly limited by challenges in obtaining AD brain biopsies. Moreover, murine models do not recapitulate completely the human

pathological phenotype at the molecular level (Koch et al., 2009a; Wichterle and Przedborski, 2010). Therefore, these difficulties may be overcome by reprogramming primary cells from AD patients into iPSC and then subsequently differentiate iPSC into functional neurons. The differentiation protocol not only maintains endogenous genome of the patients and transcriptional control mechanisms, but also recapitulates in vitro important events during disease development (Byers et al., 2012).

Due to the limitation in the clonal numbers of the PS1 mutations for iPSC generation, ESC-derived lt-NES were lentivirally transduced with different PS1 variants including PS1WT, the catalytically inactive variant PS1DN and the two FAD-linked mutations PS1LP and PS1AV to extend the study. Among these FAD-associated mutations, PS1LP is a very aggressive form which causes an onset of AD already during the second decade of life (Moehlmann et al., 2002), whereas PS1AV is a milder mutant which causes the age of onset at between 50 and 60 (Finckh et al., 2000). The ESC-derived model with overexpression of PS1 variants has been well described by assessing neuronal morphology, electrophysiology and differentiation efficiency (Koch et al., 2012).

Here, overexpression of PS1 in transgenic cells was approximately three-fold above endogenous PS1 levels. Importantly, the transgenic cells demonstrated endoproteolytic processing as shown by the predominant expression of PS1-CTFs in PS1WT and PS1-FAD mutant cells, whereas suppressed expression of PS1-CTFs in PS1DN cells. Moreover, analysis of endogenous APP processing indicated altered γ-secretase activity in PS1 mutant cell lines. As expected, expression of the inactive PS1DN resulted in a strong accumulation of APP-CTFs. Importantly, the PS1LP and PS1AV expressing cells also showed accumulation of APP-CTFs, although to a weaker extent as compared to the inactive PS1DN mutant. Importantly, as reported previously, the PS1LP mutant increased Aβ42/Aβ40 ratio due to a decreased of Aβ40 secretion, indicating a partial loss of γ-secretase activity (Koch et al., 2012). However, Aβ measurements in this study revealed unchanged Aβ42/Aβ40 ratio PS1AV cells, although Aβ40 secretion was significantly suppressed. This might be explained by the fact that overexpression of PS1AV strongly increased APP-CTF accumulation, suggesting a strong loss of γ-secretase activity.

Collectively, these findings illustrated the recapitulation of certain AD related phenotypes in neuronal models. Together with earlier reports, neurons expressing PS1 variants are proven as useful and reliable models to investigate cellular pathologies of AD in association with PS1 mutations. In addition, these neuronal cultures can provide a relevant platform for screening AD-modifying drugs, and supply postmortem and animal-based studies.

To further allow assessment of cell type-specific and general effects of PS1 on autophagy, MEF completely lacking PS1 and PS2 (MEF PSdKO) were used as parental cell line to transduce with lentivectors carrying human PS1WT and the catalytically inactive form of PS1 that lacks the crucial, catalytic site aspartate residues PS1D257A (PS1DA). Importantly, the re-expression of PS1WT and

PS1DA in MEF PSdKO allowed to distinguish PS1 activity dependent and independent effects. Additionally, MEF were included in the study for immunocytochemical analysis, because the shape of neurons limits assessment of intracellular vesicular visualization.

4.2.2. PS1 mutants and PS deficiency impair the metabolism of long-lived proteins

To investigate the role of FAD-linked mutations of PS1 on autophagic function, metabolism of $[^{35}S]$ L-methionine radiolabeled long-lived proteins was initially elucidated in iPSC-DN. Long-lived proteins are supposed to be degraded in lysosomes via autophagosomes. Notably, two independent methods of quantification revealed unchanged short-lived protein degradation between control and AD neurons. Interestingly, degradation of long-lived proteins was prevented in AD neurons. In other words, the FAD-linked PS1AV mutation does not affect UPS, but diminished autophagic function.

In addition, to verify a general involvement of PS1 in the global protein metabolism in neurons, the same experiment was performed in ESC-DN overexpressing PS1WT and PS1DN. Notably, loss of γ-secretase activity by overexpression of PS1DN also impaired the protein turn-over. This result further supports an involvement of γ-secretase activity in global protein metabolism during autophagy.

These observations in neurons derived from human pluripotent stem cells are in agreement with earlier reports in which growing genetic and biochemical evidence have identified lysosomal proteolysis failure as the principal basis for autophagy dysfunction in AD (Cataldo et al., 2004; Lee et al., 2010; Yang et al., 2011). Similarly, Lee et al demonstrated lower turn-over of long-lived proteins in human fibroblasts carrying different PS1-FAD mutants, while short-lived proteins were not affected (Lee et al., 2010). Thus, many lines of evidence support a critical role of PS1-FAD mutants on lysosomal capacity.

To further test a general involvement of PS1 in cellular protein metabolism, MEF expressing PS1WT or the inactive variant PS1DA were also included in this study. Interestingly, the expression of PS1WT in PSdKO cells increased the turn-over of long-lived proteins, whereas expression of PS1DA had no effect. Thus, the loss of γ-secretase activity reduces proteolysis of long-lived proteins in different cell types, suggesting a general role this protease complex in the regulation of cellular protein metabolism.

The mechanisms that underlie autophagic dysfunction in PS1 mutant cells, however, remain controversial. Since autophagy is a multiple-step process, the defect of autophagic capacity might result from defective autophagosomal synthesis, autophagosome-lysosome fusion or lysosomal function. Additionally, lysosomal dysfunction, could also be a consequence of reduced lysosomal acidification, accumulation of undigested by-products and decreased content or activity of lysosomal hydrolases (Wong and Cuervo, 2010).

4.2.2.1. Impaired induction of autophagy in PS1 mutant cells

To elucidate potential mechanisms contributing to the impaired proteolysis of long-lived proteins in cells expressing FAD-linked PS1 mutants or complete loss of γ-secretase activity, proteins involved in the regulation of autophagy were analyzed in more detail. Interestingly, the data obtained with iPSC-DN revealed a significant decrease in LC3-II levels and increase in LC3-I levels in AD neurons. This suggests a reduction of the conversion from LC3-I to LC3-II or autophagosomal synthesis in PS1AV mutant cells. Additionally, the data also revealed a significant decrease of Bcl-2 phosphorylation at Ser70 in AD neurons. Since the phosphorylation of Bcl-2 at Thr69, Ser70 and Ser87 results in its dissociation from BECN1 and promote autophagosomal synthesis (Laplante and Sabatini, 2009; Levine and Kroemer, 2008; Wei et al., 2008), these findings indicate a reduced induction of autophagy in AD neurons expressing PS1AV mutant.

Consistent with observations in iPSC-DN endogenously expressing the PS1AV mutant, ESC-DN overexpressing FAD-linked PS1 mutants PS1LP and PS1AV or the inactive PS1 variant also revealed reduced LC3-II and Bcl-2 phosphorylation levels as compared to PS1WT cells. To visualize autophagosomal formation, fluorescence-microscopy analysis was performed. Notably, endogenous LC3-II reactive structure in neurons derived from both iPSC and ESC were scarce and only very faint, probably indicating a high constitutive autophagic flux in neurons as described previously (Boland et al., 2008; Komatsu et al., 2007a). This might also explain the low LC3-II levels as compared to LC3-I levels observed in immunoblot analyses from these neurons. However, overexpression of RFP-LC3 revealed the presence of autophagic vesicles in ESC-DN. Interestingly, consistent with immunoblotting results, the data showed a significantly decreased number of RFP-LC3 positive punctae in cells expressing FAD-linked PS1 mutants or a complete loss of γ-secretase activity.

Moreover, the involvement of PS1 protein and γ-secretase activity in autophagic induction was verified in MEF. Indeed, re-expression of PS1WT in a PSdKO background significantly elevated both LC3-II and phosphorylated Bcl-2 levels, whereas the re-expression of the catalytically inactive PS1DA had no effect. Additionally, immunofluorescence microscopy also supported this conclusion by showing significant increase of LC3 positive punctae in PS1WT expressing, but not in PS1DA expressing cells. Thus, the data confirm the observed effects in ESC-DN, further supporting a γ-secretase–activity dependent function of PS1 in autophagy. Importantly, quantification of acquired images suggested an unchanged efficiency of autophagosome-lysosome fusion between PS1 variants. However, further investigations are needed to confirm this conclusion. Collectively, the data from ESC-DN and MEF expressing different variants of PS1 indicate an involvement of the γ-secretase in autophagy.

Due to the possibility that the observed cellular changes in LC3 might be attributed to transcriptional changes of LC3 mRNA levels, both conventional and quantitative RT-PCR were

performed in neurons and MEF expressing PS1 variants. However, LC3 mRNA levels were very similar in cells expressing different PS1 variants (data not shown), suggesting that PS1 is not involved in transcriptional control of LC3.

Taken together, human neuronal cultures and MEF indicate the inhibition of autophagic induction in FAD-associated mutations of PS1 or complete loss of γ-secretase activity, likely contributing to the impaired proteolysis of long-lived proteins. The decreased autophagosomal synthesis in PS1 mutant cells is consistent with previous reports indicating a reduced autophagic induction in AD brains. Indeed, it was reported that the increased autophagy-inhibitory mTOR signaling and strongly decreased BECN1 levels were observed in AD brain (Pickford et al., 2008; Yang et al., 2011). On the other hand, the apparent absence of LC3-II and autophagic vesicles in neurons expressing PS1 mutants are contradictory with observations in AD brains where the accumulation of autophagic vesicles is highly abundant in dystrophic neurites (Jaeger and Wyss-Coray, 2009; Kundu and Thompson, 2008; Nixon et al., 2005). For example, AD brains and a mouse model of AD pathology (PS1/APP mice, which overexpress FAD-associated mutations of human PS1 and APP) revealed abundant autophagic vacuoles, particularly within dystrophic neurites. Additionally, autophagy was also evident in the perikarya of AD affected neurons, especially in those with neurofibrillary tangles (Nixon et al., 2005; Yu et al., 2005). Thus, a possible explanation for these contradictory observations would be the difference in autophagy between the AD brains and young in vitro differentiated neurons. In healthy brains, neurons appear to have a high constitutive autophagic activity, which leads to high rates of autophagosomal turn-over. Importantly, the brain seems to be a specially protected tissue where nutrients are constantly supplied even from other organs during starvation conditions. Therefore, the increased autophagosomes observed in the AD brains likely reflect impaired autophagosomal clearance (Boland et al., 2008; Nixon et al., 2005). However, the decrease of autophagic induction and thus in lower constitutive autophagic activity, as observed here in the young neurons expressing PS1-FAD mutants might be an early event in the progress of AD pathogenesis. Consequently, the defective autophagic induction potentially promotes the gradual accumulation of intracellular undigested by-products, toxic protein aggregates and dysfunctional organelles (Son et al., 2012). Thus, it will be interesting to investigate whether these accumulations might trigger cellular pathologies that leads to the persistence of autophagosomes as observed in AD brain upon longer differentiation or aging of neurons in vitro. Moreover, the possibility that PS1 mutants exert effects on autophagic flux and thereby lead to persistence of autophagosomes cannot be excluded.

Importantly, autophagy is an essential pro-survival pathway induced by a variety of stress factors, including nutrient deprivation, growth factor withdrawal, oxidative stress, infection, and hypoxia (Kroemer et al., 2010). These factors contribute to the etiology of multiple diseases such as cancer, stroke, heart disease, and infection (Murrow and Debnath, 2013). Upon stress, autophagy degrades

damaged proteins and organelles to maintain cellular biosynthetic capacity and ATP levels. Thus, if PS1 mutant neurons are exposed to cellular stress, the low basal autophagy in these cells could lead to the accumulation of toxic protein aggregates and damaged organelles. This ultimately promotes neuronal death (Boland and Nixon, 2006). Supportively, it has been well documented that mice lacking the Atg5 or Atg7 have decreased plasma and tissue amino acid concentrations and die within the first day after birth, which is likely due to nutrient depletion during the neonatal starvation period (Komatsu et al., 2005; Kuma et al., 2004).

Altogether, the data thus reveal a novel finding that FAD-linked PS1 mutants or complete loss of γ-secretase activity reduces autophagic induction, and that this effect contributes to impaired turn-over of long-lived proteins. Therefore, one could speculate that initiation of autophagy has an important impact on AD development. By extension, it has been well documented that the abrogation of constitutive autophagy by deletion of essential autophagic genes Atg5 or Atg7 in mice results in neurodegeneration without overexpression of any pathogenic protein, demonstrating that blocked autophagic is sufficient to induce neurodegenerative phenotypes (Hara et al., 2006; Komatsu et al., 2006). Particularly, failure in autophagic induction in these mice leads to persistence of un-engulfed cargo and promoted aggregation of intracellular components, dysfunctional organelles or toxic substances (Hara et al., 2006; Komatsu et al., 2006; Komatsu et al., 2007b). Thus, compromised autophagy might underlie the etiology of several neurodegenerative disorders (Mizushima et al., 2008; Rubinsztein et al., 2012).

Despite the data highlight the involvement of phosphorylation of Bcl-2 in autophagic induction, how PS1 regulates Bcl-2 phosphorylation is still elusive. It has been demonstrated that c Jun N-terminal kinase 1 (JNK1)-mediated multi-site phosphorylation of Bcl-2 stimulates starvation- and ceramide-induced autophagy (Pattingre et al., 2009; Wei et al., 2008). However, whether JNK1 is involved in PS1 / γ-secretase -regulated autophagy and how PS1 / γ-secretase might be linked to JNK1 activation remains to be investigated. In this regard, it is interesting to note that JNK and BH3-only members of the Bcl-2 family are phosphorylated upon activation of the P75 neurotrophin receptor (P75NTR), which is a substrate of γ-secretase (Forsyth et al., 2014).

As AD and many neurodegenerative disorders are associated with the accumulation of intracellular aggregate-prone proteins, an obvious therapeutic strategy might be to reduce the concentration of these toxic proteins. Indeed, promoting the clearance of these proteins via pharmacological induction of autophagy has proved to be a useful mechanism for protecting against their toxic effects in a range of cell and animal models (Berger et al., 2006; Ravikumar et al., 2002).

4.2.2.2. Modulation of autophagy in cells expressing different PS1 variants

To gain further insight into the functional role of PS1 in the autophagic process, cell expressing the different PS1 variants were exposed to various autophagic modulators. Importantly, induction of

autophagy by either starvation or rapamycin did not alter the conversion of LC3-I to LC3-II in both iPSC- and ESC-DN, suggesting that constitutive autophagy is already high in neurons. This is consistent with no apparent autophagic induction in the mouse brain after 48 h of food deprivation (Mizushima, 2004). Additionally, these observations are also supported by a low number of autophagosomes in the normal brain (Nixon et al., 2005) and low levels of LC3-II protein in neurons (Mizushima, 2004; Pickford et al., 2008; Yu et al., 2005) as compared with other tissues.

Since stimulation of autophagy by nutrient starvation or rapamycin could not increase the conversion from LC3-I to LC3-II in neurons, the effect of PS1 on autophagosomal formation was investigated upon inhibition of autophagosomal degradation. Interestingly, LC3-II accumulation observed upon chloroquine treatment in AD neurons was much lower than in control neurons. This indicates a reduced capacity of autophagosomal synthesis in PS1AV mutant cells.

Additionally, due to the constitutive autophagy is high in neurons, starvation-induced autophagy was alternatively investigated in MEF. By subjecting MEF expressing PS1WT and PS1DA in EBSS medium for 1 and 6 h, the results suggest both a reduction of autophagic induction and degradation in PS1DA cells upon starvation. This is indeed in agreement with previous report indicating that induction of autophagy by serum withdrawal for a short time resulted in higher LC3-II levels in MEF WT, but to a much lesser extent in MEF PS1KO (Zhang et al., 2012). Importantly, these findings also demonstrate the differences between distinct cell types in autophagic activity under basal and stimulated conditions.

Taken together, modulation of autophagy further confirms reduced autophagic induction upon loss of γ-secretase function by FAD-associated PS1 mutations or catalytically inactive PS1.

4.2.2.3. Impaired lysosomal activity in PS1 mutant cells

The impaired proteolysis of long-lived proteins in cells carrying FAD-linked PS1 mutants or a complete loss of γ-secretase activity prompted us to investigate lysosomal function in these cells. Although the initiation of autophagy has been shown to be reduced in these cells, it remains controversial to date whether lysosomal function or autophagic degradation is also affected by PS1. To address this, lysosomal function was mainly assessed via the processing of Cat D. In iPSC-DN, Cat D processing was suppressed in AD neurons, suggesting a defect of lysosomal function in PS1AV mutant cells. Together with the accumulation of the autophagic substrate p62 in AD neurons, these data imply an impaired autophagic degradation in PS1AV mutant, which would also contribute to decreased turn-over of long-lived proteins.

By extension, control and AD neurons were treated with chloroquine to inhibit lysosomal acidification. Interestingly, chloroquine significantly prevented Cat D processing in control neurons, whereas less effect was observed in AD neurons. Thus, the data indicate defective lysosomal acidification in PS1AV mutant, contributing to impaired autophagic turn-over. Consistently, ESC-DN

expressing FAD-associated PS1 mutants and PS1DN also revealed a decreased Cat D processing and an increased p62 accumulation. Collectively, the data indicate a defective lysosomal function in PS1-FAD mutants and inactive variant PS1DN in both iPSC- and ESC-DN. Previous study has attributed the dysfunction of lysosome in PS deficient cells to impairment of lysosomal acidification (Lee et al., 2010). However, to verify changes in lysosomal acidity in these cells, more experiments are needed. For example, acidic organelles can be labled with LysoTracker dye to visualize in fluorescence microscopy, with LysoSensor dye or nanoparticle sensor to measure pH.

Additionally, lysosomal function was also assessed in MEF PSdKO, re-expressing functional PS1WT or inactive PS1DA. Surprisingly, both Cat D processing and P62 levels were comparable between PS1 variants, suggesting that lysosomal function is not affected by PS1 in MEF. Thus, the impaired turn-over of long-lived proteins in MEF PSdKO and PS1DA is unlikely caused by defective lysosomal function, it is rather caused by reduced autophagic induction in these cells. Together with observations in neurons, these findings suggest a cell type-dependent effect on Cat D processing or lysosomal acidification as previously proposed.

Taken together, it appears that PS1 mutants not only exert its inhibitory effect on the initiation of autophagy, but also inhibit the completion of autophagy via impairment of lysosomal function, at least in cultured neurons. Of course, it cannot be excluded that PS1 also exerts functions in the fusion between autophagosomes with endosomal-lysosomal vesicles, or the regulation of other major lysosomal proteases. Therefore, more investigations are needed to figure out the comprehensive roles of PS1 in autophagy.
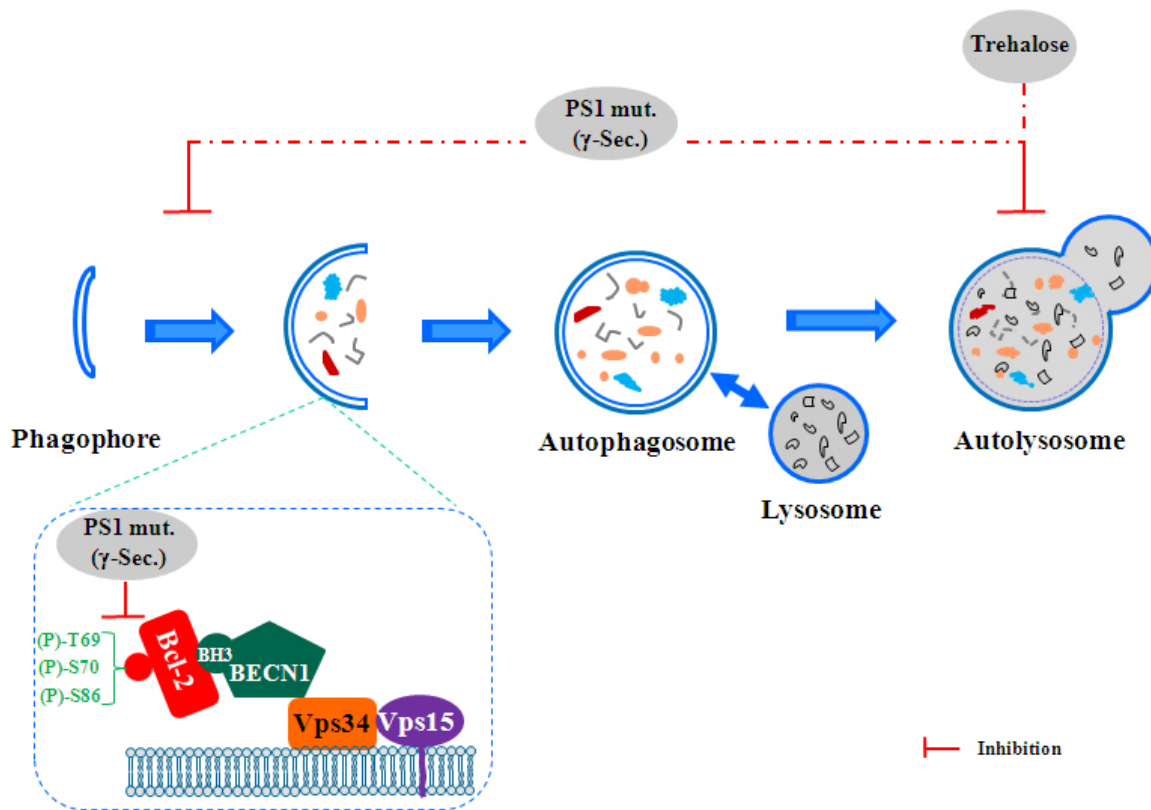
Figure 4.1: Inhibitory targets of trehalose and FAD-linked PS1 mutants (PS1 mut.)/loss of γ-secretase (γ-sec.) activity on autophagic pathway. Trehalose impairs lysosomal acidification. PS1-FAD mutants or loss of γ-secretase activity impairs both autophagosomal synthesis and Cat D processing-dependent lysosomal function in human differentiated neurons. PS1/γ-secretase targets the BECN1/Bcl-2 interaction via phosphorylation of Bcl-2.

Since FAD-associated mutations of PS1 are widely believed to cause loss-of-function of the γ-secretase activity thereby leading to the overall reduction of Aβ levels, the persistence of amyloid plaques observed in FAD patients carrying PS mutations suggests the dysfunction of other regulatory mechanisms (Cacquevel et al., 2012). Together with our findings, the accumulation of amyloid plaques is likely attributed to autophagic dysfunction. Supportively, autophagic activation by rapamycin or nutrient starvation leads to increased Aβ production in autophagic vesicles, which is principally delivered to lysosomes where it is degraded (Bahr and Bendiske, 2002; Florez-McClure et al., 2007; Yu et al., 2005). In addition, the deletion of Cat D leads to an increase of cerebral brain Aβ42 levels threefold higher than those in wild-type littermates (Saido and Leissring, 2012). Similarly, Cat B deletion elevates Aβ levels in mice brain (Mueller-Steiner et al., 2006). Moreover, the severe autophagic pathology not only appears in cases of EO-FAD, but also in later onset SAD (Nixon et al., 2008). This dysfunction could initiate a pathogenic cascade by impaired recycling of metabolites and accumulation of cellular waste products ultimately leading to neurodegeneration. Indeed, neurons in the AD brain accumulate intraneuronal Aβ, and recent data suggest that intracellular Aβ causes neurodegeneration by increased ER stress, endosomal/lysosomal leakage

and dysfunction mitochondria (Umeda et al., 2011). Especially, CNS neurons appear to be particularly dependent on lysosome function for eliminating Aβ from endocytic-autophagic pathways (LeBlanc and Goodyer, 1999). Interestingly, recent study provided evidence that autophagosomes can fuse with endosomes and subsequently with plasma membrane to release their contents and Aβ into extracellular fluids (Nilsson et al., 2013). Thus, autophagy plays important roles in both intracellular degradation and secretion of Aβ, thereby affecting Aβ plaque formation. Recently, growing evidence has also indicated that autophagy substantially contributes to the turn-over of tau proteins (Brown et al., 2005; Feuillette et al., 2005; Hamano et al., 2008; Lee et al., 2013; Wang et al., 2010). Collectively, autophagy plays a crucial role in AD pathology and could be a potential AD drug target.

Thus, understanding the roles of FAD-linked mutations of PS1 on autophagic initiation and flux has important implications for AD research. In autophagy, the lysosome is a key subcellular organelle in the execution of the degradation of different substrates. However, at the present, little is known whether lysosomal function is controlled during the process of autophagy. A very recent study has provided evidence that inactivation of mTOR complex 1 enhances lysosomal function although it is also known to triggers autophagosomal synthesis. Particularly, suppression of mTOR activity by starvation or two mTOR catalytic inhibitors (PP242 and Torin1) leads to increased lysosomal activity (Zhou et al., 2013). Thus, regulation of mTOR complex 1 inactivation might be a potential therapeutic target for autophagic dysfunction-related AD and other disorders. Additionally, genetic deletion of the endogenous lysosomal-associated cysteine protease inhibitor, cystatin B, has restored lysosomal clearance in autophagy-deficient TgCRND8 mice overexpressing mutant human APP695 (Yang et al., 2011). Moreover, it has been also indicated that autophagosome-lysosome fusion is crucial for lysosomal activation (Zhou et al., 2013).

Future perspectives

AD is increasingly being recognized as one of the most important medical and social problems in older people world-wide (Yiannopoulou and Papageorgiou, 2013). To date, there are no effective pharmacotherapeutic options for prevention or cure of AD, only symptomatic treatments exist for this disease. On the basis of findings on AD pathogenesis, novel treatments are challenged by the multiple pathogenic changes during the disease development, including the deposition of extracellular amyloid plaques and intracellular neurofibrillary tangles, inflammation, oxidative damage, iron deregulation and cholesterol metabolism (Yiannopoulou and Papageorgiou, 2013). In fact, the hypothesis that Aβ aggregation leads to toxic oligomeres has stimulated broad therapeutic efforts to suppress Aβ generation or to remove amyloid plaques from the brain (Golde, 2005). For example, the passive immunotherapy with anti-Aβ antibodies bapineuzumab and solanezumab has been used for phase III clinical trial in North America. Solanezumab aimed to recognize and block amyloid-β before it forms plaques. However, in patients with mild and moderate forms of disease,

solanezumab failed to slowdown the decline in memory and other cognitive measures. With bapineuzumab, the antibody aimed to stimulate the immune system to clear plaques from the brain, but again, there was no cognitive benefit overall (Callaway, 2012). Additionally, three more studies have been begun in 2013 to test whether anti-amyloid drugs can forestall early symptoms of Alzheimer's and arrest cognitive decline. These tests are carried out in patients who, on the basis of genetic predisposition or Aβ levels, have been identified as being at increased risk of developing the disease (Callaway, 2012). The major trial focuses on a large Colombian cohort that shares a rare genetic mutation PS1 E280A predisposing to develop Alzheimer's symptoms around age 45 (Callaway, 2012). Although the cognitive benefits of these new trials have not been elucidated, the failures of the previous trials with Aβ passive immunization suggest the insufficiency of targeting plaques or extracellular Aβ in PS1 mutant cases. Therefore, AD might be prevented or effectively treated by a combination of therapies aiming to reduce the formation and removal of both amyloid plaques and neurofibrillary tangles. For many diseases, the upregulation of autophagy is a promising therapeutic target to remove the toxic aggregate or misfolded proteins (Hochfeld et al., 2013). Therefore, combining knowledge of the potential mechanisms for the formation of amyloid plaques and neurofibrillary tangles with knowledge on the role of autophagy in AD pathogenesis, might help to develop novel strategies for therapy or prevention of this disease.

5. Abbreviations

Abbreviation	Full name
Aβ	Amyloid beta
AD	Alzheimer's disease
ADAM	A disintegrin and metalloprotease
AICD	APP intracellular domain
APH-1	Anterior pharynx defective-1
Apo E	Apolipoprotein E
APP	β-Amyloid precursor protein
sAPPα	Soluble APP generated by α-secretase cleavage
sAPPβ	Soluble APP generated by β-secretase cleavage
APP-CTFs	Carboxy-terminal fragments of APP
APP-CTFα/CTFβ	APP C-terminal fragment generated by α-/β-secretase cleavage
APS	Ammonium persulfate
ATG	Autophagy-related gene
BACE	β-site APP cleaving enzyme
Bcl-2	B-cell lymphoma 2
BDNF	Brain-derived neurotrophic factor
BECN1	Beclin 1
BSA	Bovine serum albumin
cDNA	Complementary DNA
CNS	Central nervous system
C83	APP C-terminal fagment generated by α-secretase cleavage
C99	APP C-terminal fagment generated by β-secretase cleavage
DAPI	4',6-Diamidino-2-phenylindole
DAPT	N-[N-(3,5-Difluorophenacetyl)-L-alanyl]-S-phenylglycine t-butyl ester
dKO	Double knock-out
DMSO	Dimethyl sulfoxide
DMEM	Dulbecco's Modified Eagle's Medium
DNA	Deoxy ribonucleic acid
dNTPs	Nucleoside triphosphate
Dox	Doxycycline
DTT	Dithiothreitol
EBSS	Earle's Balanced Salt Solution
ECL	Enhanced chemiluminescence
EDTA	Ethylenediamintetraacetic acid
ER	Endoplasmic reticulum
FAD	Familial Alzheimer's disease
FCSi	Fatal calf serum heat-inactivated

FL	Full-length
GFP	Green fluorescent protein
HBSS	Hank's balanced salt solution
HEK	Human embryonic kidney cells
HEPES	4-(2-hydroxyethyl)-1-piperazineethanesulfonic acid
hES cells	Human embryonic stem cells
hPS cells	Human pluripotent stem cells
HRP	Horse radish peroxidase
HD	Huntington's disease
ICC	Immunocytochemistry
ICD	Intracellular domain
IP	Immunoprecipitation
iPS cells	Induced pluripotent stem cells
LB medium	Lauria-Bertani medium
Lt-NES cells	Long-term self-renewing neuroepithelial stem cells
MAPK	Mitogen activated protein kinase
mRNA	Messenger RNA
mTOR	Mammalian target of rapamycin
NFTs	Neurofibrillary tangles
NMDA	N-methyl-D-aspartate
NSC	Neural stem cells
NTF	N-terminal fragment
PAGE	Polyacrylamid gel electrophoresis
PBS	Phosphate buffered saline
PD	Parkinson's disease
PCR	Polymerase chain reaction
PEN-2	Presenilin enhancer-2
Pen/Strep	Penicillin/Streptomycin
PFA	Paraformaldehyde
PHF	Paired helical filaments
PI	Phosphatidylinositol
PI3K	Phosphatidylinositol-3 kinase
PI3P	Phosphatidylinositol-3-phosphate
PM	Plasma membrane
PS	Presenilin
PVDF	Polyvinylidine Fluoride
RFP	Red fluorescent protein
RNA	Ribonucleic acid
RT-PCR	Reverse trascriptase-PCR
SDS	Sodium dodecyl sulfate

TBS	Tris buffered saline
TEMED	N,N,N',N'-Tetramethylethylenediamine
Tet-On	Tetracycline regulatable gene induction system
TGN	Trans-Golgi network
WB	Western blot
WT	Wild type

Amino acid abbreviations

Amino acid	3-letter	1-letter
Alanine	Ala	A
Arginine	Arg	R
Asparagine	Asn	N
Aspartic acid	Asp	D
Cysteine	Cys	C
Glutamine	Gln	Q
Glutamic acid	Glu	E
Glycine	Gly	G
Histidine	His	H
Isoleucine	Ile	I
Leucine	Leu	L
Lysine	Lys	K
Methionine	Met	M
Phenylalanine	Phe	F
Proline	Pro	P
Serine	Ser	S
Threonine	Thr	T
Tryptophan	Trp	W
Tyrosine	Tyr	Y
Valine	Val	V

6. Abstract

Alzheimer's disease (AD) is the most common form of neurodegenerative diseases, which is associated with extracellular deposits of the amyloid β-peptide (Aβ) and intraneuronal aggregates of hyperphosphorylated tau protein in the brain. Aβ is generated by cleavage of APP C-terminal fragment β (APP-CTFβ) by γ-secretase. Thus, metabolism of APP-CTF is crucial for amyloid plaque deposition. Although many studies have been focused on understanding proteolytic cleavage of APP and amyloid plaque deposition, less is known about mechanisms that control the cellular metabolism of APP and its derivatives APP-CTFs. Autophagy plays an important role in intracellular protein quality control, especially of long-lived, misfolded and aggregated proteins (Nixon et al., 2008). Dysfunction of autophagy is implicated in the pathogenesis of AD-associated neurodegeneration (Kundu and Thompson, 2008).

This study revealed an important role of autophagy in APP-CTF metabolism by using different autophagic modulations, such as nutrient starvation medium, lipid accumulation, and lysosomal inhibition. In the course of this study, the function of trehalose, which is well recognized as a stimulator of autophagy, has been revisited. Unexpectedly, this study demonstrated rather an inhibitory role of trehalose on lysosomal activity and thus, autophagic flux.

The main project of this dissertation focused on the role of PS1 mutants on autophagy. Mutations in PS1 are the major cause of early-onset familial AD (EO-FAD). Recently, PS proteins have been shown to play role in lysosomal or autophagic capacity. However, these studies used non-neuronal models and the results were controversial. By using various cell models carrying different PS1 variants, ranging from human neurons derived from induced pluripotent or embryonic stem cells to mouse embryonic fibroblasts, the study indicated a decreased turn-over of long-lived proteins or autophagic capacity in FAD-linked PS1 mutant cells. Particularly, PS1 mutants or genetic deficiency reduced autophagic initiation via decreased phosphorylation of Bcl-2, which regulates the interaction with Beclin-1, and thereby decreased autophagosome formation. Additionally, PS1 mutant cells also revealed decreased autophagic flux by impairment of lysosomal function. Thus, the results support the hypothesis that autophagy is defective in AD brains, and elucidated two distinct effects of PS1 on induction and completion of autophagy. The findings further indicate that autophagy is an interesting targeted for therapeutic or preventive strategies in AD treatment.

7. References

Aguib, Y., Heiseke, A., Gilch, S., Riemer, C., Baier, M., Schatzl, H.M., and Ertmer, A. (2009). Autophagy induction by trehalose counteracts cellular prion infection. Autophagy *5*, 361-369.

Allinson, T.M., Parkin, E.T., Turner, A.J., and Hooper, N.M. (2003). ADAMs family members as amyloid precursor protein alpha-secretases. J Neurosci Res *74*, 342-352.

Alonso, A.C., Grundke-Iqbal, I., and Iqbal, K. (1996). Alzheimer's disease hyperphosphorylated tau sequesters normal tau into tangles of filaments and disassembles microtubules. Nat Med *2*, 783-787.

Alonso, A.D., Grundke-Iqbal, I., Barra, H.S., and Iqbal, K. (1997). Abnormal phosphorylation of tau and the mechanism of Alzheimer neurofibrillary degeneration: sequestration of microtubule-associated proteins 1 and 2 and the disassembly of microtubules by the abnormal tau. Proc Natl Acad Sci U S A *94*, 298-303.

Andersson, E., Tryggvason, U., Deng, Q., Friling, S., Alekseenko, Z., Robert, B., Perlmann, T., and Ericson, J. (2006). Identification of intrinsic determinants of midbrain dopamine neurons. Cell *124*, 393-405.

Armstrong, R.A. (2011). Spatial patterns of beta-amyloid (Abeta) deposits in familial and sporadic Alzheimer's disease. Folia Neuropathol *49*, 153-161.

Auer, I.A., Schmidt, M.L., Lee, V.M., Curry, B., Suzuki, K., Shin, R.W., Pentchev, P.G., Carstea, E.D., and Trojanowski, J.Q. (1995). Paired helical filament tau (PHFtau) in Niemann-Pick type C disease is similar to PHFtau in Alzheimer's disease. Acta Neuropathol *90*, 547-551.

Axe, E.L., Walker, S.A., Manifava, M., Chandra, P., Roderick, H.L., Habermann, A., Griffiths, G., and Ktistakis, N.T. (2008). Autophagosome formation from membrane compartments enriched in phosphatidylinositol 3-phosphate and dynamically connected to the endoplasmic reticulum. J Cell Biol *182*, 685-701.

Bach, J.H., Chae, H.S., Rah, J.C., Lee, M.W., Park, C.H., Choi, S.H., Choi, J.K., Lee, S.H., Kim, Y.S., Kim, K.Y., *et al.* (2001). C-terminal fragment of amyloid precursor protein induces astrocytosis. J Neurochem *78*, 109-120.

Backer, J.M. (2008). The regulation and function of Class III PI3Ks: novel roles for Vps34. Biochem J *410*, 1-17.

Bahr, B.A., and Bendiske, J. (2002). The neuropathogenic contributions of lysosomal dysfunction. J Neurochem *83*, 481-489.

Bain, G., Kitchens, D., Yao, M., Huettner, J.E., and Gottlieb, D.I. (1995). Embryonic stem cells express neuronal properties in vitro. Dev Biol *168*, 342-357.

Bales, K.R. (2010). Brain lipid metabolism, apolipoprotein E and the pathophysiology of Alzheimer's disease. Neuropharmacology *59*, 295-302.

Bales, K.R., Verina, T., Cummins, D.J., Du, Y., Dodel, R.C., Saura, J., Fishman, C.E., DeLong, C.A., Piccardo, P., Petegnief, V., *et al.* (1999). Apolipoprotein E is essential for amyloid deposition in the APP(V717F) transgenic mouse model of Alzheimer's disease. Proc Natl Acad Sci U S A *96*, 15233-15238.

Basi, G., Frigon, N., Barbour, R., Doan, T., Gordon, G., McConlogue, L., Sinha, S., and Zeller, M. (2003). Antagonistic effects of beta-site amyloid precursor protein-cleaving enzymes 1 and 2 on beta-amyloid peptide production in cells. J Biol Chem *278*, 31512-31520.

Bauer, P., Balding, D.J., Klunemann, H.H., Linden, D.E., Ory, D.S., Pineda, M., Priller, J., Sedel, F., Muller, A., Chadha-Boreham, H.*, et al.* (2013). Genetic screening for Niemann-Pick disease type C in adults with neurological and psychiatric symptoms: findings from the ZOOM study. Hum Mol Genet *22*, 4349-4356.

Bayer, T.A., Cappai, R., Masters, C.L., Beyreuther, K., and Multhaup, G. (1999). It all sticks together--the APP-related family of proteins and Alzheimer's disease. Mol Psychiatry *4*, 524-528.

Beel, A.J., and Sanders, C.R. (2008). Substrate specificity of gamma-secretase and other intramembrane proteases. Cell Mol Life Sci *65*, 1311-1334.

Benes, P., Vetvicka, V., and Fusek, M. (2008). Cathepsin D--many functions of one aspartic protease. Crit Rev Oncol Hematol *68*, 12-28.

Bennett, B.L., Sasaki, D.T., Murray, B.W., O'Leary, E.C., Sakata, S.T., Xu, W., Leisten, J.C., Motiwala, A., Pierce, S., Satoh, Y.*, et al.* (2001). SP600125, an anthrapyrazolone inhibitor of Jun N-terminal kinase. Proc Natl Acad Sci U S A *98*, 13681-13686.

Berger, Z., Ravikumar, B., Menzies, F.M., Oroz, L.G., Underwood, B.R., Pangalos, M.N., Schmitt, I., Wullner, U., Evert, B.O., O'Kane, C.J.*, et al.* (2006). Rapamycin alleviates toxicity of different aggregate-prone proteins. Hum Mol Genet *15*, 433-442.

Bezprozvanny, I., and Mattson, M.P. (2008). Neuronal calcium mishandling and the pathogenesis of Alzheimer's disease. Trends Neurosci *31*, 454-463.

Bjorkoy, G., Lamark, T., Brech, A., Outzen, H., Perander, M., Overvatn, A., Stenmark, H., and Johansen, T. (2005). p62/SQSTM1 forms protein aggregates degraded by autophagy and has a protective effect on huntingtin-induced cell death. J Cell Biol *171*, 603-614.

Blurton-Jones, M., Kitazawa, M., Martinez-Coria, H., Castello, N.A., Muller, F.J., Loring, J.F., Yamasaki, T.R., Poon, W.W., Green, K.N., and LaFerla, F.M. (2009). Neural stem cells improve cognition via BDNF in a transgenic model of Alzheimer disease. Proc Natl Acad Sci U S A *106*, 13594-13599.

Boissart, C., Poulet, A., Georges, P., Darville, H., Julita, E., Delorme, R., Bourgeron, T., Peschanski, M., and Benchoua, A. (2013). Differentiation from human pluripotent stem cells of cortical neurons of the superficial layers amenable to psychiatric disease modeling and high-throughput drug screening. Transl Psychiatry *3*, e294.

Boland, B., Kumar, A., Lee, S., Platt, F.M., Wegiel, J., Yu, W.H., and Nixon, R.A. (2008). Autophagy induction and autophagosome clearance in neurons: relationship to autophagic pathology in Alzheimer's disease. J Neurosci *28*, 6926-6937.

Boland, B., and Nixon, R.A. (2006). Neuronal macroautophagy: from development to degeneration. Mol Aspects Med *27*, 503-519.

Borchelt, D.R., Thinakaran, G., Eckman, C.B., Lee, M.K., Davenport, F., Ratovitsky, T., Prada, C.M., Kim, G., Seekins, S., Yager, D.*, et al.* (1996). Familial Alzheimer's disease-linked presenilin 1 variants elevate Abeta1-42/1-40 ratio in vitro and in vivo. Neuron *17*, 1005-1013.

Brown, M.R., Bondada, V., Keller, J.N., Thorpe, J., and Geddes, J.W. (2005). Proteasome or calpain inhibition does not alter cellular tau levels in neuroblastoma cells or primary neurons. J Alzheimers Dis *7*, 15-24.

Brustle, O., Spiro, A.C., Karram, K., Choudhary, K., Okabe, S., and McKay, R.D. (1997). In vitro-generated neural precursors participate in mammalian brain development. Proc Natl Acad Sci U S A *94*, 14809-14814.

Buerger, K., Ewers, M., Pirttila, T., Zinkowski, R., Alafuzoff, I., Teipel, S.J., DeBernardis, J., Kerkman, D., McCulloch, C., Soininen, H.*, et al.* (2006). CSF phosphorylated tau protein correlates with neocortical neurofibrillary pathology in Alzheimer's disease. Brain *129*, 3035-3041.

Buerger, K., Teipel, S.J., Zinkowski, R., Blennow, K., Arai, H., Engel, R., Hofmann-Kiefer, K., McCulloch, C., Ptok, U., Heun, R.*, et al.* (2002). CSF tau protein phosphorylated at threonine 231 correlates with cognitive decline in MCI subjects. Neurology *59*, 627-629.

Buxbaum, J.D., Gandy, S.E., Cicchetti, P., Ehrlich, M.E., Czernik, A.J., Fracasso, R.P., Ramabhadran, T.V., Unterbeck, A.J., and Greengard, P. (1990). Processing of Alzheimer beta/A4 amyloid precursor protein: modulation by agents that regulate protein phosphorylation. Proc Natl Acad Sci U S A *87*, 6003-6006.

Byers, B., Lee, H.L., and Reijo Pera, R. (2012). Modeling Parkinson's disease using induced pluripotent stem cells. Curr Neurol Neurosci Rep *12*, 237-242.

Caccamo, A., Magri, A., Medina, D.X., Wisely, E.V., Lopez-Aranda, M.F., Silva, A.J., and Oddo, S. (2013). mTOR regulates tau phosphorylation and degradation: implications for Alzheimer's disease and other tauopathies. Aging Cell *12*, 370-380.

Cacquevel, M., Aeschbach, L., Houacine, J., and Fraering, P.C. (2012). Alzheimer's disease-linked mutations in presenilin-1 result in a drastic loss of activity in purified gamma-secretase complexes. PLoS One *7*, e35133.

Cai, H., Wang, Y., McCarthy, D., Wen, H., Borchelt, D.R., Price, D.L., and Wong, P.C. (2001). BACE1 is the major beta-secretase for generation of Abeta peptides by neurons. Nat Neurosci *4*, 233-234.

Cai, X.D., Golde, T.E., and Younkin, S.G. (1993). Release of excess amyloid beta protein from a mutant amyloid beta protein precursor. Science *259*, 514-516.

Caiazzo, M., Dell'Anno, M.T., Dvoretskova, E., Lazarevic, D., Taverna, S., Leo, D., Sotnikova, T.D., Menegon, A., Roncaglia, P., Colciago, G.*, et al.* (2011). Direct generation of functional dopaminergic neurons from mouse and human fibroblasts. Nature *476*, 224-227.

Callaway, E. (2012). Alzheimer's drugs take a new tack. Nature *489*, 13-14.

Campion, D., Dumanchin, C., Hannequin, D., Dubois, B., Belliard, S., Puel, M., Thomas-Anterion, C., Michon, A., Martin, C., Charbonnier, F.*, et al.* (1999). Early-onset autosomal dominant Alzheimer disease: prevalence, genetic heterogeneity, and mutation spectrum. Am J Hum Genet *65*, 664-670.

Caporaso, G.L., Takei, K., Gandy, S.E., Matteoli, M., Mundigl, O., Greengard, P., and De Camilli, P. (1994). Morphologic and biochemical analysis of the intracellular trafficking of the Alzheimer beta/A4 amyloid precursor protein. J Neurosci *14*, 3122-3138.

Casarejos, M.J., Solano, R.M., Gomez, A., Perucho, J., de Yebenes, J.G., and Mena, M.A. (2011). The accumulation of neurotoxic proteins, induced by proteasome inhibition, is reverted by trehalose, an enhancer of autophagy, in human neuroblastoma cells. Neurochem Int *58*, 512-520.

Caselli, R.J., Dueck, A.C., Locke, D.E., Sabbagh, M.N., Ahern, G.L., Rapcsak, S.Z., Baxter, L.C., Yaari, R., Woodruff, B.K., Hoffman-Snyder, C.*, et al.* (2011). Cerebrovascular risk factors and preclinical memory decline in healthy APOE epsilon4 homozygotes. Neurology *76*, 1078-1084.

Castano, E.M., Prelli, F., Wisniewski, T., Golabek, A., Kumar, R.A., Soto, C., and Frangione, B. (1995). Fibrillogenesis in Alzheimer's disease of amyloid beta peptides and apolipoprotein E. Biochem J *306 (Pt 2)*, 599-604.

Castellano, J.M., Kim, J., Stewart, F.R., Jiang, H., DeMattos, R.B., Patterson, B.W., Fagan, A.M., Morris, J.C., Mawuenyega, K.G., Cruchaga, C.*, et al.* (2011). Human apoE isoforms differentially regulate brain amyloid-beta peptide clearance. Sci Transl Med *3*, 89ra57.

Cataldo, A.M., Peterhoff, C.M., Schmidt, S.D., Terio, N.B., Duff, K., Beard, M., Mathews, P.M., and Nixon, R.A. (2004). Presenilin mutations in familial Alzheimer disease and transgenic mouse models accelerate neuronal lysosomal pathology. J Neuropathol Exp Neurol *63*, 821-830.

Chang, K.A., and Suh, Y.H. (2005). Pathophysiological roles of amyloidogenic carboxy-terminal fragments of the beta-amyloid precursor protein in Alzheimer's disease. J Pharmacol Sci *97*, 461-471.

Cheung, K.H., Shineman, D., Muller, M., Cardenas, C., Mei, L., Yang, J., Tomita, T., Iwatsubo, T., Lee, V.M., and Foskett, J.K. (2008). Mechanism of Ca2+ disruption in Alzheimer's disease by presenilin regulation of InsP3 receptor channel gating. Neuron *58*, 871-883.

Chin, M.H., Pellegrini, M., Plath, K., and Lowry, W.E. (2010). Molecular analyses of human induced pluripotent stem cells and embryonic stem cells. Cell Stem Cell *7*, 263-269.

Choi, A.M., Ryter, S.W., and Levine, B. (2013). Autophagy in human health and disease. N Engl J Med *368*, 1845-1846.

Chong, Y. (1997). Effect of a carboxy-terminal fragment of the Alzheimer's amyloid precursor protein on expression of proinflammatory cytokines in rat glial cells. Life Sci *61*, 2323-2333.

Citron, M., Oltersdorf, T., Haass, C., McConlogue, L., Hung, A.Y., Seubert, P., Vigo-Pelfrey, C., Lieberburg, I., and Selkoe, D.J. (1992). Mutation of the beta-amyloid precursor protein in familial Alzheimer's disease increases beta-protein production. Nature *360*, 672-674.

Coen, K., Flannagan, R.S., Baron, S., Carraro-Lacroix, L.R., Wang, D., Vermeire, W., Michiels, C., Munck, S., Baert, V., Sugita, S.*, et al.* (2012). Lysosomal calcium homeostasis defects, not proton pump defects, cause endo-lysosomal dysfunction in PSEN-deficient cells. J Cell Biol *198*, 23-35.

Cole, S.L., and Vassar, R. (2008). BACE1 structure and function in health and Alzheimer's disease. Curr Alzheimer Res *5*, 100-120.

Conti, L., and Cattaneo, E. (2010). Neural stem cell systems: physiological players or in vitro entities? Nat Rev Neurosci *11*, 176-187.

Conti, L., Pollard, S.M., Gorba, T., Reitano, E., Toselli, M., Biella, G., Sun, Y., Sanzone, S., Ying, Q.L., Cattaneo, E.*, et al.* (2005). Niche-independent symmetrical self-renewal of a mammalian tissue stem cell. PLoS Biol *3*, e283.

Conti, L., Reitano, E., and Cattaneo, E. (2006). Neural stem cell systems: diversities and properties after transplantation in animal models of diseases. Brain Pathol *16*, 143-154.

Corder, E.H., Saunders, A.M., Strittmatter, W.J., Schmechel, D.E., Gaskell, P.C., Small, G.W., Roses, A.D., Haines, J.L., and Pericak-Vance, M.A. (1993). Gene dose of apolipoprotein E type 4 allele and the risk of Alzheimer's disease in late onset families. Science *261*, 921-923.

Criollo, A., Maiuri, M.C., Tasdemir, E., Vitale, I., Fiebig, A.A., Andrews, D., Molgo, J., Diaz, J., Lavandero, S., Harper, F.*, et al.* (2007). Regulation of autophagy by the inositol trisphosphate receptor. Cell Death Differ *14*, 1029-1039.

Cundiff, P.E., and Anderson, S.A. (2011). Impact of induced pluripotent stem cells on the study of central nervous system disease. Curr Opin Genet Dev *21*, 354-361.

Das, A., Banik, N.L., and Ray, S.K. (2007). Garlic compounds generate reactive oxygen species leading to activation of stress kinases and cysteine proteases for apoptosis in human glioblastoma T98G and U87MG cells. Cancer *110*, 1083-1095.

Daviglus, M.L., Bell, C.C., Berrettini, W., Bowen, P.E., Connolly, E.S., Jr., Cox, N.J., Dunbar-Jacob, J.M., Granieri, E.C., Hunt, G., McGarry, K.*, et al.* (2010). National Institutes of Health State-of-the-Science Conference statement: preventing alzheimer disease and cognitive decline. Ann Intern Med *153*, 176-181.

De Strooper, B., Annaert, W., Cupers, P., Saftig, P., Craessaerts, K., Mumm, J.S., Schroeter, E.H., Schrijvers, V., Wolfe, M.S., Ray, W.J.*, et al.* (1999). A presenilin-1-dependent gamma-secretase-like protease mediates release of Notch intracellular domain. Nature *398*, 518-522.

De Strooper, B., Iwatsubo, T., and Wolfe, M.S. (2012). Presenilins and gamma-secretase: structure, function, and role in Alzheimer Disease. Cold Spring Harb Perspect Med *2*, a006304.

Dries, D.R., Shah, S., Han, Y.H., Yu, C., Yu, S., Shearman, M.S., and Yu, G. (2009). Glu-333 of nicastrin directly participates in gamma-secretase activity. J Biol Chem *284*, 29714-29724.

Duff, K., Eckman, C., Zehr, C., Yu, X., Prada, C.M., Perez-tur, J., Hutton, M., Buee, L., Harigaya, Y., Yager, D.*, et al.* (1996). Increased amyloid-beta42(43) in brains of mice expressing mutant presenilin 1. Nature *383*, 710-713.

Duff, K., and Suleman, F. (2004). Transgenic mouse models of Alzheimer's disease: how useful have they been for therapeutic development? Brief Funct Genomic Proteomic *3*, 47-59.

Efeyan, A., and Sabatini, D.M. (2010). mTOR and cancer: many loops in one pathway. Curr Opin Cell Biol *22*, 169-176.

Ejlerskov, P., Rasmussen, I., Nielsen, T.T., Bergstrom, A.L., Tohyama, Y., Jensen, P.H., and Vilhardt, F. (2013). Tubulin polymerization-promoting protein (TPPP/p25alpha) promotes unconventional secretion of alpha-synuclein through exophagy by impairing autophagosome-lysosome fusion. J Biol Chem *288*, 17313-17335.

Engele, J., Schubert, D., and Bohn, M.C. (1991). Conditioned media derived from glial cell lines promote survival and differentiation of dopaminergic neurons in vitro: role of mesencephalic glia. J Neurosci Res *30*, 359-371.

Epple, U.D., Suriapranata, I., Eskelinen, E.L., and Thumm, M. (2001). Aut5/Cvt17p, a putative lipase essential for disintegration of autophagic bodies inside the vacuole. J Bacteriol *183*, 5942-5955.

Esselens, C., Oorschot, V., Baert, V., Raemaekers, T., Spittaels, K., Serneels, L., Zheng, H., Saftig, P., De Strooper, B., Klumperman, J., *et al.* (2004). Presenilin 1 mediates the turnover of telencephalin in hippocampal neurons via an autophagic degradative pathway. J Cell Biol *166*, 1041-1054.

Fahrenholz, F., Gilbert, S., Kojro, E., Lammich, S., and Postina, R. (2000). Alpha-secretase activity of the disintegrin metalloprotease ADAM 10. Influences of domain structure. Ann N Y Acad Sci *920*, 215-222.

Faiz, M., and Nagy, A. (2013). Induced Pluripotent Stem Cells and Disorders of the Nervous System: Progress, Problems, and Prospects. Neuroscientist.

Falk, A., Koch, P., Kesavan, J., Takashima, Y., Ladewig, J., Alexander, M., Wiskow, O., Tailor, J., Trotter, M., Pollard, S., *et al.* (2012). Capture of neuroepithelial-like stem cells from pluripotent stem cells provides a versatile system for in vitro production of human neurons. PLoS One *7*, e29597.

Farrer, L.A., Cupples, L.A., Haines, J.L., Hyman, B., Kukull, W.A., Mayeux, R., Myers, R.H., Pericak-Vance, M.A., Risch, N., and van Duijn, C.M. (1997). Effects of age, sex, and ethnicity on the association between apolipoprotein E genotype and Alzheimer disease. A meta-analysis. APOE and Alzheimer Disease Meta Analysis Consortium. JAMA *278*, 1349-1356.

Fernandez-Estevez, M.A., Casarejos, M.J., Lopez Sendon, J., Garcia Caldentey, J., Ruiz, C., Gomez, A., Perucho, J., de Yebenes, J.G., and Mena, M.A. (2014). Trehalose reverses cell malfunction in fibroblasts from normal and Huntington's disease patients caused by proteosome inhibition. PLoS One *9*, e90202.

Feuillette, S., Blard, O., Lecourtois, M., Frebourg, T., Campion, D., and Dumanchin, C. (2005). Tau is not normally degraded by the proteasome. J Neurosci Res *80*, 400-405.

Finckh, U., Muller-Thomsen, T., Mann, U., Eggers, C., Marksteiner, J., Meins, W., Binetti, G., Alberici, A., Hock, C., Nitsch, R.M., *et al.* (2000). High prevalence of pathogenic mutations in patients with early-onset dementia detected by sequence analyses of four different genes. Am J Hum Genet *66*, 110-117.

Florez-McClure, M.L., Hohsfield, L.A., Fonte, G., Bealor, M.T., and Link, C.D. (2007). Decreased insulin-receptor signaling promotes the autophagic degradation of beta-amyloid peptide in C. elegans. Autophagy *3*, 569-580.

Fluhrer, R., Capell, A., Westmeyer, G., Willem, M., Hartung, B., Condron, M.M., Teplow, D.B., Haass, C., and Walter, J. (2002). A non-amyloidogenic function of BACE-2 in the secretory pathway. J Neurochem *81*, 1011-1020.

Forsyth, P.A., Krishna, N., Lawn, S., Valadez, J.G., Qu, X., Fenstermacher, D.A., Fournier, M., Potthast, L., Chinnaiyan, P., Gibney, G.T., *et al.* (2014). p75 Neurotrophin Receptor Cleavage by alpha- and gamma-Secretases is required for Neurotrophin mediated proliferation of Brain Tumor Initiating Cells. J Biol Chem.

Francis, R., McGrath, G., Zhang, J., Ruddy, D.A., Sym, M., Apfeld, J., Nicoll, M., Maxwell, M., Hai, B., Ellis, M.C., *et al.* (2002). aph-1 and pen-2 are required for Notch pathway signaling, gamma-secretase cleavage of betaAPP, and presenilin protein accumulation. Dev Cell *3*, 85-97.

Fukumoto, H., Rosene, D.L., Moss, M.B., Raju, S., Hyman, B.T., and Irizarry, M.C. (2004). Beta-secretase activity increases with aging in human, monkey, and mouse brain. Am J Pathol *164*, 719-725.

Gaspard, N., Bouschet, T., Herpoel, A., Naeije, G., van den Ameele, J., and Vanderhaeghen, P. (2009). Generation of cortical neurons from mouse embryonic stem cells. Nat Protoc *4*, 1454-1463.

Gaspard, N., Bouschet, T., Hourez, R., Dimidschstein, J., Naeije, G., van den Ameele, J., Espuny-Camacho, I., Herpoel, A., Passante, L., Schiffmann, S.N.*, et al.* (2008). An intrinsic mechanism of corticogenesis from embryonic stem cells. Nature *455*, 351-357.

Georgakopoulos, A., Litterst, C., Ghersi, E., Baki, L., Xu, C., Serban, G., and Robakis, N.K. (2006). Metalloproteinase/Presenilin1 processing of ephrinB regulates EphB-induced Src phosphorylation and signaling. EMBO J *25*, 1242-1252.

Gieselmann, V., Hasilik, A., and von Figura, K. (1985). Processing of human cathepsin D in lysosomes in vitro. J Biol Chem *260*, 3215-3220.

Glat, M.J., and Offen, D. (2013). Cell and gene therapy in Alzheimer's disease. Stem Cells Dev *22*, 1490-1496.

Glenner, G.G., and Wong, C.W. (1984). Alzheimer's disease: initial report of the purification and characterization of a novel cerebrovascular amyloid protein. Biochem Biophys Res Commun *120*, 885-890.

Golde, T.E. (2005). The Abeta hypothesis: leading us to rationally-designed therapeutic strategies for the treatment or prevention of Alzheimer disease. Brain Pathol *15*, 84-87.

Golde, T.E., and Kukar, T.L. (2009). Medicine. Avoiding unintended toxicity. Science *324*, 603-604.

Goldstein, L.S. (2012). Axonal transport and neurodegenerative disease: can we see the elephant? Prog Neurobiol *99*, 186-190.

Gomez-Isla, T., Price, J.L., McKeel, D.W., Jr., Morris, J.C., Growdon, J.H., and Hyman, B.T. (1996). Profound loss of layer II entorhinal cortex neurons occurs in very mild Alzheimer's disease. J Neurosci *16*, 4491-4500.

Gouras, G.K., Tsai, J., Naslund, J., Vincent, B., Edgar, M., Checler, F., Greenfield, J.P., Haroutunian, V., Buxbaum, J.D., Xu, H.*, et al.* (2000). Intraneuronal Abeta42 accumulation in human brain. Am J Pathol *156*, 15-20.

Green, D.R., Galluzzi, L., and Kroemer, G. (2011). Mitochondria and the autophagy-inflammation-cell death axis in organismal aging. Science *333*, 1109-1112.

Green, K.N., Demuro, A., Akbari, Y., Hitt, B.D., Smith, I.F., Parker, I., and LaFerla, F.M. (2008). SERCA pump activity is physiologically regulated by presenilin and regulates amyloid beta production. J Cell Biol *181*, 1107-1116.

Greenfield, J.P., Tsai, J., Gouras, G.K., Hai, B., Thinakaran, G., Checler, F., Sisodia, S.S., Greengard, P., and Xu, H. (1999). Endoplasmic reticulum and trans-Golgi network generate distinct populations of Alzheimer beta-amyloid peptides. Proc Natl Acad Sci U S A *96*, 742-747.

Grehan, S., Tse, E., and Taylor, J.M. (2001). Two distal downstream enhancers direct expression of the human apolipoprotein E gene to astrocytes in the brain. J Neurosci *21*, 812-822.

Gyure, K.A., Durham, R., Stewart, W.F., Smialek, J.E., and Troncoso, J.C. (2001). Intraneuronal abeta-amyloid precedes development of amyloid plaques in Down syndrome. Arch Pathol Lab Med *125*, 489-492.

Haan, M.N., Shemanski, L., Jagust, W.J., Manolio, T.A., and Kuller, L. (1999). The role of APOE epsilon4 in modulating effects of other risk factors for cognitive decline in elderly persons. JAMA *282*, 40-46.

Haass, C., Hung, A.Y., Schlossmacher, M.G., Oltersdorf, T., Teplow, D.B., and Selkoe, D.J. (1993a). Normal cellular processing of the beta-amyloid precursor protein results in the secretion of the amyloid beta peptide and related molecules. Ann N Y Acad Sci *695*, 109-116.

Haass, C., Hung, A.Y., Schlossmacher, M.G., Teplow, D.B., and Selkoe, D.J. (1993b). beta-Amyloid peptide and a 3-kDa fragment are derived by distinct cellular mechanisms. J Biol Chem *268*, 3021-3024.

Haass, C., Kaether, C., Thinakaran, G., and Sisodia, S. (2012). Trafficking and proteolytic processing of APP. Cold Spring Harb Perspect Med *2*, a006270.

Haass, C., Koo, E.H., Mellon, A., Hung, A.Y., and Selkoe, D.J. (1992). Targeting of cell-surface beta-amyloid precursor protein to lysosomes: alternative processing into amyloid-bearing fragments. Nature *357*, 500-503.

Haass, C., and Selkoe, D.J. (2007). Soluble protein oligomers in neurodegeneration: lessons from the Alzheimer's amyloid beta-peptide. Nat Rev Mol Cell Biol *8*, 101-112.

Haass, C., and Steiner, H. (2002). Alzheimer disease gamma-secretase: a complex story of GxGD-type presenilin proteases. Trends Cell Biol *12*, 556-562.

Haga, S., Akai, K., and Ishii, T. (1989). Demonstration of microglial cells in and around senile (neuritic) plaques in the Alzheimer brain. An immunohistochemical study using a novel monoclonal antibody. Acta Neuropathol *77*, 569-575.

Hailey, D.W., Rambold, A.S., Satpute-Krishnan, P., Mitra, K., Sougrat, R., Kim, P.K., and Lippincott-Schwartz, J. (2010). Mitochondria supply membranes for autophagosome biogenesis during starvation. Cell *141*, 656-667.

Hamano, T., Gendron, T.F., Causevic, E., Yen, S.H., Lin, W.L., Isidoro, C., Deture, M., and Ko, L.W. (2008). Autophagic-lysosomal perturbation enhances tau aggregation in transfectants with induced wild-type tau expression. Eur J Neurosci *27*, 1119-1130.

Hamasaki, M., Furuta, N., Matsuda, A., Nezu, A., Yamamoto, A., Fujita, N., Oomori, H., Noda, T., Haraguchi, T., Hiraoka, Y.*, et al.* (2013a). Autophagosomes form at ER-mitochondria contact sites. Nature *495*, 389-393.

Hamasaki, M., Shibutani, S.T., and Yoshimori, T. (2013b). Up-to-date membrane biogenesis in the autophagosome formation. Curr Opin Cell Biol.

Hara, T., Nakamura, K., Matsui, M., Yamamoto, A., Nakahara, Y., Suzuki-Migishima, R., Yokoyama, M., Mishima, K., Saito, I., Okano, H.*, et al.* (2006). Suppression of basal autophagy in neural cells causes neurodegenerative disease in mice. Nature *441*, 885-889.

Hardy, J. (2001). Genetic dissection of primary neurodegenerative diseases. Biochem Soc Symp, 51-57.

Hasegawa, H., Sanjo, N., Chen, F., Gu, Y.J., Shier, C., Petit, A., Kawarai, T., Katayama, T., Schmidt, S.D., Mathews, P.M.*, et al.* (2004). Both the sequence and length of the C terminus of PEN-2 are critical for intermolecular interactions and function of presenilin complexes. J Biol Chem *279*, 46455-46463.

Hawkins, R.D., Hon, G.C., Lee, L.K., Ngo, Q., Lister, R., Pelizzola, M., Edsall, L.E., Kuan, S., Luu, Y., Klugman, S.*, et al.* (2010). Distinct epigenomic landscapes of pluripotent and lineage-committed human cells. Cell Stem Cell *6*, 479-491.

Hayashi-Nishino, M., Fujita, N., Noda, T., Yamaguchi, A., Yoshimori, T., and Yamamoto, A. (2009). A subdomain of the endoplasmic reticulum forms a cradle for autophagosome formation. Nat Cell Biol *11*, 1433-1437.

Hayrapetyan, V., Rybalchenko, V., Rybalchenko, N., and Koulen, P. (2008). The N-terminus of presenilin-2 increases single channel activity of brain ryanodine receptors through direct protein-protein interaction. Cell Calcium *44*, 507-518.

He, C., and Klionsky, D.J. (2009). Regulation mechanisms and signaling pathways of autophagy. Annu Rev Genet *43*, 67-93.

He, C., and Levine, B. (2010). The Beclin 1 interactome. Curr Opin Cell Biol *22*, 140-149.

Hochfeld, W.E., Lee, S., and Rubinsztein, D.C. (2013). Therapeutic induction of autophagy to modulate neurodegenerative disease progression. Acta Pharmacol Sin *34*, 600-604.

Holtzman, D.M., Bales, K.R., Wu, S., Bhat, P., Parsadanian, M., Fagan, A.M., Chang, L.K., Sun, Y., and Paul, S.M. (1999). Expression of human apolipoprotein E reduces amyloid-beta deposition in a mouse model of Alzheimer's disease. J Clin Invest *103*, R15-R21.

Holtzman, D.M., Fagan, A.M., Mackey, B., Tenkova, T., Sartorius, L., Paul, S.M., Bales, K., Ashe, K.H., Irizarry, M.C., and Hyman, B.T. (2000). Apolipoprotein E facilitates neuritic and cerebrovascular plaque formation in an Alzheimer's disease model. Ann Neurol *47*, 739-747.

Holtzman, D.M., Morris, J.C., and Goate, A.M. (2011). Alzheimer's disease: the challenge of the second century. Sci Transl Med *3*, 77sr71.

Howell, S., Nalbantoglu, J., and Crine, P. (1995). Neutral endopeptidase can hydrolyze beta-amyloid(1-40) but shows no effect on beta-amyloid precursor protein metabolism. Peptides *16*, 647-652.

Huang, Y., and Mucke, L. (2012). Alzheimer mechanisms and therapeutic strategies. Cell *148*, 1204-1222.

Israel, M.A., Yuan, S.H., Bardy, C., Reyna, S.M., Mu, Y., Herrera, C., Hefferan, M.P., Van Gorp, S., Nazor, K.L., Boscolo, F.S.*, et al.* (2012). Probing sporadic and familial Alzheimer's disease using induced pluripotent stem cells. Nature *482*, 216-220.

Iwata, N., Tsubuki, S., Takaki, Y., Shirotani, K., Lu, B., Gerard, N.P., Gerard, C., Hama, E., Lee, H.J., and Saido, T.C. (2001). Metabolic regulation of brain Abeta by neprilysin. Science *292*, 1550-1552.

Jaeger, P.A., Pickford, F., Sun, C.H., Lucin, K.M., Masliah, E., and Wyss-Coray, T. (2010). Regulation of amyloid precursor protein processing by the Beclin 1 complex. PLoS One *5*, e11102.

Jaeger, P.A., and Wyss-Coray, T. (2009). All-you-can-eat: autophagy in neurodegeneration and neuroprotection. Mol Neurodegener *4*, 16.

Jarrett, J.T., Berger, E.P., and Lansbury, P.T., Jr. (1993). The carboxy terminus of the beta amyloid protein is critical for the seeding of amyloid formation: implications for the pathogenesis of Alzheimer's disease. Biochemistry *32*, 4693-4697.

Jeyakumar, M., Thomas, R., Elliot-Smith, E., Smith, D.A., van der Spoel, A.C., d'Azzo, A., Perry, V.H., Butters, T.D., Dwek, R.A., and Platt, F.M. (2003). Central nervous system inflammation is a hallmark of pathogenesis in mouse models of GM1 and GM2 gangliosidosis. Brain *126*, 974-987.

Jonsson, T., Atwal, J.K., Steinberg, S., Snaedal, J., Jonsson, P.V., Bjornsson, S., Stefansson, H., Sulem, P., Gudbjartsson, D., Maloney, J., *et al.* (2012). A mutation in APP protects against Alzheimer's disease and age-related cognitive decline. Nature *488*, 96-99.

Jordan, P.M., Cain, L.D., and Wu, P. (2008). Astrocytes enhance long-term survival of cholinergic neurons differentiated from human fetal neural stem cells. J Neurosci Res *86*, 35-47.

Kaether, C., Schmitt, S., Willem, M., and Haass, C. (2006). Amyloid precursor protein and Notch intracellular domains are generated after transport of their precursors to the cell surface. Traffic *7*, 408-415.

Kar, S., and Quirion, R. (2004). Amyloid beta peptides and central cholinergic neurons: functional interrelationship and relevance to Alzheimer's disease pathology. Prog Brain Res *145*, 261-274.

Karten, B., Peake, K.B., and Vance, J.E. (2009). Mechanisms and consequences of impaired lipid trafficking in Niemann-Pick type C1-deficient mammalian cells. Biochim Biophys Acta *1791*, 659-670.

Kawasaki, H., Mizuseki, K., Nishikawa, S., Kaneko, S., Kuwana, Y., Nakanishi, S., Nishikawa, S.I., and Sasai, Y. (2000). Induction of midbrain dopaminergic neurons from ES cells by stromal cell-derived inducing activity. Neuron *28*, 31-40.

Kelleher, R.J., 3rd, and Shen, J. (2010). Genetics. Gamma-secretase and human disease. Science *330*, 1055-1056.

Khandekar, N., Lie, K.H., Sachdev, P.S., and Sidhu, K.S. (2012). Amyloid precursor proteins, neural differentiation of pluripotent stem cells and its relevance to Alzheimer's disease. Stem Cells Dev *21*, 997-1006.

Khatoon, S., Grundke-Iqbal, I., and Iqbal, K. (1992). Brain levels of microtubule-associated protein tau are elevated in Alzheimer's disease: a radioimmuno-slot-blot assay for nanograms of the protein. J Neurochem *59*, 750-753.

Kim, I., Rodriguez-Enriquez, S., and Lemasters, J.J. (2007). Selective degradation of mitochondria by mitophagy. Arch Biochem Biophys *462*, 245-253.

Kim, J., Su, S.C., Wang, H., Cheng, A.W., Cassady, J.P., Lodato, M.A., Lengner, C.J., Chung, C.Y., Dawlaty, M.M., Tsai, L.H., *et al.* (2011). Functional integration of dopaminergic neurons directly converted from mouse fibroblasts. Cell Stem Cell *9*, 413-419.

Klimanskaya, I., Chung, Y., Becker, S., Lu, S.J., and Lanza, R. (2006). Human embryonic stem cell lines derived from single blastomeres. Nature *444*, 481-485.

Klionsky, D.J. (2007). Autophagy: from phenomenology to molecular understanding in less than a decade. Nat Rev Mol Cell Biol *8*, 931-937.

Klionsky, D.J., Abdalla, F.C., Abeliovich, H., Abraham, R.T., Acevedo-Arozena, A., Adeli, K., Agholme, L., Agnello, M., Agostinis, P., Aguirre-Ghiso, J.A., *et al.* (2012). Guidelines for the use and interpretation of assays for monitoring autophagy. Autophagy *8*, 445-544.

Koch, P., Kokaia, Z., Lindvall, O., and Brustle, O. (2009a). Emerging concepts in neural stem cell research: autologous repair and cell-based disease modelling. Lancet Neurol *8*, 819-829.

Koch, P., Opitz, T., Steinbeck, J.A., Ladewig, J., and Brustle, O. (2009b). A rosette-type, self-renewing human ES cell-derived neural stem cell with potential for in vitro instruction and synaptic integration. Proc Natl Acad Sci U S A *106*, 3225-3230.

Koch, P., Tamboli, I.Y., Mertens, J., Wunderlich, P., Ladewig, J., Stuber, K., Esselmann, H., Wiltfang, J., Brustle, O., and Walter, J. (2012). Presenilin-1 L166P mutant human pluripotent stem cell-derived neurons exhibit partial loss of gamma-secretase activity in endogenous amyloid-beta generation. Am J Pathol *180*, 2404-2416.

Kojro, E., and Fahrenholz, F. (2005). The non-amyloidogenic pathway: structure and function of alpha-secretases. Subcell Biochem *38*, 105-127.

Komatsu, M., Ueno, T., Waguri, S., Uchiyama, Y., Kominami, E., and Tanaka, K. (2007a). Constitutive autophagy: vital role in clearance of unfavorable proteins in neurons. Cell Death Differ *14*, 887-894.

Komatsu, M., Waguri, S., Chiba, T., Murata, S., Iwata, J., Tanida, I., Ueno, T., Koike, M., Uchiyama, Y., Kominami, E.*, et al.* (2006). Loss of autophagy in the central nervous system causes neurodegeneration in mice. Nature *441*, 880-884.

Komatsu, M., Waguri, S., Koike, M., Sou, Y.S., Ueno, T., Hara, T., Mizushima, N., Iwata, J., Ezaki, J., Murata, S.*, et al.* (2007b). Homeostatic levels of p62 control cytoplasmic inclusion body formation in autophagy-deficient mice. Cell *131*, 1149-1163.

Komatsu, M., Waguri, S., Ueno, T., Iwata, J., Murata, S., Tanida, I., Ezaki, J., Mizushima, N., Ohsumi, Y., Uchiyama, Y.*, et al.* (2005). Impairment of starvation-induced and constitutive autophagy in Atg7-deficient mice. J Cell Biol *169*, 425-434.

Komatsu, M., Wang, Q.J., Holstein, G.R., Friedrich, V.L., Jr., Iwata, J., Kominami, E., Chait, B.T., Tanaka, K., and Yue, Z. (2007c). Essential role for autophagy protein Atg7 in the maintenance of axonal homeostasis and the prevention of axonal degeneration. Proc Natl Acad Sci U S A *104*, 14489-14494.

Koo, E.H., and Squazzo, S.L. (1994). Evidence that production and release of amyloid beta-protein involves the endocytic pathway. J Biol Chem *269*, 17386-17389.

Kopke, E., Tung, Y.C., Shaikh, S., Alonso, A.C., Iqbal, K., and Grundke-Iqbal, I. (1993). Microtubule-associated protein tau. Abnormal phosphorylation of a non-paired helical filament pool in Alzheimer disease. J Biol Chem *268*, 24374-24384.

Kroemer, G., and Jaattela, M. (2005). Lysosomes and autophagy in cell death control. Nat Rev Cancer *5*, 886-897.

Kroemer, G., Marino, G., and Levine, B. (2010). Autophagy and the integrated stress response. Mol Cell *40*, 280-293.

Kruger, U., Wang, Y., Kumar, S., and Mandelkow, E.M. (2012). Autophagic degradation of tau in primary neurons and its enhancement by trehalose. Neurobiol Aging *33*, 2291-2305.

Kulic, L., Walter, J., Multhaup, G., Teplow, D.B., Baumeister, R., Romig, H., Capell, A., Steiner, H., and Haass, C. (2000). Separation of presenilin function in amyloid beta-peptide generation and endoproteolysis of Notch. Proc Natl Acad Sci U S A *97*, 5913-5918.

Kuma, A., Hatano, M., Matsui, M., Yamamoto, A., Nakaya, H., Yoshimori, T., Ohsumi, Y., Tokuhisa, T., and Mizushima, N. (2004). The role of autophagy during the early neonatal starvation period. Nature *432*, 1032-1036.

Kundu, M., and Thompson, C.B. (2008). Autophagy: basic principles and relevance to disease. Annu Rev Pathol *3*, 427-455.

Ladewig, J., Mertens, J., Kesavan, J., Doerr, J., Poppe, D., Glaue, F., Herms, S., Wernet, P., Kogler, G., Muller, F.J*., et al.* (2012). Small molecules enable highly efficient neuronal conversion of human fibroblasts. Nat Methods.

Lamb, C.A., Yoshimori, T., and Tooze, S.A. (2013). The autophagosome: origins unknown, biogenesis complex. Nat Rev Mol Cell Biol *14*, 759-774.

Lang, T., Schaeffeler, E., Bernreuther, D., Bredschneider, M., Wolf, D.H., and Thumm, M. (1998). Aut2p and Aut7p, two novel microtubule-associated proteins are essential for delivery of autophagic vesicles to the vacuole. EMBO J *17*, 3597-3607.

Laplante, M., and Sabatini, D.M. (2009). mTOR signaling at a glance. J Cell Sci *122*, 3589-3594.

Larner, A.J., and Doran, M. (2006). Clinical phenotypic heterogeneity of Alzheimer's disease associated with mutations of the presenilin-1 gene. J Neurol *253*, 139-158.

LaVoie, M.J., Fraering, P.C., Ostaszewski, B.L., Ye, W., Kimberly, W.T., Wolfe, M.S., and Selkoe, D.J. (2003). Assembly of the gamma-secretase complex involves early formation of an intermediate subcomplex of Aph-1 and nicastrin. J Biol Chem *278*, 37213-37222.

LeBlanc, A.C., and Goodyer, C.G. (1999). Role of endoplasmic reticulum, endosomal-lysosomal compartments, and microtubules in amyloid precursor protein metabolism of human neurons. J Neurochem *72*, 1832-1842.

Lee, G., Kim, H., Elkabetz, Y., Al Shamy, G., Panagiotakos, G., Barberi, T., Tabar, V., and Studer, L. (2007). Isolation and directed differentiation of neural crest stem cells derived from human embryonic stem cells. Nat Biotechnol *25*, 1468-1475.

Lee, G.H., Kim, D.S., Kim, H.T., Lee, J.W., Chung, C.H., Ahn, T., Lim, J.M., Kim, I.K., Chae, H.J., and Kim, H.R. (2011a). Enhanced lysosomal activity is involved in Bax inhibitor-1-induced regulation of the endoplasmic reticulum (ER) stress response and cell death against ER stress: involvement of vacuolar H+-ATPase (V-ATPase). J Biol Chem *286*, 24743-24753.

Lee, J.H., Yu, W.H., Kumar, A., Lee, S., Mohan, P.S., Peterhoff, C.M., Wolfe, D.M., Martinez-Vicente, M., Massey, A.C., Sovak, G*., et al.* (2010). Lysosomal proteolysis and autophagy require presenilin 1 and are disrupted by Alzheimer-related PS1 mutations. Cell *141*, 1146-1158.

Lee, M.J., Lee, J.H., and Rubinsztein, D.C. (2013). Tau degradation: the ubiquitin-proteasome system versus the autophagy-lysosome system. Prog Neurobiol *105*, 49-59.

Lee, V.M., Brunden, K.R., Hutton, M., and Trojanowski, J.Q. (2011b). Developing therapeutic approaches to tau, selected kinases, and related neuronal protein targets. Cold Spring Harb Perspect Med *1*, a006437.

Leissring, M.A., Farris, W., Chang, A.Y., Walsh, D.M., Wu, X., Sun, X., Frosch, M.P., and Selkoe, D.J. (2003). Enhanced proteolysis of beta-amyloid in APP transgenic mice prevents plaque formation, secondary pathology, and premature death. Neuron *40*, 1087-1093.

Levine, B., and Kroemer, G. (2008). Autophagy in the pathogenesis of disease. Cell *132*, 27-42.

Levitan, D., Lee, J., Song, L., Manning, R., Wong, G., Parker, E., and Zhang, L. (2001). PS1 N- and C-terminal fragments form a complex that functions in APP processing and Notch signaling. Proc Natl Acad Sci U S A *98*, 12186-12190.

Levy, E., Carman, M.D., Fernandez-Madrid, I.J., Power, M.D., Lieberburg, I., van Duinen, S.G., Bots, G.T., Luyendijk, W., and Frangione, B. (1990). Mutation of the Alzheimer's disease amyloid gene in hereditary cerebral hemorrhage, Dutch type. Science *248*, 1124-1126.

Li, L., Zhang, X., and Le, W. (2010). Autophagy dysfunction in Alzheimer's disease. Neurodegener Dis *7*, 265-271.

Lian, X.Y., and Stringer, J.L. (2004). Astrocytes contribute to regulation of extracellular calcium and potassium in the rat cerebral cortex during spreading depression. Brain Res *1012*, 177-184.

Lowry, W.E., Richter, L., Yachechko, R., Pyle, A.D., Tchieu, J., Sridharan, R., Clark, A.T., and Plath, K. (2008). Generation of human induced pluripotent stem cells from dermal fibroblasts. Proc Natl Acad Sci U S A *105*, 2883-2888.

Lujan, E., Chanda, S., Ahlenius, H., Sudhof, T.C., and Wernig, M. (2012). Direct conversion of mouse fibroblasts to self-renewing, tripotent neural precursor cells. Proc Natl Acad Sci U S A *109*, 2527-2532.

Lum, J.J., Bauer, D.E., Kong, M., Harris, M.H., Li, C., Lindsten, T., and Thompson, C.B. (2005). Growth factor regulation of autophagy and cell survival in the absence of apoptosis. Cell *120*, 237-248.

Luo, Y., Bolon, B., Kahn, S., Bennett, B.D., Babu-Khan, S., Denis, P., Fan, W., Kha, H., Zhang, J., Gong, Y.*, et al.* (2001). Mice deficient in BACE1, the Alzheimer's beta-secretase, have normal phenotype and abolished beta-amyloid generation. Nat Neurosci *4*, 231-232.

Luyckx, J., and Baudouin, C. (2011). Trehalose: an intriguing disaccharide with potential for medical application in ophthalmology. Clin Ophthalmol *5*, 577-581.

Ma, J., Yee, A., Brewer, H.B., Jr., Das, S., and Potter, H. (1994). Amyloid-associated proteins alpha 1-antichymotrypsin and apolipoprotein E promote assembly of Alzheimer beta-protein into filaments. Nature *372*, 92-94.

Magazu, S., Migliardo, F., and Telling, M.T. (2007). Study of the dynamical properties of water in disaccharide solutions. Eur Biophys J *36*, 163-171.

Mahley, R.W., Weisgraber, K.H., and Huang, Y. (2006). Apolipoprotein E4: a causative factor and therapeutic target in neuropathology, including Alzheimer's disease. Proc Natl Acad Sci U S A *103*, 5644-5651.

Maiuri, M.C., Le Toumelin, G., Criollo, A., Rain, J.C., Gautier, F., Juin, P., Tasdemir, E., Pierron, G., Troulinaki, K., Tavernarakis, N.*, et al.* (2007a). Functional and physical interaction between Bcl-X(L) and a BH3-like domain in Beclin-1. EMBO J *26*, 2527-2539.

Maiuri, M.C., Zalckvar, E., Kimchi, A., and Kroemer, G. (2007b). Self-eating and self-killing: crosstalk between autophagy and apoptosis. Nat Rev Mol Cell Biol *8*, 741-752.

Mandelkow, E.M., and Mandelkow, E. (2012). Biochemistry and cell biology of tau protein in neurofibrillary degeneration. Cold Spring Harb Perspect Med *2*, a006247.

Martinez-Vicente, M., and Cuervo, A.M. (2007). Autophagy and neurodegeneration: when the cleaning crew goes on strike. Lancet Neurol *6*, 352-361.

Martinez-Vicente, M., Talloczy, Z., Wong, E., Tang, G., Koga, H., Kaushik, S., de Vries, R., Arias, E., Harris, S., Sulzer, D.*, et al.* (2010). Cargo recognition failure is responsible for inefficient autophagy in Huntington's disease. Nat Neurosci *13*, 567-576.

Massey, A., Kiffin, R., and Cuervo, A.M. (2004). Pathophysiology of chaperone-mediated autophagy. Int J Biochem Cell Biol *36*, 2420-2434.

Masters, C.L., Simms, G., Weinman, N.A., Multhaup, G., McDonald, B.L., and Beyreuther, K. (1985). Amyloid plaque core protein in Alzheimer disease and Down syndrome. Proc Natl Acad Sci U S A *82*, 4245-4249.

Mauch, D.H., Nagler, K., Schumacher, S., Goritz, C., Muller, E.C., Otto, A., and Pfrieger, F.W. (2001). CNS synaptogenesis promoted by glia-derived cholesterol. Science *294*, 1354-1357.

McCarthy, J.V., Twomey, C., and Wujek, P. (2009). Presenilin-dependent regulated intramembrane proteolysis and gamma-secretase activity. Cell Mol Life Sci *66*, 1534-1555.

McPhie, D.L., Lee, R.K., Eckman, C.B., Olstein, D.H., Durham, S.P., Yager, D., Younkin, S.G., Wurtman, R.J., and Neve, R.L. (1997). Neuronal expression of beta-amyloid precursor protein Alzheimer mutations causes intracellular accumulation of a C-terminal fragment containing both the amyloid beta and cytoplasmic domains. J Biol Chem *272*, 24743-24746.

Meijer, A.J., and Codogno, P. (2006). Signalling and autophagy regulation in health, aging and disease. Mol Aspects Med *27*, 411-425.

Mertens, J., Stuber, K., Wunderlich, P., Ladewig, J., Kesavan, J.C., Vandenberghe, R., Vandenbulcke, M., van Damme, P., Walter, J., Brustle, O.*, et al.* (2013). APP Processing in Human Pluripotent Stem Cell-Derived Neurons Is Resistant to NSAID-Based gamma-Secretase Modulation. Stem Cell Reports *1*, 491-498.

Metcalf, P., and Fusek, M. (1993). Two crystal structures for cathepsin D: the lysosomal targeting signal and active site. EMBO J *12*, 1293-1302.

Meziane, H., Dodart, J.C., Mathis, C., Little, S., Clemens, J., Paul, S.M., and Ungerer, A. (1998). Memory-enhancing effects of secreted forms of the beta-amyloid precursor protein in normal and amnestic mice. Proc Natl Acad Sci U S A *95*, 12683-12688.

Mills, J., and Reiner, P.B. (1999). Mitogen-activated protein kinase is involved in N-methyl-D-aspartate receptor regulation of amyloid precursor protein cleavage. Neuroscience *94*, 1333-1338.

Mindell, J.A. (2012). Lysosomal acidification mechanisms. Annu Rev Physiol *74*, 69-86.

Mizushima, N. (2004). Methods for monitoring autophagy. Int J Biochem Cell Biol *36*, 2491-2502.

Mizushima, N. (2007). Autophagy: process and function. Genes Dev *21*, 2861-2873.

Mizushima, N. (2010). The role of the Atg1/ULK1 complex in autophagy regulation. Curr Opin Cell Biol *22*, 132-139.

Mizushima, N., Levine, B., Cuervo, A.M., and Klionsky, D.J. (2008). Autophagy fights disease through cellular self-digestion. Nature *451*, 1069-1075.

Moehlmann, T., Winkler, E., Xia, X., Edbauer, D., Murrell, J., Capell, A., Kaether, C., Zheng, H., Ghetti, B., Haass, C., *et al.* (2002). Presenilin-1 mutations of leucine 166 equally affect the generation of the Notch and APP intracellular domains independent of their effect on Abeta 42 production. Proc Natl Acad Sci U S A *99*, 8025-8030.

Mohamed, N.V., Plouffe, V., Remillard-Labrosse, G., Planel, E., and Leclerc, N. (2014). Starvation and inhibition of lysosomal function increased tau secretion by primary cortical neurons. Sci Rep *4*, 5715.

Moreau, K., Renna, M., and Rubinsztein, D.C. (2013). Connections between SNAREs and autophagy. Trends Biochem Sci *38*, 57-63.

Morris, M., Maeda, S., Vossel, K., and Mucke, L. (2011). The many faces of tau. Neuron *70*, 410-426.

Mowrer, K.R., and Wolfe, M.S. (2008). Promotion of BACE1 mRNA alternative splicing reduces amyloid beta-peptide production. J Biol Chem *283*, 18694-18701.

Mueller-Steiner, S., Zhou, Y., Arai, H., Roberson, E.D., Sun, B., Chen, J., Wang, X., Yu, G., Esposito, L., Mucke, L., *et al.* (2006). Antiamyloidogenic and neuroprotective functions of cathepsin B: implications for Alzheimer's disease. Neuron *51*, 703-714.

Mullins, C., and Bonifacino, J.S. (2001). The molecular machinery for lysosome biogenesis. Bioessays *23*, 333-343.

Murrow, L., and Debnath, J. (2013). Autophagy as a stress-response and quality-control mechanism: implications for cell injury and human disease. Annu Rev Pathol *8*, 105-137.

Nair, U., Jotwani, A., Geng, J., Gammoh, N., Richerson, D., Yen, W.L., Griffith, J., Nag, S., Wang, K., Moss, T., *et al.* (2011). SNARE proteins are required for macroautophagy. Cell *146*, 290-302.

Nakai, A., Yamaguchi, O., Takeda, T., Higuchi, Y., Hikoso, S., Taniike, M., Omiya, S., Mizote, I., Matsumura, Y., Asahi, M., *et al.* (2007). The role of autophagy in cardiomyocytes in the basal state and in response to hemodynamic stress. Nat Med *13*, 619-624.

Neely, K.M., Green, K.N., and LaFerla, F.M. (2011). Presenilin is necessary for efficient proteolysis through the autophagy-lysosome system in a gamma-secretase-independent manner. J Neurosci *31*, 2781-2791.

Ni, H.M., Bockus, A., Wozniak, A.L., Jones, K., Weinman, S., Yin, X.M., and Ding, W.X. (2011). Dissecting the dynamic turnover of GFP-LC3 in the autolysosome. Autophagy *7*, 188-204.

Nilsberth, C., Westlind-Danielsson, A., Eckman, C.B., Condron, M.M., Axelman, K., Forsell, C., Stenh, C., Luthman, J., Teplow, D.B., Younkin, S.G., *et al.* (2001). The 'Arctic' APP mutation (E693G) causes Alzheimer's disease by enhanced Abeta protofibril formation. Nat Neurosci *4*, 887-893.

Nilsson, P., Loganathan, K., Sekiguchi, M., Matsuba, Y., Hui, K., Tsubuki, S., Tanaka, M., Iwata, N., Saito, T., and Saido, T.C. (2013). Abeta secretion and plaque formation depend on autophagy. Cell Rep *5*, 61-69.

Nixon, R.A. (2006). Autophagy in neurodegenerative disease: friend, foe or turncoat? Trends Neurosci *29*, 528-535.

Nixon, R.A. (2007). Autophagy, amyloidogenesis and Alzheimer disease. J Cell Sci *120*, 4081-4091.

Nixon, R.A., Wegiel, J., Kumar, A., Yu, W.H., Peterhoff, C., Cataldo, A., and Cuervo, A.M. (2005). Extensive involvement of autophagy in Alzheimer disease: an immuno-electron microscopy study. J Neuropathol Exp Neurol *64*, 113-122.

Nixon, R.A., Yang, D.S., and Lee, J.H. (2008). Neurodegenerative lysosomal disorders: a continuum from development to late age. Autophagy *4*, 590-599.

Nyabi, O., Pype, S., Mercken, M., Herreman, A., Saftig, P., Craessaerts, K., Serneels, L., Annaert, W., and De Strooper, B. (2002). No endogenous A beta production in presenilin-deficient fibroblasts. Nat Cell Biol *4*, E164; author reply E165-166.

O'Brien, R.J., and Wong, P.C. (2011). Amyloid precursor protein processing and Alzheimer's disease. Annu Rev Neurosci *34*, 185-204.

Oh, E.S., Savonenko, A.V., King, J.F., Fangmark Tucker, S.M., Rudow, G.L., Xu, G., Borchelt, D.R., and Troncoso, J.C. (2009). Amyloid precursor protein increases cortical neuron size in transgenic mice. Neurobiol Aging *30*, 1238-1244.

Ohno, H., Stewart, J., Fournier, M.C., Bosshart, H., Rhee, I., Miyatake, S., Saito, T., Gallusser, A., Kirchhausen, T., and Bonifacino, J.S. (1995). Interaction of tyrosine-based sorting signals with clathrin-associated proteins. Science *269*, 1872-1875.

Okabe, S., Forsberg-Nilsson, K., Spiro, A.C., Segal, M., and McKay, R.D. (1996). Development of neuronal precursor cells and functional postmitotic neurons from embryonic stem cells in vitro. Mech Dev *59*, 89-102.

Pacheco, C.D., and Lieberman, A.P. (2008). The pathogenesis of Niemann-Pick type C disease: a role for autophagy? Expert Rev Mol Med *10*, e26.

Palop, J.J., and Mucke, L. (2010). Amyloid-beta-induced neuronal dysfunction in Alzheimer's disease: from synapses toward neural networks. Nat Neurosci *13*, 812-818.

Pankiv, S., Clausen, T.H., Lamark, T., Brech, A., Bruun, J.A., Outzen, H., Overvatn, A., Bjorkoy, G., and Johansen, T. (2007). p62/SQSTM1 binds directly to Atg8/LC3 to facilitate degradation of ubiquitinated protein aggregates by autophagy. J Biol Chem *282*, 24131-24145.

Pasternak, S.H., Bagshaw, R.D., Guiral, M., Zhang, S., Ackerley, C.A., Pak, B.J., Callahan, J.W., and Mahuran, D.J. (2003). Presenilin-1, nicastrin, amyloid precursor protein, and gamma-secretase activity are co-localized in the lysosomal membrane. J Biol Chem *278*, 26687-26694.

Pattingre, S., Bauvy, C., Carpentier, S., Levade, T., Levine, B., and Codogno, P. (2009). Role of JNK1-dependent Bcl-2 phosphorylation in ceramide-induced macroautophagy. J Biol Chem *284*, 2719-2728.

Pattingre, S., Tassa, A., Qu, X., Garuti, R., Liang, X.H., Mizushima, N., Packer, M., Schneider, M.D., and Levine, B. (2005). Bcl-2 antiapoptotic proteins inhibit Beclin 1-dependent autophagy. Cell *122*, 927-939.

Perrier, A.L., Tabar, V., Barberi, T., Rubio, M.E., Bruses, J., Topf, N., Harrison, N.L., and Studer, L. (2004). Derivation of midbrain dopamine neurons from human embryonic stem cells. Proc Natl Acad Sci U S A *101*, 12543-12548.

Pfisterer, U., Kirkeby, A., Torper, O., Wood, J., Nelander, J., Dufour, A., Bjorklund, A., Lindvall, O., Jakobsson, J., and Parmar, M. (2011). Direct conversion of human fibroblasts to dopaminergic neurons. Proc Natl Acad Sci U S A *108*, 10343-10348.

Pickford, F., Masliah, E., Britschgi, M., Lucin, K., Narasimhan, R., Jaeger, P.A., Small, S., Spencer, B., Rockenstein, E., Levine, B.*, et al.* (2008). The autophagy-related protein beclin 1 shows reduced

expression in early Alzheimer disease and regulates amyloid beta accumulation in mice. J Clin Invest *118*, 2190-2199.

Pihlaja, R., Koistinaho, J., Malm, T., Sikkila, H., Vainio, S., and Koistinaho, M. (2008). Transplanted astrocytes internalize deposited beta-amyloid peptides in a transgenic mouse model of Alzheimer's disease. Glia *56*, 154-163.

Pitas, R.E., Boyles, J.K., Lee, S.H., Foss, D., and Mahley, R.W. (1987). Astrocytes synthesize apolipoprotein E and metabolize apolipoprotein E-containing lipoproteins. Biochim Biophys Acta *917*, 148-161.

Poirier, J. (1996). Apolipoprotein E in the brain and its role in Alzheimer's disease. J Psychiatry Neurosci *21*, 128-134.

Polson, H.E., de Lartigue, J., Rigden, D.J., Reedijk, M., Urbe, S., Clague, M.J., and Tooze, S.A. (2010). Mammalian Atg18 (WIPI2) localizes to omegasome-anchored phagophores and positively regulates LC3 lipidation. Autophagy *6*, 506-522.

Prasher, V.P., Farrer, M.J., Kessling, A.M., Fisher, E.M., West, R.J., Barber, P.C., and Butler, A.C. (1998). Molecular mapping of Alzheimer-type dementia in Down's syndrome. Ann Neurol *43*, 380-383.

Primakoff, P., and Myles, D.G. (2000). The ADAM gene family: surface proteins with adhesion and protease activity. Trends Genet *16*, 83-87.

Qiang, L., Fujita, R., Yamashita, T., Angulo, S., Rhinn, H., Rhee, D., Doege, C., Chau, L., Aubry, L., Vanti, W.B., *et al.* (2011). Directed conversion of Alzheimer's disease patient skin fibroblasts into functional neurons. Cell *146*, 359-371.

Qu, T., Brannen, C.L., Kim, H.M., and Sugaya, K. (2001). Human neural stem cells improve cognitive function of aged brain. Neuroreport *12*, 1127-1132.

Rabinowitz, J.D., and White, E. (2010). Autophagy and metabolism. Science *330*, 1344-1348.

Ratovitski, T., Slunt, H.H., Thinakaran, G., Price, D.L., Sisodia, S.S., and Borchelt, D.R. (1997). Endoproteolytic processing and stabilization of wild-type and mutant presenilin. J Biol Chem *272*, 24536-24541.

Ravikumar, B., Duden, R., and Rubinsztein, D.C. (2002). Aggregate-prone proteins with polyglutamine and polyalanine expansions are degraded by autophagy. Hum Mol Genet *11*, 1107-1117.

Repetto, E., Yoon, I.S., Zheng, H., and Kang, D.E. (2007). Presenilin 1 regulates epidermal growth factor receptor turnover and signaling in the endosomal-lysosomal pathway. J Biol Chem *282*, 31504-31516.

Richo, G.R., and Conner, G.E. (1994). Structural requirements of procathepsin D activation and maturation. J Biol Chem *269*, 14806-14812.

Ridet, J.L., Malhotra, S.K., Privat, A., and Gage, F.H. (1997). Reactive astrocytes: cellular and molecular cues to biological function. Trends Neurosci *20*, 570-577.

Rocca, W.A., Hofman, A., Brayne, C., Breteler, M.M., Clarke, M., Copeland, J.R., Dartigues, J.F., Engedal, K., Hagnell, O., Heeren, T.J., *et al.* (1991). Frequency and distribution of Alzheimer's disease in Europe: a collaborative study of 1980-1990 prevalence findings. The EURODEM-Prevalence Research Group. Ann Neurol *30*, 381-390.

Roch, J.M., Masliah, E., Roch-Levecq, A.C., Sundsmo, M.P., Otero, D.A., Veinbergs, I., and Saitoh, T. (1994). Increase of synaptic density and memory retention by a peptide representing the trophic domain of the amyloid beta/A4 protein precursor. Proc Natl Acad Sci U S A *91*, 7450-7454.

Rojo, L.E., Fernandez, J.A., Maccioni, A.A., Jimenez, J.M., and Maccioni, R.B. (2008). Neuroinflammation: implications for the pathogenesis and molecular diagnosis of Alzheimer's disease. Arch Med Res *39*, 1-16.

Rosendorff, C., Beeri, M.S., and Silverman, J.M. (2007). Cardiovascular risk factors for Alzheimer's disease. Am J Geriatr Cardiol *16*, 143-149.

Rowland, A.M., Richmond, J.E., Olsen, J.G., Hall, D.H., and Bamber, B.A. (2006). Presynaptic terminals independently regulate synaptic clustering and autophagy of GABAA receptors in Caenorhabditis elegans. J Neurosci *26*, 1711-1720.

Rubinsztein, D.C. (2006). The roles of intracellular protein-degradation pathways in neurodegeneration. Nature *443*, 780-786.

Rubinsztein, D.C., Codogno, P., and Levine, B. (2012). Autophagy modulation as a potential therapeutic target for diverse diseases. Nat Rev Drug Discov *11*, 709-730.

Rubinsztein, D.C., Gestwicki, J.E., Murphy, L.O., and Klionsky, D.J. (2007). Potential therapeutic applications of autophagy. Nat Rev Drug Discov *6*, 304-312.

Russell, R.C., Yuan, H.X., and Guan, K.L. (2014). Autophagy regulation by nutrient signaling. Cell Res *24*, 42-57.

Saido, T., and Leissring, M.A. (2012). Proteolytic degradation of amyloid beta-protein. Cold Spring Harb Perspect Med *2*, a006379.

Sarkar, S., Carroll, B., Buganim, Y., Maetzel, D., Ng, A.H., Cassady, J.P., Cohen, M.A., Chakraborty, S., Wang, H., Spooner, E.*, et al.* (2013). Impaired autophagy in the lipid-storage disorder Niemann-Pick type C1 disease. Cell Rep *5*, 1302-1315.

Sarkar, S., Davies, J.E., Huang, Z., Tunnacliffe, A., and Rubinsztein, D.C. (2007). Trehalose, a novel mTOR-independent autophagy enhancer, accelerates the clearance of mutant huntingtin and alpha-synuclein. J Biol Chem *282*, 5641-5652.

Sarkar, S., and Rubinsztein, D.C. (2008). Small molecule enhancers of autophagy for neurodegenerative diseases. Mol Biosyst *4*, 895-901.

Saura, C.A., Choi, S.Y., Beglopoulos, V., Malkani, S., Zhang, D., Shankaranarayana Rao, B.S., Chattarji, S., Kelleher, R.J., 3rd, Kandel, E.R., Duff, K.*, et al.* (2004). Loss of presenilin function causes impairments of memory and synaptic plasticity followed by age-dependent neurodegeneration. Neuron *42*, 23-36.

Schaeffer, V., Lavenir, I., Ozcelik, S., Tolnay, M., Winkler, D.T., and Goedert, M. (2012). Stimulation of autophagy reduces neurodegeneration in a mouse model of human tauopathy. Brain *135*, 2169-2177.

Schousboe, A., and Waagepetersen, H.S. (2005). Role of astrocytes in glutamate homeostasis: implications for excitotoxicity. Neurotox Res *8*, 221-225.

Schultz, S.S., and Lucas, P.A. (2006). Human stem cells isolated from adult skeletal muscle differentiate into neural phenotypes. J Neurosci Methods *152*, 144-155.

Selkoe, D.J. (1998). The cell biology of beta-amyloid precursor protein and presenilin in Alzheimer's disease. Trends Cell Biol *8*, 447-453.

Selkoe, D.J. (1999). Translating cell biology into therapeutic advances in Alzheimer's disease. Nature *399*, A23-31.

Selkoe, D.J. (2001). Alzheimer's disease: genes, proteins, and therapy. Physiol Rev *81*, 741-766.

Selkoe, D.J. (2011). Alzheimer's disease. Cold Spring Harb Perspect Biol *3*.

Serneels, L., Dejaegere, T., Craessaerts, K., Horre, K., Jorissen, E., Tousseyn, T., Hebert, S., Coolen, M., Martens, G., Zwijsen, A.*, et al.* (2005). Differential contribution of the three Aph1 genes to gamma-secretase activity in vivo. Proc Natl Acad Sci U S A *102*, 1719-1724.

Serneels, L., Van Biervliet, J., Craessaerts, K., Dejaegere, T., Horre, K., Van Houtvin, T., Esselmann, H., Paul, S., Schafer, M.K., Berezovska, O.*, et al.* (2009). gamma-Secretase heterogeneity in the Aph1 subunit: relevance for Alzheimer's disease. Science *324*, 639-642.

Settembre, C., Di Malta, C., Polito, V.A., Garcia Arencibia, M., Vetrini, F., Erdin, S., Erdin, S.U., Huynh, T., Medina, D., Colella, P.*, et al.* (2011). TFEB links autophagy to lysosomal biogenesis. Science *332*, 1429-1433.

Settembre, C., Fraldi, A., Jahreiss, L., Spampanato, C., Venturi, C., Medina, D., de Pablo, R., Tacchetti, C., Rubinsztein, D.C., and Ballabio, A. (2008a). A block of autophagy in lysosomal storage disorders. Hum Mol Genet *17*, 119-129.

Settembre, C., Fraldi, A., Rubinsztein, D.C., and Ballabio, A. (2008b). Lysosomal storage diseases as disorders of autophagy. Autophagy *4*, 113-114.

Settembre, C., Zoncu, R., Medina, D.L., Vetrini, F., Erdin, S., Huynh, T., Ferron, M., Karsenty, G., Vellard, M.C., Facchinetti, V.*, et al.* (2012). A lysosome-to-nucleus signalling mechanism senses and regulates the lysosome via mTOR and TFEB. EMBO J *31*, 1095-1108.

Shah, S., Lee, S.F., Tabuchi, K., Hao, Y.H., Yu, C., LaPlant, Q., Ball, H., Dann, C.E., 3rd, Sudhof, T., and Yu, G. (2005). Nicastrin functions as a gamma-secretase-substrate receptor. Cell *122*, 435-447.

Shen, J., and Kelleher, R.J., 3rd (2007). The presenilin hypothesis of Alzheimer's disease: evidence for a loss-of-function pathogenic mechanism. Proc Natl Acad Sci U S A *104*, 403-409.

Sherrington, R., Rogaev, E.I., Liang, Y., Rogaeva, E.A., Levesque, G., Ikeda, M., Chi, H., Lin, C., Li, G., Holman, K.*, et al.* (1995). Cloning of a gene bearing missense mutations in early-onset familial Alzheimer's disease. Nature *375*, 754-760.

Shi, C.S., and Kehrl, J.H. (2008). MyD88 and Trif target Beclin 1 to trigger autophagy in macrophages. J Biol Chem *283*, 33175-33182.

Shirotani, K., Edbauer, D., Capell, A., Schmitz, J., Steiner, H., and Haass, C. (2003). Gamma-secretase activity is associated with a conformational change of nicastrin. J Biol Chem *278*, 16474-16477.

Singh, P.P., Singh, M., and Mastana, S.S. (2006). APOE distribution in world populations with new data from India and the UK. Ann Hum Biol *33*, 279-308.

Sinha, S., Anderson, J.P., Barbour, R., Basi, G.S., Caccavello, R., Davis, D., Doan, M., Dovey, H.F., Frigon, N., Hong, J., *et al.* (1999). Purification and cloning of amyloid precursor protein beta-secretase from human brain. Nature *402*, 537-540.

Sinha, S., and Levine, B. (2008). The autophagy effector Beclin 1: a novel BH3-only protein. Oncogene *27 Suppl 1*, S137-148.

Sisodia, S.S. (1992). Beta-amyloid precursor protein cleavage by a membrane-bound protease. Proc Natl Acad Sci U S A *89*, 6075-6079.

Sisodia, S.S., and St George-Hyslop, P.H. (2002). gamma-Secretase, Notch, Abeta and Alzheimer's disease: where do the presenilins fit in? Nat Rev Neurosci *3*, 281-290.

Son, E.Y., Ichida, J.K., Wainger, B.J., Toma, J.S., Rafuse, V.F., Woolf, C.J., and Eggan, K. (2011). Conversion of mouse and human fibroblasts into functional spinal motor neurons. Cell Stem Cell *9*, 205-218.

Son, J.H., Shim, J.H., Kim, K.H., Ha, J.Y., and Han, J.Y. (2012). Neuronal autophagy and neurodegenerative diseases. Exp Mol Med *44*, 89-98.

Steiner, H., and Haass, C. (2000). Intramembrane proteolysis by presenilins. Nat Rev Mol Cell Biol *1*, 217-224.

Steiner, H., Winkler, E., Edbauer, D., Prokop, S., Basset, G., Yamasaki, A., Kostka, M., and Haass, C. (2002). PEN-2 is an integral component of the gamma-secretase complex required for coordinated expression of presenilin and nicastrin. J Biol Chem *277*, 39062-39065.

Stockley, J.H., and O'Neill, C. (2008). Understanding BACE1: essential protease for amyloid-beta production in Alzheimer's disease. Cell Mol Life Sci *65*, 3265-3289.

Stromhaug, P.E., Berg, T.O., Fengsrud, M., and Seglen, P.O. (1998). Purification and characterization of autophagosomes from rat hepatocytes. Biochem J *335 (Pt 2)*, 217-224.

Takahashi, K., Okita, K., Nakagawa, M., and Yamanaka, S. (2007). Induction of pluripotent stem cells from fibroblast cultures. Nat Protoc *2*, 3081-3089.

Takami, M., Nagashima, Y., Sano, Y., Ishihara, S., Morishima-Kawashima, M., Funamoto, S., and Ihara, Y. (2009). gamma-Secretase: successive tripeptide and tetrapeptide release from the transmembrane domain of beta-carboxyl terminal fragment. J Neurosci *29*, 13042-13052.

Takamura, A., Higaki, K., Kajimaki, K., Otsuka, S., Ninomiya, H., Matsuda, J., Ohno, K., Suzuki, Y., and Nanba, E. (2008). Enhanced autophagy and mitochondrial aberrations in murine G(M1)-gangliosidosis. Biochem Biophys Res Commun *367*, 616-622.

Tamboli, I.Y., Hampel, H., Tien, N.T., Tolksdorf, K., Breiden, B., Mathews, P.M., Saftig, P., Sandhoff, K., and Walter, J. (2011a). Sphingolipid storage affects autophagic metabolism of the amyloid precursor protein and promotes Abeta generation. J Neurosci *31*, 1837-1849.

Tamboli, I.Y., Tien, N.T., and Walter, J. (2011b). Sphingolipid storage impairs autophagic clearance of Alzheimer-associated proteins. Autophagy *7*, 645-646.

Tanida, I., Minematsu-Ikeguchi, N., Ueno, T., and Kominami, E. (2005). Lysosomal turnover, but not a cellular level, of endogenous LC3 is a marker for autophagy. Autophagy *1*, 84-91.

Tannenberg, R.K., Scott, H.L., Westphalen, R.I., and Dodd, P.R. (2004). The identification and characterization of excitotoxic nerve-endings in Alzheimer disease. Curr Alzheimer Res *1*, 11-25.

Tanzi, R.E., and Bertram, L. (2005). Twenty years of the Alzheimer's disease amyloid hypothesis: a genetic perspective. Cell *120*, 545-555.

Tebar, F., Bohlander, S.K., and Sorkin, A. (1999). Clathrin assembly lymphoid myeloid leukemia (CALM) protein: localization in endocytic-coated pits, interactions with clathrin, and the impact of overexpression on clathrin-mediated traffic. Mol Biol Cell *10*, 2687-2702.

Terman, A., Kurz, T., Navratil, M., Arriaga, E.A., and Brunk, U.T. (2010). Mitochondrial turnover and aging of long-lived postmitotic cells: the mitochondrial-lysosomal axis theory of aging. Antioxid Redox Signal *12*, 503-535.

Terry, R.D., Hansen, L.A., DeTeresa, R., Davies, P., Tobias, H., and Katzman, R. (1987). Senile dementia of the Alzheimer type without neocortical neurofibrillary tangles. J Neuropathol Exp Neurol *46*, 262-268.

Teter, S.A., Eggerton, K.P., Scott, S.V., Kim, J., Fischer, A.M., and Klionsky, D.J. (2001). Degradation of lipid vesicles in the yeast vacuole requires function of Cvt17, a putative lipase. J Biol Chem *276*, 2083-2087.

Thinakaran, G., Borchelt, D.R., Lee, M.K., Slunt, H.H., Spitzer, L., Kim, G., Ratovitsky, T., Davenport, F., Nordstedt, C., Seeger, M.*, et al.* (1996). Endoproteolysis of presenilin 1 and accumulation of processed derivatives in vivo. Neuron *17*, 181-190.

Thomson, J.A., Itskovitz-Eldor, J., Shapiro, S.S., Waknitz, M.A., Swiergiel, J.J., Marshall, V.S., and Jones, J.M. (1998). Embryonic stem cell lines derived from human blastocysts. Science *282*, 1145-1147.

Tian, Y., Bassit, B., Chau, D., and Li, Y.M. (2010). An APP inhibitory domain containing the Flemish mutation residue modulates gamma-secretase activity for Abeta production. Nat Struct Mol Biol *17*, 151-158.

Tian, Y., Chang, J.C., Greengard, P., and Flajolet, M. (2014). The convergence of endosomal and autophagosomal pathways: Implications for APP-CTF degradation. Autophagy *10*.

Tiraboschi, P., Hansen, L.A., Masliah, E., Alford, M., Thal, L.J., and Corey-Bloom, J. (2004). Impact of APOE genotype on neuropathologic and neurochemical markers of Alzheimer disease. Neurology *62*, 1977-1983.

Tu, H., Nelson, O., Bezprozvanny, A., Wang, Z., Lee, S.F., Hao, Y.H., Serneels, L., De Strooper, B., Yu, G., and Bezprozvanny, I. (2006). Presenilins form ER Ca2+ leak channels, a function disrupted by familial Alzheimer's disease-linked mutations. Cell *126*, 981-993.

Umeda, T., Tomiyama, T., Sakama, N., Tanaka, S., Lambert, M.P., Klein, W.L., and Mori, H. (2011). Intraneuronal amyloid beta oligomers cause cell death via endoplasmic reticulum stress, endosomal/lysosomal leakage, and mitochondrial dysfunction in vivo. J Neurosci Res *89*, 1031-1042.

Van Den Heuvel, C., Thornton, E., and Vink, R. (2007). Traumatic brain injury and Alzheimer's disease: a review. Prog Brain Res *161*, 303-316.

van Echten-Deckert, G., and Walter, J. (2012). Sphingolipids: critical players in Alzheimer's disease. Prog Lipid Res *51*, 378-393.

Vassar, R., Bennett, B.D., Babu-Khan, S., Kahn, S., Mendiaz, E.A., Denis, P., Teplow, D.B., Ross, S., Amarante, P., Loeloff, R.*, et al.* (1999). Beta-secretase cleavage of Alzheimer's amyloid precursor protein by the transmembrane aspartic protease BACE. Science *286*, 735-741.

Venables, M.C., Brouns, F., and Jeukendrup, A.E. (2008). Oxidation of maltose and trehalose during prolonged moderate-intensity exercise. Med Sci Sports Exerc *40*, 1653-1659.

Vicencio, J.M., Ortiz, C., Criollo, A., Jones, A.W., Kepp, O., Galluzzi, L., Joza, N., Vitale, I., Morselli, E., Tailler, M*., et al.* (2009). The inositol 1,4,5-trisphosphate receptor regulates autophagy through its interaction with Beclin 1. Cell Death Differ *16*, 1006-1017.

Vierbuchen, T., Ostermeier, A., Pang, Z.P., Kokubu, Y., Sudhof, T.C., and Wernig, M. (2010). Direct conversion of fibroblasts to functional neurons by defined factors. Nature *463*, 1035-1041.

Wakabayashi, T., Craessaerts, K., Bammens, L., Bentahir, M., Borgions, F., Herdewijn, P., Staes, A., Timmerman, E., Vandekerckhove, J., Rubinstein, E*., et al.* (2009). Analysis of the gamma-secretase interactome and validation of its association with tetraspanin-enriched microdomains. Nat Cell Biol *11*, 1340-1346.

Wakabayashi, T., and De Strooper, B. (2008). Presenilins: members of the gamma-secretase quartets, but part-time soloists too. Physiology (Bethesda) *23*, 194-204.

Walter, J. (2006). Control of amyloid-beta-peptide generation by subcellular trafficking of the beta-amyloid precursor protein and beta-secretase. Neurodegener Dis *3*, 247-254.

Walter, J., Capell, A., Grunberg, J., Pesold, B., Schindzielorz, A., Prior, R., Podlisny, M.B., Fraser, P., Hyslop, P.S., Selkoe, D.J*., et al.* (1996). The Alzheimer's disease-associated presenilins are differentially phosphorylated proteins located predominantly within the endoplasmic reticulum. Mol Med *2*, 673-691.

Walter, J., Grunberg, J., Capell, A., Pesold, B., Schindzielorz, A., Citron, M., Mendla, K., George-Hyslop, P.S., Multhaup, G., Selkoe, D.J*., et al.* (1997). Proteolytic processing of the Alzheimer disease-associated presenilin-1 generates an in vivo substrate for protein kinase C. Proc Natl Acad Sci U S A *94*, 5349-5354.

Walter, J., Kaether, C., Steiner, H., and Haass, C. (2001). The cell biology of Alzheimer's disease: uncovering the secrets of secretases. Curr Opin Neurobiol *11*, 585-590.

Walter, J., and van Echten-Deckert, G. (2013a). Cross-talk of membrane lipids and Alzheimer-related proteins. Mol Neurodegener *8*, 34.

Walter, J., and van Echten-Deckert, G. (2013b). Cross-talk of membrane lipids and Alzheimer-related proteins. Mol Neurodegener *8*, 34.

Wang, Y., Martinez-Vicente, M., Kruger, U., Kaushik, S., Wong, E., Mandelkow, E.M., Cuervo, A.M., and Mandelkow, E. (2010). Synergy and antagonism of macroautophagy and chaperone-mediated autophagy in a cell model of pathological tau aggregation. Autophagy *6*, 182-183.

Wei, Y., Pattingre, S., Sinha, S., Bassik, M., and Levine, B. (2008). JNK1-mediated phosphorylation of Bcl-2 regulates starvation-induced autophagy. Mol Cell *30*, 678-688.

Weidemann, A., Eggert, S., Reinhard, F.B., Vogel, M., Paliga, K., Baier, G., Masters, C.L., Beyreuther, K., and Evin, G. (2002). A novel epsilon-cleavage within the transmembrane domain of the Alzheimer amyloid precursor protein demonstrates homology with Notch processing. Biochemistry *41*, 2825-2835.

Weidemann, A., Konig, G., Bunke, D., Fischer, P., Salbaum, J.M., Masters, C.L., and Beyreuther, K. (1989). Identification, biogenesis, and localization of precursors of Alzheimer's disease A4 amyloid protein. Cell *57*, 115-126.

Weiss, J.H., Yin, H.Z., and Choi, D.W. (1994). Basal forebrain cholinergic neurons are selectively vulnerable to AMPA/kainate receptor-mediated neurotoxicity. Neuroscience *60*, 659-664.

Wichterle, H., and Przedborski, S. (2010). What can pluripotent stem cells teach us about neurodegenerative diseases? Nat Neurosci *13*, 800-804.

Williamson, W.R., and Hiesinger, P.R. (2010). On the role of v-ATPase V0a1-dependent degradation in Alzheimer disease. Commun Integr Biol *3*, 604-607.

Wilson, C.A., Murphy, D.D., Giasson, B.I., Zhang, B., Trojanowski, J.Q., and Lee, V.M. (2004). Degradative organelles containing mislocalized alpha-and beta-synuclein proliferate in presenilin-1 null neurons. J Cell Biol *165*, 335-346.

Winslow, A.R., and Rubinsztein, D.C. (2008). Autophagy in neurodegeneration and development. Biochim Biophys Acta *1782*, 723-729.

Wolfe, D.M., Lee, J.H., Kumar, A., Lee, S., Orenstein, S.J., and Nixon, R.A. (2013). Autophagy failure in Alzheimer's disease and the role of defective lysosomal acidification. Eur J Neurosci *37*, 1949-1961.

Wolfe, M.S., Xia, W., Moore, C.L., Leatherwood, D.D., Ostaszewski, B., Rahmati, T., Donkor, I.O., and Selkoe, D.J. (1999a). Peptidomimetic probes and molecular modeling suggest that Alzheimer's gamma-secretase is an intramembrane-cleaving aspartyl protease. Biochemistry *38*, 4720-4727.

Wolfe, M.S., Xia, W., Ostaszewski, B.L., Diehl, T.S., Kimberly, W.T., and Selkoe, D.J. (1999b). Two transmembrane aspartates in presenilin-1 required for presenilin endoproteolysis and gamma-secretase activity. Nature *398*, 513-517.

Wong, E., and Cuervo, A.M. (2010). Autophagy gone awry in neurodegenerative diseases. Nat Neurosci *13*, 805-811.

Xu, H., Sweeney, D., Wang, R., Thinakaran, G., Lo, A.C., Sisodia, S.S., Greengard, P., and Gandy, S. (1997). Generation of Alzheimer beta-amyloid protein in the trans-Golgi network in the apparent absence of vesicle formation. Proc Natl Acad Sci U S A *94*, 3748-3752.

Yang, D.S., Stavrides, P., Mohan, P.S., Kaushik, S., Kumar, A., Ohno, M., Schmidt, S.D., Wesson, D., Bandyopadhyay, U., Jiang, Y., *et al.* (2011). Reversal of autophagy dysfunction in the TgCRND8 mouse model of Alzheimer's disease ameliorates amyloid pathologies and memory deficits. Brain *134*, 258-277.

Yang, Z., and Klionsky, D.J. (2010). Mammalian autophagy: core molecular machinery and signaling regulation. Curr Opin Cell Biol *22*, 124-131.

Yankner, B.A. (1996). Mechanisms of neuronal degeneration in Alzheimer's disease. Neuron *16*, 921-932.

Yiannopoulou, K.G., and Papageorgiou, S.G. (2013). Current and future treatments for Alzheimer's disease. Ther Adv Neurol Disord *6*, 19-33.

Ying, Q.L., Stavridis, M., Griffiths, D., Li, M., and Smith, A. (2003). Conversion of embryonic stem cells into neuroectodermal precursors in adherent monoculture. Nat Biotechnol *21*, 183-186.

Yla-Anttila, P., Vihinen, H., Jokitalo, E., and Eskelinen, E.L. (2009). 3D tomography reveals connections between the phagophore and endoplasmic reticulum. Autophagy *5*, 1180-1185.

Yoshimori, T., Yamamoto, A., Moriyama, Y., Futai, M., and Tashiro, Y. (1991). Bafilomycin A1, a specific inhibitor of vacuolar-type H(+)-ATPase, inhibits acidification and protein degradation in lysosomes of cultured cells. J Biol Chem *266*, 17707-17712.

Young-Pearse, T.L., Bai, J., Chang, R., Zheng, J.B., LoTurco, J.J., and Selkoe, D.J. (2007). A critical function for beta-amyloid precursor protein in neuronal migration revealed by in utero RNA interference. J Neurosci *27*, 14459-14469.

Young, J.E., and Goldstein, L.S. (2012). Alzheimer's disease in a dish: promises and challenges of human stem cell models. Hum Mol Genet *21*, R82-89.

Yu, G., Nishimura, M., Arawaka, S., Levitan, D., Zhang, L., Tandon, A., Song, Y.Q., Rogaeva, E., Chen, F., Kawarai, T.*, et al.* (2000). Nicastrin modulates presenilin-mediated notch/glp-1 signal transduction and betaAPP processing. Nature *407*, 48-54.

Yu, L., McPhee, C.K., Zheng, L., Mardones, G.A., Rong, Y., Peng, J., Mi, N., Zhao, Y., Liu, Z., Wan, F.*, et al.* (2010). Termination of autophagy and reformation of lysosomes regulated by mTOR. Nature *465*, 942-946.

Yu, W.H., Cuervo, A.M., Kumar, A., Peterhoff, C.M., Schmidt, S.D., Lee, J.H., Mohan, P.S., Mercken, M., Farmery, M.R., Tjernberg, L.O.*, et al.* (2005). Macroautophagy--a novel Beta-amyloid peptide-generating pathway activated in Alzheimer's disease. J Cell Biol *171*, 87-98.

Yu, W.H., Kumar, A., Peterhoff, C., Shapiro Kulnane, L., Uchiyama, Y., Lamb, B.T., Cuervo, A.M., and Nixon, R.A. (2004). Autophagic vacuoles are enriched in amyloid precursor protein-secretase activities: implications for beta-amyloid peptide over-production and localization in Alzheimer's disease. Int J Biochem Cell Biol *36*, 2531-2540.

Zalckvar, E., Berissi, H., Mizrachy, L., Idelchuk, Y., Koren, I., Eisenstein, M., Sabanay, H., Pinkas-Kramarski, R., and Kimchi, A. (2009). DAP-kinase-mediated phosphorylation on the BH3 domain of beclin 1 promotes dissociation of beclin 1 from Bcl-XL and induction of autophagy. EMBO Rep *10*, 285-292.

Zhang, S.C., Wernig, M., Duncan, I.D., Brustle, O., and Thomson, J.A. (2001). In vitro differentiation of transplantable neural precursors from human embryonic stem cells. Nat Biotechnol *19*, 1129-1133.

Zhang, X., Garbett, K., Veeraraghavalu, K., Wilburn, B., Gilmore, R., Mirnics, K., and Sisodia, S.S. (2012). A Role for Presenilins in Autophagy Revisited: Normal Acidification of Lysosomes in Cells Lacking PSEN1 and PSEN2. J Neurosci *32*, 8633-8648.

Zhang, Z., Nadeau, P., Song, W., Donoviel, D., Yuan, M., Bernstein, A., and Yankner, B.A. (2000). Presenilins are required for gamma-secretase cleavage of beta-APP and transmembrane cleavage of Notch-1. Nat Cell Biol *2*, 463-465.

Zhou, J., Tan, S.H., Nicolas, V., Bauvy, C., Yang, N.D., Zhang, J., Xue, Y., Codogno, P., and Shen, H.M. (2013). Activation of lysosomal function in the course of autophagy via mTORC1 suppression and autophagosome-lysosome fusion. Cell Res *23*, 508-523.

8. Acknowledgement

My deepest and warmest gratitude go to my supervisor Prof. Dr. Jochen Walter, for giving me opportunity to join his laboratory as a PhD student and for his fantastic support during my study. This voyage would have not been possible without his helpful suggestions and excellent care of my works. I am especially thankful that he provided the optimal research conditions, and gave me valuable advice and the independence to develop my research skills. I greatly appreciate that he was always very patient, willing to help and discuss with careful instructions.

I would like to express my special gratitude to Dr. Irfan Y. Tamboli, who has accepted me to carry out my PhD research from his grant and supervised me in the early stages of my thesis. He guided me always with patience and encouragement as a mentor, counselor and colleague. His helpfulness and great advice are extremely important for the development of my works. Especially, I really appreciate that he always had time for discussion and helped me overcome challenges of the new working environment.

I am grateful to my thesis committee Prof. Dr. Jörg Höhfeld, Prof. Dr. Waldemar Kolanus and PD Dr. Philipp Koch for their valuable time. I especially want to thank Prof. Höhfeld for his kind agreement to be the second referee for this dissertation.

I would sincerely like to thank PD. Dr. Philipp Koch, Dr. Jerome Mertens and Kathrin Stüber from the group of Prof. Dr. Oliver Brüstle for providing the human pluripotent stem cells – derived neurons. Their great valuable cell types are the fundamental materials for my research. I especially want to thank Jerome and Kathrin for valuable discussions and excellent collaboration. I greatly appreciated their kind support and contributions into my project. I hope our data will be published in near future.

I sincerely thank to my colleagues both past and present for their help, friendship and creating a nice working atmosphere Dr. Patrick Wunderlich, Dr. Martin Siepmann, Dr. Sathish Kumar, Dr. Konstantin Glebov, Esterban, Eva, Ilker, Janina, Josefine, Marie, Nadja, Sandra, Angela, Sonia, Jessica, Heike, Esther, Manish, and the members of the neurobiology lab. Many thanks for their willingness to help out in the lab and for interesting discussions. I deeply appreciate Patrick, Angela, Esterban, and Sonia for reading and commenting on my dissertation. I wish to thank Sonia for her kind help to carry out some experiments. My special thanks to Patrick for the instructive conversations and his helpfulness at all points.

Con cảm ơn bố mẹ và các em vì những ưu ái và ủng hộ dành cho con. Bố mẹ hãy xem đây như là việc con đã hoàn thành một mục tiêu, kế hoạch của mình. Mặc dù lấy bằng tiến sỹ không đảm bảo cho sự thành công trong cuộc sống, nhưng con nghĩ là con đã lựa chọn cái phù hợp nhất, cái con muốn theo đuổi nhất tại thời điểm 5 năm trước. Quan trọng hơn cả, con cảm thấy mình may mắn, hạnh phúc vì được đi đến nhiều nơi mà con muốn, được trải nghiệm cuộc sống và tiếp xúc với nhiều nền văn hóa. Đó là điều vô cùng quý giá đối với con.

Phương Nam, cảm ơn em vì những chia sẻ trong cuộc sống cũng như trong nghiên cứu. Đặc biệt là những thiệt thòi và khó khăn khi không có anh bên cạnh để chăm sóc em và con. Sự hy sinh và cố gắng của em là động lực lớn để anh cố gắng hoàn thành tốt nhất nghiên cứu của mình. Cảm ơn con gái yêu Tuệ-Anh vì con đã đến với bố mẹ, con là động lực lớn cho cuộc sống của bố mẹ.

9. Curriculum Vitae

Full name: Nguyen, Thanh Tien

Works and University Education

Oct. 2009 – Oct. 2014	PhD student: Molecular Cell Biology, Neurology, University Hospital of Bonn, Germany. Graduate student of the International graduate school Threotical and Experimental Medicine (THEME), University of Bonn, Germany *Thesis*: Involvement of autophagy in metabolism of Amyloid Precursor Protein and effects of familial Alzheimer's disease-associated mutations of Presenilin-1
Sep. 2008 – Jul. 2009	Research assistant: Department of Anatomy & Cell Biology, University of Ulsan College of Medicine, S. Korea. Main projects: - The processing of Amyloid Precursor Protein - Rat primary cortical and hippocampal neuronal preparation
Sep. 2006 – Aug. 2008	Master student: Lab of Skin Biotechnology, College of Life Science, KyungHee University, S. Korea. *Thesis*: Comparison of Resin Components of *Rhus succedanea* Linne and *Rhus verniciflua* Stokes
Aug. 2005 – Jul. 2006	Research assistant: Center for Experimental Biology, National Center for Technological Progress, Viet Nam Projects: - Cultivation and harvest of microalgae Dunaliella, Chlorella, Spirulina. - Analyses of industrial wastewaters.
Sep. 2001 – Jun. 2005	Bachelor program: Biological Education, Vietnam National University Hanoi, Viet Nam *Thesis*: Comparing and optimising various outdoor culture conditions for *in vitro* growth of microalgal *Dunaliella salina.*

Scientific records

EURON and THEME joint PhD meeting – University of Bonn, September 22-23, 2011	**Talk**: Tien Nguyen, Irfan Tamboli and Jochen Walter. Familial Alzheimer disease-associated Presenilin mutants regulate autophagic activity – implication for Alzheimer's disease
AD/PD 2011 Barcelona, Spain, March 9-13, 2011	**Poster**: Tien Nguyen, Jochen Walter and Irfan Tamboli. Presenilin-1 regulates induction of autophagy
THEME PhD meeting – University of Bonn, September 2010	**Poster**: Tien Nguyen, Jochen Walter and Irfan Tamboli. Presenilin 1 regulates autophagic response to stress

Trainings

1. Stem cell biology, 28.4.2011 – 30.4.2011, Institute of Reconstructive Neurobiology, University of Bonn, Germany.
2. Human molecular genetics, 3.8.2011 – 7.9.2011, Institute of Human Genetics, University of Bonn, Germany.

Publications

1. **Nguyen T. Tien**, Irfan Y. Tamboli, and Jochen Walter. Trehalose decreases the degradation of the amyloid precursor protein by inhibition of lysosomal activity. (Submitted)

2. **Nguyen T. Tien**, Philipp Koch, Jerome Mertens, Irfan Y. Tamboli, Kathrin Stuber, Oliver Brüstle and Jochen Walter. Familial Alzheimer's disease - associated Presenilin 1 mutants regulate autophagy in human pluripotent stem cells-derived neurons. (In preparation)

3. Patrick Wunderlich, Konstantin Glebov, Nadja Kemmerling, **Nguyen T. Tien**, Harald Neumann and Jochen Walter. Sequential proteolytic processing of the triggering receptor expressed on myeloid cells-2 (TREM2) by ectodomain shedding and γ-secretase dependent intramembranous cleavage. J Biol Chem. 2013 Nov 15; 288 (46): 33027-36.

4. Irfan Y. Tamboli, **Nguyen T. Tien** and Jochen Walter. Sphingolipid storage impairs autophagic clearance of Alzheimer-associated proteins. Autophagy. 2011 Jun; 7 (6): 645-6.

5. Irfan Y. Tamboli, Heike Hampel, **Nguyen T. Tien**, Karen Tolksdorf, Bernadette Breiden, Paul M. Mathews, Paul Saftig, Konrad Sandhoff, and Jochen Walter. Sphingolipid Storage Affects Autophagic Metabolism of the Amyloid Precursor Protein and Promotes Aβ Generation. J Neurosci. 2011 Feb 2; 31 (5): 1837-49.

6. S. M. Kim, S. Y. Yoon, J. E. Choi, J. S. Park, J. M. Choi, **T. Nguyen,** and D. H. Kim. Activation of eukaryotic initiation factor-2α-kinases in okadaic acid-treated neurons. Neuroscience. 2010 Sep 15; 169 (4): 1831-9.

Scholarships and Awards

- Scholarship from BK21 Korea Research Foundation for Master program (2006-2008).

- Scholarship from E. Land foundation for Master Program (2006-2008).

- Scholarship with financial support, from Vietnam Ministry of Education and Training for undergraduate students (2004-2005).

- Certificate of Merit for poor family's students with excellent achievements in studies and scientific research, granted by the Dean of Pedagogy Faculty, Vietnam National University, Hanoi (VNU) (2005).

Languages

- English: Fluent (communication and scientific writing)
- Korean, German: Elementary level; Dutch: Beginner
- Vietnamese: Native speaker

Skills

- Molecular biology techniques: ELISA, RT-PCR, IHC, ICC, fluorescence microscope, Western blot, Cloning, Gene transfection, exosome preparation, electron microscope…
- Cell cultures: human pluripotent stem cells - derived neurons, rat primary cortical and hippocampal neurons, glia, neuroglioma, macrophages, fibroblasts, epithelial cells...
- Extraction of herbal compounds, silica gel column chromatography, thin layer chromatography…
- IT skills: Word, Excel, PowerPoint, GraphPad Prism, Photoshop…
- Teamwork, communication, organization, project management…